



UK RACE TO SPACE

Final Engine Documentation 2023

Cranfield University

CranSEDS HRMTS 22-23

H.Y.D.R.A.

HYbrid engine Development for
Rocketry Applications

Mentors: Daniel Sieradzki

Aaron Sidhu

Contents

1	Introduction	1
1.1	History and background of engine development at the university	1
1.2	Engine type	2
1.3	Current sponsors and funding	2
2	Project Management	3
2.1	Assigned Roles and Team Roster	3
2.2	Team roles and Responsibilities	3
2.3	Stakeholder Map	4
2.4	Work Package Breakdown Structure	5
2.5	Preliminary Budget	5
2.6	Project Risks, COSHH and Mitigations	5
2.7	Project Plan	6
2.8	Team Management	6
3	Requirements	7
4	Propellants	8
4.1	Liquid Oxidiser	8
4.2	Solid Fuel	9
5	Detailed Design	10
5.1	Engine Design	11
5.1.1	Fuel Grain and Combustion Casing Geometry	11
5.2	Propulsion Design	12
5.2.1	Motor Sizing	12
5.2.2	Injector	13

5.2.3	Nozzle Design	15
5.2.4	Ignition Mechanism	17
5.2.5	Thrust Adapter Assembly	17
5.3	Feed System Design	19
5.3.1	Valves	21
5.3.2	Controls and DAQ Electronics	21
5.4	Engine Mount	25
5.4.1	Test Stand	25
5.4.2	Support sub-assembly	27
5.5	Material Selection	28
5.6	Cooling Plan and Thermal Analyses	28
6	Design Calculations	30
6.1	Engine Sizing	30
6.2	Fuel Grain Geometry	31
6.3	Regression Rate	31
6.4	Combustion Chamber Length	32
6.5	Nozzle Shape	32
6.6	Thermochemistry for combustion reaction	33
6.7	Pressure Drop	35
6.7.1	Feed Line Pressure Drop	35
6.7.2	Injector Pressure Drop	36
6.8	Injector Design	36
6.8.1	Injector Sizing	36
6.8.2	Injector holes	37
6.9	Flange Sizing	38
6.10	Chamber thin wall stress calculations	38
7	CFD Simulations	40
7.1	Methodology	40
7.1.1	Step 1: Modelling the geometry	40
7.1.2	Step 2: Meshing	41
7.1.3	Step 3: Setting boundary conditions	42

7.1.4	Step 4: Solver pre-processing (Setup)	42
7.2	Results	43
7.3	Future Work	46
8	Manufacturing	47
8.1	Timeline and lead time overview	47
8.2	Manufacturers used	51
8.3	Assembly overview and Sub-assembly testing	52
8.3.1	Hydrostatic Pressure Testing	52
8.3.2	Cold Flow Testing	53
9	Engine Setup and Hot-Fire Sequence	54
9.1	Engine Integration	54
9.1.1	Engine Structure	54
9.1.2	Feed Line System	55
9.1.3	Controls and DAQ System	55
9.2	Manufacturing: Test-Firing Procedure and Operations	56
9.2.1	Combustion Sequence Overview	56
9.2.2	Assembly and maintenance	56
9.2.3	Safety Checks	58
9.2.4	Run System	58
10	Knowledge Transfer Plan	60
Bibliography		62
11 Appendices		63
11.1	Sub-System Requirements	63
11.1.1	Structures	63
11.1.2	Propulsion	64
11.1.3	Controls	65
11.2	Engineering Drawings	66
11.3	Material Datasheets	72
11.3.1	Graphite Datasheet	72
11.4	Simulation Output	74

11.4.1 ProPEP3	74
11.4.2 RPA	78
11.5 Temperature Graph Matlab Code	80
11.6 Load cell DAQ Arduino code	81
11.7 Project Budgets	84
11.7.1 Cost and Mass Budget	84
11.7.2 Propellant Budget	85
11.7.3 Power Budget	85
11.8 Engine Test Setup	86
11.9 Risk Assessment	89
11.9.1 Risk Assessment	89
11.9.2 Test House 11 CranSEDS HRMTS Risk Review	99
11.9.3 COSHH Assessment for Nitrous Oxide	100
11.10 Project Gantt Chart	103

List of Figures

1.1	Team Logos: Old (left) and New (right). Source: Own.	1
2.1	Stakeholders Map. Source: Own.	4
2.2	Project Work Breakdown Overview. Source: Own.	5
5.1	Hybrid Engine Assembly on the ICD Bench. Source: Own.	10
5.2	Engine Chamber Cross Sectional View. Source: Own.	11
5.3	Fuel Grain geometry inside the combustion chamber. Source: Own.	11
5.4	FEA results of combustion chamber steel casing: Deformation: $7 \mu m$ (left); Max. Stress: 28.2 MPa (FOS: 8.86) (right). Source: Own.	12
5.5	Designed Injector: Isometric View (left), Cross-Sectional View (right). Source: Own.	14
5.6	FEA results of injector plate of mild steel: Deformation: $0.6 \mu m$ (left); Max. Stress: 19.1 MPa (FOS: 13.1) (right). Source: Own.	15
5.7	FEA results of injector flange of mild steel: Deformation: $4.9 \mu m$ (left); Max. Stress: 93.3 MPa (FOS: 2.7) (right). Source: Own.	15
5.8	Graphite Nozzle Design: Isometric View (left), Cross-Sectional View (right; Short high curve edge is the convergent part facing the combustion chamber). Source: Own.	16
5.9	FEA results of the graphite bell nozzle: Deformation: $5.9 \mu m$ (left); Max. Stress: 3.6 MPa (FOS: 16.6) (right). Source: Own.	16
5.10	FEA results of steel nozzle casing: Deformation: $0.9 \mu m$ (left); Max. Stress: 6.6 MPa (FOS: 37.8) (right). Source: Own.	17
5.11	Schematic of Ignition System. Source: Own. [1]	17
5.12	Thruster Assembly (The rectangular section in the back is the S-type Load cell). Source: Own.	18
5.13	FEA results of the thrust adapter's front plate: Deformation: $5 \mu m$ (left); Max. Stress: 33.9 MPa (FOS: 7.3) (right). Source: Own.	18
5.14	FEA results of the thrust adapter's rear plate: Deformation: 0.03 mm (left); Max. Stress: 48.04 MPa (FOS: 5.2) (right). Source: Own.	19
5.15	FEA results of the thrust adapter's connector: Deformation: $0.8 \mu m$ (left); Max. Stress: 8.2 MPa (FOS: 30) (right). Source: Own.	19

5.16 FEA results of the thrust adapter's 3D printed bushing (ASA material): Deformation: 5.5 μm (left); Max. Stress: 3.8 MPa (FOS: 8.6) (right). Source: Own.	19
5.17 Feed System Schematic. Source: Own.	20
5.18 Control Box setup schematic. Source: Own.	22
5.19 Control Box setup schematic. Source: Own.	23
5.20 Sensor placement on the combustion chamber. Source: Own.	24
5.21 Data acquisition sub-system circuit schematic diagram. Source: Own.	25
5.22 Test Stand. Source: Own.	25
5.23 Test Stand on the ICD Bench. Source: Own.	26
5.24 FEA results of the engine test stand: Deformation: 0.05 mm (left); Max. Stress: 19.23 MPa (FOS: 13) (right). Source: Own.	27
5.25 Ring Clamp System. Source: Own.	27
5.26 FEA results of the steel support plate: Deformation: 0.91 mm (left); Max. Stress: 176.91 MPa (FOS: 1.4) (right). Source: Own.	28
 6.1 Exponential rate graph for temperature with time	35
 7.1 Model geometry for CFD simulation of the engine nozzle. Source: Own.	41
7.2 Meshed geometry for CFD simulation of the engine nozzle. Source: Own.	42
7.3 Obtained results for CFD simulation of the engine nozzle: Density contour. Source: Own.	44
7.4 Obtained results for CFD simulation of the engine nozzle: Pressure contour. Source: Own.	45
7.5 Obtained results for CFD simulation of the engine nozzle: Temperature contour. Source: Own.	45
7.6 Obtained results for CFD simulation of the engine nozzle: Velocity contour. Source: Own.	46
 8.1 Manufactured test stand. Source: Own.	47
8.2 Manufactured combustion chamber. Source: Own.	47
8.3 Manufactured and assembled injector plate. Source: Own.	48
8.4 Manufactured and assembled fuel grain and liner sub-assembly. Source: Own.	48
8.5 Manufactured and assembled thruster assembly. Source: Own.	49
8.6 Manufactured bend support plate. Source: Own.	49
8.7 Manufactured and assembled nozzle sub-assembly. Source: Own.	50
8.8 Assembled control box. Source: Own.	50
8.9 Assembled data acquisition system for the load cell. Source: Own.	51

8.10 Test House for Assembly and Fire Testing. Source: Own.	52
8.11 Pressure testing on the combustion chamber. Source: Own.	53
8.12 Pressure tested combustion chamber. Source: Own.	53
9.1 Engine test stand structure assembly. Source: Own.	54
9.2 Assembled Control Box. Source: Own.	56
11.1 Sub-System Requirements: Structures (HY-2XXX)	63
11.2 Hybrid Engine Assembly on Test Stand. Source: Own.	66
11.3 Engine Test Stand. Source: Own.	66
11.4 Thrust Adapter Rear Plate. Source: Own.	67
11.5 Thrust Adapter Front Plate. Source: Own.	67
11.6 Thrust Adapter Connecting Tie rods. Source: Own.	68
11.7 Engine Chamber Ring Clamp System Support Plates. Source: Own.	68
11.8 Engine Injector Flange. Source: Own.	69
11.9 Engine Injector Plate. Source: Own.	69
11.10 Combustion Chamber Casing. Source: Own.	70
11.11 Combustion Chamber Casing End Flanges. Source: Own.	70
11.12 Metal Nozzle Casing. Source: Own.	71
11.13 Graphite Nozzle. Source: Own.	71
11.14 Simulation Outputs. Source: Own.	74
11.15 Nozzle Impulse vs Expansion Ratio response curve. Source: Own.	74
11.16 Chamber Pressure vs Burn Rate Results. Source: Own.	74
11.17 Combustion Chamber and Nozzle Stabilized Temperature Curve. Source: Own.	78
11.18 Combustion Chamber and Nozzle Stabilized Wall Heat Flux Curve. Source: Own.	78
11.19 Welding on the combustion chamber and end flange connection. Source: Own.	86
11.20 Internal hole for pressure transducer to measure internal combustion chamber pressure. Source: Own.	86
11.21 Injector plate assembly. Source: Own.	86
11.22 Line assembly of the combustion chamber. Source: Own.	87
11.23 Structural assembly of the engine setup. Source: Own.	87
11.24 Pressure testing machine for the combustion chamber. Source: Own.	88
11.25 Etching on combustion chamber after passing the pressure test. Source: Own.	88
11.26 Pareto diagram. Source: Own.	89

List of Tables

1.1	List of Project Sponsors	2
2.1	Team members and their roles	3
2.2	Cost Budget and Acquisitions	5
3.1	Top-Level Requirements for the Project (HY-1XXX)	7
4.1	Assembly and Equipment level requirements Source: Own.	8
4.2	Liquid Oxidiser propellant selection trade study	9
5.1	Sizing results from parameters from ProPEP simulation	13
5.2	Input values to determine the number of holes on the injector plate.	14
7.1	Tabulated results obtained from CFD simulation of the C-D nozzle	43
11.1	Sub-System Requirements: Propulsion (HY-3XXX)	64
11.2	Sub-System Requirements: Controls (HY-4XXX)	65
11.3	Cost and Mass Budget	84
11.4	Propellant Budget	85
11.5	Electrical Power Budget	85

Acknowledgments

We would like to express our deepest thanks and gratitude to all the people who helped shape this design work and report:

We thank our supervisor Professor Adam Baker for his insights and zeal driving this project over the years, and his technical expertise, helping us out in times of need.

To David Thompson and the manufacturing team at the Test facility of Cranfield University for helping us in manufacturing and making the process as smooth as possible.

To Scott Booden and his team for aiding us right from the project's inception and helping us to accomplish the project's design, ready enough to be built and test fired. Without you guys, we would have been unable to fast-pace our design for the combustion chamber, feed and controls system.

To all our mentors, Dan Sieradzki, Aaron Sidhu, Ben Kanda, Zoe Ashford, Adriano Isoldi, Dario Del Gatto, Giuseppe Gallo, and Sammukh Khadtare who have gone above and beyond to aid the project. They have consistently provided a friendly and concise yet greatly effective mentorship, employing their knowledge, skills and experiences to help us in our design and manufacturing phase.

And, to the Race to Space competition team for organizing this contest, giving us the unique opportunity to grow and gain an amazing experience.

To our sponsors, SmallSpark, CranSEDS, and the Cranfield Student's Association, for their financial support and technical backing.

To the ASE course professors from the School of Aerospace, Transport and Manufacturing, Cranfield University, for their technical guidance and constructive suggestions.

To the tireless committee team at CranSEDS and Cranfield Student's Association, who helped in the facilitation of our requests and encouraged the team to propel through the dark clouds.

To Gregor Arbuckle for his help in designing the team's logo.

And to the passion and drive within all of the team members to learn, explore and embark on this journey and always keep pushing their limits.

Chapter 1

Introduction

1.1 History and background of engine development at the university

CranSEDS is Cranfield University's local chapter of UKSEDS and is comprised of students interested in space exploration. The association promotes students' practical learning in the space sector by organising several competitions in the field of rocketry, robotics, and satellite design. The Hybrid Rocket Test Stand project was proposed as an independent activity to design, build and test a hybrid rocket motor and a test stand table at the Test Facility of Cranfield University. The team's supervisor, Dr Adam Baker, advised to start the project on Hybrid Engine and gain essential experience to move forward and develop a completely student-built Liquid Bi-Propellant Engine.

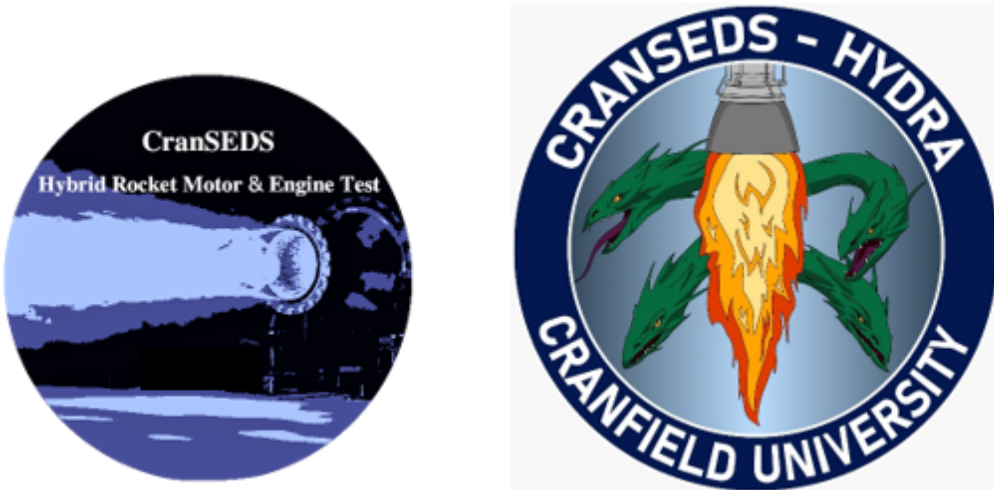


Figure 1.1: Team Logos: Old (left) and New (right). Source: Own.

This project has the objective of fostering interest and developing students' skills in the field of space propulsion as well as giving the opportunity to future CranSEDS students to work on hybrid motor projects. Another objective for this project is to provide an enrichment ground for the Cranfield students, and potentially other university students, to develop their research projects and thesis with the help of the Hybrid engine built by the team. Originally started in 2020, the long-term goals of the project are to integrate the hybrid motor into a rocket and move on to the development of liquid engines.

From its initiation, the past 2 years, teams have been working tirelessly to set out the mission statement, objectives, requirements and work that needs to be undertaken for developing a real-life Hybrid Engine, along with securing crucial sponsorships and assistance from the University. Unfortunately,

due to COVID, the team's progress on the manufacturing side dipped down. However, that didn't stop the team from keeping working virtually and refining their design. Our task this year is to refine the design with respect to the manufacturing parameters and eventually build the Hybrid Engine and have a Hot Fire Testing.

1.2 Engine type

The team has a plan to build a Small Horizontal Hybrid Engine with a mean thrust of 300 N using liquid oxidiser propellant as Nitrous Oxide and solid fuel propellant as HDPE (High-Density Poly-Ethylene) Grain case. The following report describes the initial design and operation plan of the team and the next steps that the team needs to take for designing, manufacturing, testing and validating the Hybrid Engine before presenting the engine at the Race to Space competition in July 2023.

1.3 Current sponsors and funding

The team's sponsors have been mentioned in the list below. They have been utterly helpful in aiding the team to develop the engine and mould the members into better engineers. The sponsors have aided the team with technical support for the Hybrid engine, financial support and support for developing the managerial and Systems model for the project.

Table 1.1: List of Project Sponsors

Sponsor	Assistance type
Centre for Autonomous and Cyber-Physical Systems, Cranfield University	Financial Support
SmallSpark	Financial Support
School of Aerospace, Transport and Manufacturing	Financial Support, Technical Support
CranSEDS	Financial Support
Cranfield University Test Facility	Technical Support

The team is actively looking for sponsors to aid the team in refining our project design and, with time, develop the project team to take up the task of building Cranfield University's 1st Student team-built Hybrid and Liquid Engine. The funding and current budget of the project has been tabulated below. The table indicates the overview of the budget allocation between various sub-systems and the overall estimated cost of the project at this stage. A general margin of 20 percent has been used for sub-systems and as an overhead cost.

Chapter 2

Project Management

2.1 Assigned Roles and Team Roster

2.2 Team roles and Responsibilities

The team has been sub-divided into 5 sub-systems which work in concordance with each other to develop their sub-system to an optimal level while ensuring proper integration between every sub-system to yield an efficient system of a working Hybrid Engine. The members of the team and their respective roles have been attached herewith.

Table 2.1: Team members and their roles

Name	Role	Email ID	Course
Triyan Pal Arora	Project Manager; Technical Lead	triyanol.arora.225@cranfield.ac.uk	ASE
Sanmukh Khadtare	Emeritus Project Manager	sanmukhskhadtare@gmail.com	ASE
Yi Qiang Ji Zhang	Systems Lead	yiqiang.jizhang.444@cranfield.ac.uk	ASE
Corentin Julie	Controls Lead	corentin.julie.655@cranfield.ac.uk	ASE
Peter Kirman	Manufacturing Lead	peter.kirman.810@cranfield.ac.uk	ASE
Emeric Tenailleau	Propulsion Lead	emeric.tenailleau.389@cranfield.ac.uk	ASE
Eeshaan Kamath	Structures Lead	eeshaan.kamath.810@cranfield.ac.uk	ASE
Augustin Pedo	CFD Lead	augustin.pedo.381@cranfield.ac.uk	AD'

* ASE: Astronautics and Space Engineering;

' AD: Aerospace Dynamics.

The team has been working under Professor Adam Baker as the main supervisor for the project, who has been crucial in the design and operation of the project. For the Work Package Distribution, the team attempted to classify the work without any major inter-dependency; however, overlaps between the works packages can't be avoided, and the team took it as an affirmation of the collaborative work the members need to put in for the system as a whole.

2.3 Stakeholder Map

The stakeholders are anyone internally or externally involved with the organisation and project and have an impact based on the project's output. As a crucial exercise to start any project, it is a good practice to envision them, to realise the areas in which they can be categorised and their interest in the project. Being reminded of them through the project can help raise a positive outcome and identify any negative impact early on. The stakeholder classification has been highlighted in figure 2.1.

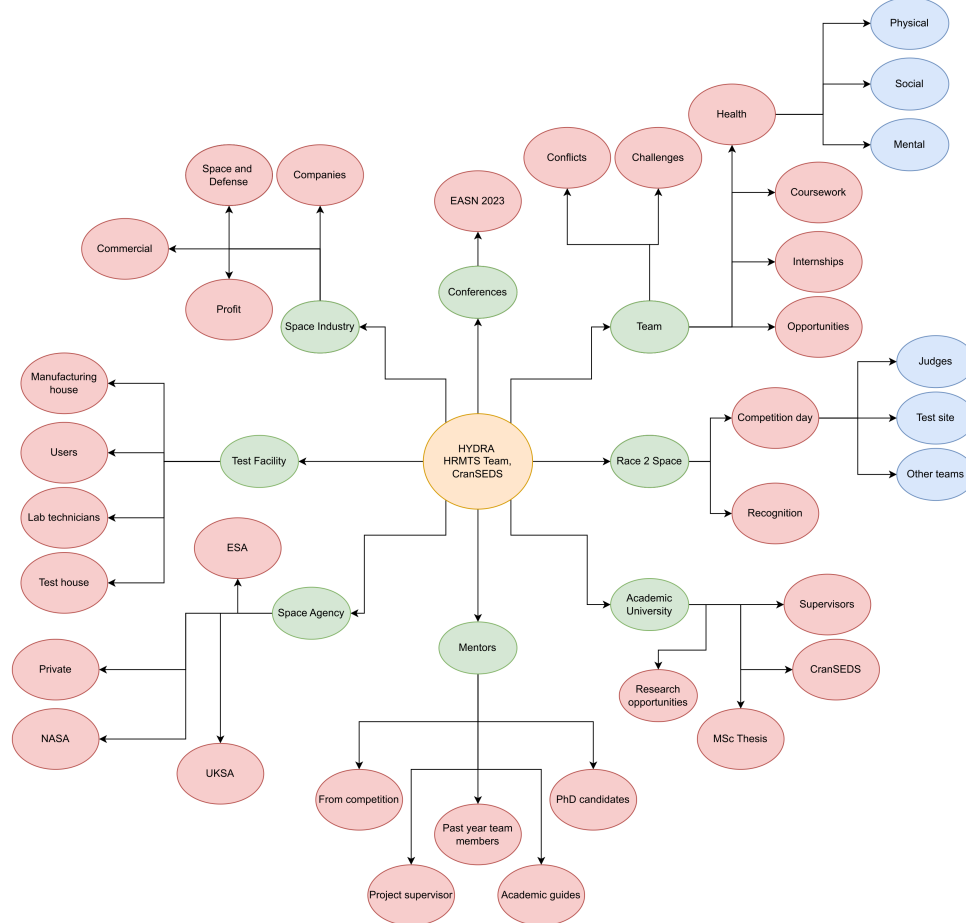


Figure 2.1: Stakeholders Map. Source: Own.

2.4 Work Package Breakdown Structure

The **Work Breakdown Structure** (WBS) is a visual, hierarchical and deliverable-oriented deconstruction of a project. This tool arranges and breaks down the project scope by displaying all deliverables into work packages. By doing this, it is easier to track and monitor the tasks that each subsystem is performing. It also assists in scheduling and keeping track of the schedule done in the Gantt Chart [11.10](#). The work breakdown overview for the team is shown in [2.2](#). A **stakeholders map** is also detailed in [2.3](#).

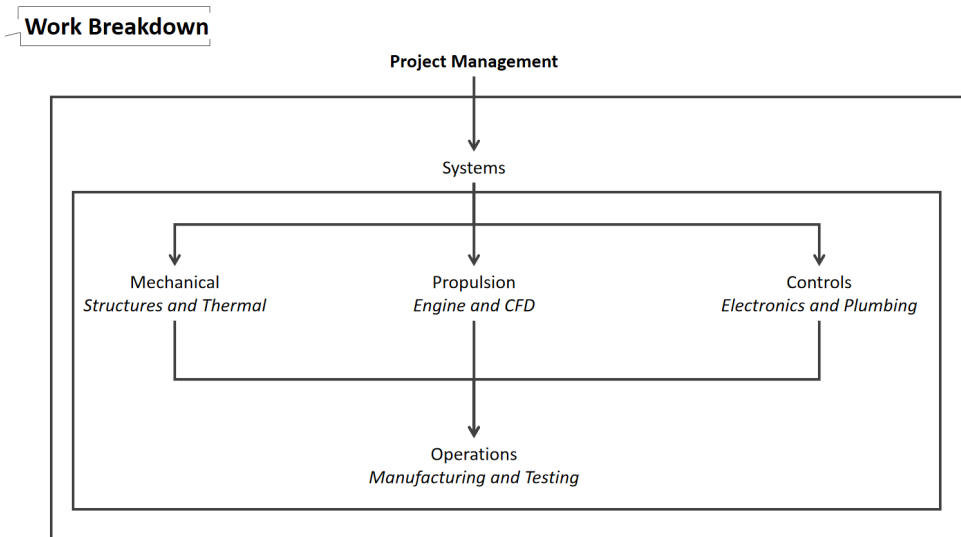


Figure 2.2: Project Work Breakdown Overview. Source: Own.

2.5 Preliminary Budget

The current status of the cost budget is shown in [2.2](#) below. This depicts the total cost for component and material procurement, manufacturing and covering staff costs for each sub-system.

Table 2.2: Cost Budget and Acquisitions

Subsystem	Net Cost (£)	Acquired (£)	To be raised (£)
Propulsion	154.30	154.30	0
Structures	1471.54	1471.54	0
Manufacturing and Supervision	4580.0	4474.65	105.35
Feed Line System	724.26	674.16	50.1
Data Acquisition System	10	10	10
Sponsorships	2500	2300	200

Appendix [11.7.1](#) shows a more detailed breakdown of the parts included in the total above.

2.6 Project Risks, COSHH and Mitigations

At the start of the project and through its duration before firing, risks were identified by each sub-system and for the whole system. These risks were accompanied by a separate COSHH assessment for the propellants. Several strategies were implemented to reduce their likelihood of occurrence. These have since been closely monitored, and an updated status table has been presented in Appendix [11.9](#).

2.7 Project Plan

The use of a **Gantt chart** here facilitates the preliminary scheduling for the entire project. This tool depicts a graphical representation of activities and deliverables against time. It is a simple and efficient way of overseeing the status of the project. While it may seem like a big chunk of project work time, this was also put in place to allow for a buffer in case more work of assembly, integration and testing was required. The **full Gantt chart** elaborated for this project is depicted in Appendix [11.10](#).

2.8 Team Management

Weekly meetings were held for the whole team for general updates and discussions, in which the designs were finalised and the project plan was updated. Microsoft Teams continued to be used to track time spent and store all data.

The workload and timings of the student courses meant that some of these meetings between teams could not be held, and this placed stress on completing team deadlines. **Work meetings** of more than 2 hours were added to the weekly schedule to dedicate time to the tasks and ensure they were achieved. The benefit of this meant communication to make design choices between sub-systems could be done quickly in person, saving time and building team rapport.

As the project continued, some members chose to leave due to other commitments. Because of this, WP tasks were reallocated and shared by the rest of the team. The team was encouraged to engage with the Race to Space and their assigned mentors.

Chapter 3

Requirements

The top-level requirements set out by the team for the project are as shown below. From these requirements, all sub-systems derived their requirements and designed the system to satisfy all the sub-system and top-level requirements while keeping the design simple and easy to manufacture, assemble and test.

Table 3.1: Top-Level Requirements for the Project (HY-1XXX)

ID	Parameter	Requirements	Traceability
HY-1001	Thrust	The Engine shall be designed to deliver a thrust of 300 N	
HY-1002	Burn Time	The burn time shall be greater than 5 seconds	
HY-1003	Propellants	The liquid propellants used shall be Nitrous Oxide or IPA	AEL-J1 Nitrous Oxide Test-Rig ICD
HY-1004	Ignition System	The engine shall be ignited using an external fuse wire to create sparks in the combustion chamber	
HY-1005	Mass flow rate	The mass flow rate of propellants shall be lower than 2.3 kg/sec (Nitrous Oxide), 0.5 kg/sec (IPA)	AEL-J1 Nitrous Oxide Test-Rig ICD
HY-1006	Feed Pressure	The feed line shall be able to hold pressures up to 80 bars.	AEL-J1 Nitrous Oxide Test-Rig ICD
HY-1007	Chamber Pressure	The chamber pressure for the complete fire sequence shall be lower than 51 bars (Nitrous Oxide Vapor Pressure)	
HY-1008	Mounting bracket	The mounting bracket shall provide support in all 3 axes from the experienced loads	

Sub-system-specific requirements can be found in Appendix 11.1. Those requirements are derived from these top-level requirements.

Chapter 4

Propellants

A combination of solid fuel and liquid oxidiser was selected as the propellants for the hybrid engine, as it provides a safe alternative during manufacturing. The fuel and oxidiser themselves only react and combust when at high temperatures, which makes it an ideal configuration to be applied by the student team for a small scaled hybrid engine project and work on its research aspects.

This section comprises of the propellant selection for the liquid oxidizer, solid fuel.

The purging gas selected for the engine is Nitrogen gas, and the pre-charge will be performed using liquid oxygen gas at low pressures, providing an oxygen-rich environment inside the combustion chamber.

4.1 Liquid Oxidiser

The liquid oxidiser is required to be non-reactive. However, it shall only react with the solid fuel at high temperatures ensuring safety during the assembling and setup phase. The propellant used shall be a standard propellant issued to be used by the university, testing facility and international standards. These requirements with other parameters will be used to trade off the alternatives for the final selection. The selected alternatives are Nitrous oxide (N_2O), Isopropyl Alcohol (IPA) and liquid Oxygen (LOx).

The trade study performed is summarized in the table 4.2. While the rubrics used for preparing the trade-off table have been presented in table 4.1.

Table 4.1: Assembly and Equipment level requirements Source: Own.

Requirement ID	Statement
Number	Description
Weighting Rubric	
1	Low priority
2	Medium priority
3	High priority
Scoring Rubric	
1	<20 % of the desired value
2	20-40 % of desired value
3	40-60 % of desired value
4	60-80 % of desired value
5	80-100 % of desired value

NOTE: Desired value can be maximum achievable or minimum achievable or according to a set standard.

Table 4.2: Liquid Oxidiser propellant selection trade study

Alternative	Availability	Simplicity	Reactivity	Oxidising potential	Stability	Compatibility with the fuel	Vapour Pressure	Temperature sensitivity	Safety	Feasibility	Total (110)
Weights	2	1	3	2	2	3	3	1	3	2	
N_2O	4	4	4	5	3	5	5	2	5	4	95
LOx	3	5	5	4	2	5	2	1	2	3	72
IPA	5	4	2	3	5	5	3	5	4	5	87

So the final selection for the liquid oxidiser for the hybrid engine is **nitrous oxide (N_2O)**.

The N_2O will be kept in a liquid state for the combustion to have a better performance. The average mixture ratio O/F is fixed at 7.6. This value was determined via calculations from the software RPA (Rocket Propulsion Analysis) at a nominal pressure in the combustion chamber of 3.35 MPa as shown in Appendix 11.4.

The oxidiser volume used is 1.1L, resulting in 0.905kg of N_2O at 15°C and with the chosen O/F, a fuel mass of 0.119kg is used. The average regression rate is 0.7 mm/s, the average oxidizer flux is $273.7 \text{ kg m}^{-2} \text{ s}$ (kept below $350 \text{ kg m}^{-2} \text{ s}$ to prevent blow-out). The numbers were obtained assuming frozen flow and neglecting the vapour phase.

4.2 Solid Fuel

The solid fuel that needs to be selected for the hybrid engine shall be readily available, easily manufacturable, non-reactive in the atmosphere, shall not have explosive properties when reacting with the liquid oxidizer, and shall be feasible to procure. These parameters, along with the requirement on the engine performance of sustaining a 300 N producing engine for more than 5 seconds and the combustion products shall not be harmful, makes it really constricted on the alternatives that can be considered for use as the solid fuel.

In-depth research work was performed by the previous year's team, which has been used as the baseline for the current propellant selection. The general consensus was to select a plastic that can easily be manufactured and will react with nitrous oxide at high temperatures to sustain the combustion of the hybrid engine.

After many discussions and iterations, the final selection for solid fuel was made to be **high density polyethylene (HDPE)**.

The products obtained after the combustion are CO_2 , N_2O , and N_2 . HDPE is readily available, feasible and easily manufacturable. As its main application is in thermosetting plastics, it is non-reactive. However, nitrous oxide is able to corrode and break down the polymer to its constituent monomers and react with the hydrocarbon monomer for successful combustion. This makes it a great choice for the current design.

The thermochemical reaction is presented in detail in the design calculation section 6.6.

Acrylonitrile butadiene (ABS) and polylactic acid (PLA) were also among the top contenders, in lieu of their properties of 3D printing. However, they were unable to satisfy the system requirement of providing a minimum of 300 N thrust. And so, the final selection for the solid fuel is **HDPE**.

Chapter 5

Detailed Design

The current design of the Hybrid Engine has been inspired by the old design of the previous year's team. The design methodology was a small combustion chamber with axial support from the L-shaped engine mount at the back and 2 planar supports positioning the chamber horizontally to the ground. Their baseline design concept has been carried over to this year, with modifications made at the interfaces of components, new requirements and manufacturing constraints, a new feed line system and the implementation of a data acquisition system. The requirements on propellants used are that they shall comply with safety standards in place at the university's test facility and shall be available during the race to space competition. So, liquid nitrous oxide (N_2O) is used as the oxidiser, and HDPE (high density Polyethylene) is used as the fuel, which will be cast into the desired shape with one circular port. The target firing time is over 5 seconds, and the expected peak thrust output is 300 N. For the ignition process, the chamber will be pre-charged with liquid oxygen (LOx) at low pressures, followed by spark ignition, which will be achieved remotely by igniting a fuse which enters the combustion chamber through the nozzle. Gaseous nitrogen (N_2) will be used to purge the system after each firing. The feeding system incorporates multiple safety features, such as valve isolation between the tanks and the chamber.

The final design of the Hybrid Engine on the ICD Bench is shown in figure 5.1. The engineering drawings for the component parts have been attached in Appendix 11.2.

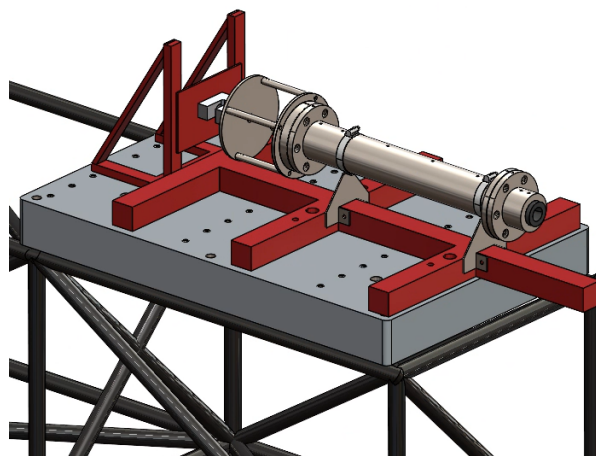


Figure 5.1: Hybrid Engine Assembly on the ICD Bench. Source: Own.

5.1 Engine Design

The drawings of the hybrid motor combustion chamber and its components are attached in appendix [11.2](#).

The section view of the combustion chamber with components is shown in figure [5.2](#). It comprises of an injector plate with 6 injector holes of 1 mm for propellant atomization. It is followed by the combustion casing locked in on both edges with welded flange and an inner layering of the engine cork liner. Following is the Graphite nozzle inside the nozzle casing with a welded flange over it to hold it within the combustion chamber casing environment.

The material used for the components is generally heat-treated Mild Steel. Further discussion on the material selection can be found in the section [5.5](#).

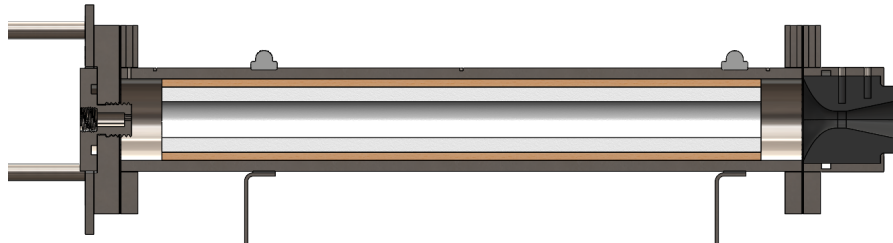


Figure 5.2: Engine Chamber Cross Sectional View. Source: Own.

To calculate the hoop stress in a chamber (thin wall pressure vessel), the following equation is used:

$$\sigma_\theta = \frac{P \cdot D_m}{2 \cdot t} \quad (5.1)$$

The calculations for the thin wall stress, along with the description for the math used, have been shown in the section [6.10](#).

5.1.1 Fuel Grain and Combustion Casing Geometry

As a circular bore produces a progressive-regressive thrust curve, it is the chosen geometry for the fuel grain. For initial trials, a circular bore is selected for simple geometry and easy production. The team needs to discuss with the manufacturer the perspective of different cross-sectional configurations for the solid fuel grain, such as star shape, annular shape, and others, as they provide better performance and consistent burn rate [\[2\]](#) [\[3\]](#). To keep the initial testing straightforward, a circular bored configuration is selected, as shown in figure [5.3](#). The fuel grain and steel combustion chamber casing are separated by a 5 mm thick layer of insulation made out of off-shelf cork. Further assembly is discussed in Chapter [9](#)

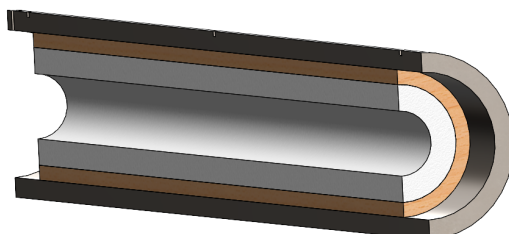


Figure 5.3: Fuel Grain geometry inside the combustion chamber. Source: Own.

The interface holding the combustion chamber over the test stand is held by 2 ring clamp systems, which are in turn mounted on Steel plates attached and fixed to the Test Stand. The design of the ring

clamp system is depicted in figure 5.25. To assess the deformation and maximum stress associated with this holding configuration, and other components of structures, a detailed FEA was performed for all components.

The combustion casing has been evaluated for structural performance through Finite Element Analysis (FEA). The resulting deformation and induced stress are indicated in figure 5.4. The analysis result showcases the maximum stress in the worst-case scenario of maximum thrust, with the worst temperature and vibrations modelled in the software.

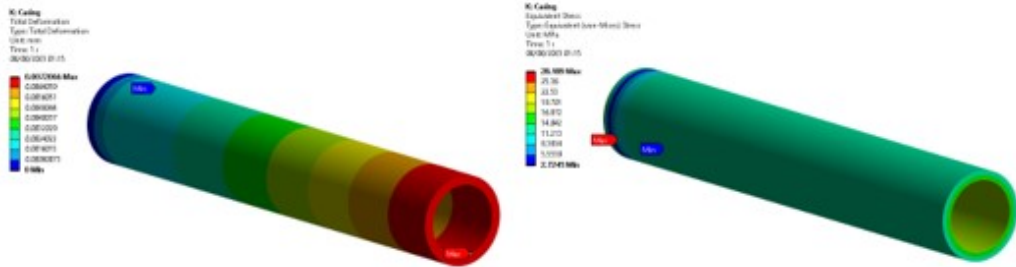


Figure 5.4: FEA results of combustion chamber steel casing: Deformation: $7 \mu\text{m}$ (left); Max. Stress: 28.2 MPa (FOS: 8.86) (right). Source: Own.

5.2 Propulsion Design

This section describes the design of the propulsion system of the motor. All the tasks performed are presented in the sections: Motor Sizing, Injector, Nozzle Design, Ignition Mechanism and Thrust Adapter.

5.2.1 Motor Sizing

The chosen propellants are Nitrous Oxide (N_2O) (liquid oxidiser) and HDPE (solid), based on safety, accessibility, data available and budget. The N_2O will be stored in a liquid state for the combustion to have a better performance. The final O/F ratio is initialized at a fixed value of 7.6.

The software ProPEP3 and RPA were used to simulate and obtain the basic properties of the motor, such as the temperature at the throat (nozzle section), the specific impulse, isentropic exponent, characteristic velocity and performance. The results have been summed up in table 5.1, while the direct outputs obtained have been attached in the Appendix 11.4.

The initialisation inputs given to the software were:

- Temperature of ingredient of 298 K (ambient condition)
- Chamber pressure of 3.35 MPa
- Exhaust pressure of 0.1013 MPa (1 bar: ambient condition)
- The mass of propellant used – Nitrous Oxide: 905.3 grams, and HDPE: 119.1 grams.

Taking into account the final burning rate of 1.84 mm/s and mass flux of 270 kg.s⁻¹.m⁻², the following table was tabulated, showing the final sizing results from the software simulations.

The calculations for the values obtained and used as input have been detailed in Chapter 6.

Note: Numbers were obtained assuming frozen flow and neglecting the vapour phase.

Table 5.1: Sizing results from parameters from ProPEP simulation

Initial Conditions	Value	Units
Burn time	6.26	s
Oxidiser to fuel ratio	7.6	
Thrust	300	N
Chamber pressure	3.35	MPa
Exit pressure	0.1013	MPa
Specific impulse	203.49	m s^{-1}
Thrust coefficient	1.185	
Total mass flow rate	0.164	kg s^{-1}
Fuel density	935	kg s^{-1}
Regression rate	$1.84 \cdot 10^{-3}$	m s^{-1}
Initial steps for the sizing		
Throat area	$7.55 \cdot 10^{-5}$	m^2
Throat diameter	$9.81 \cdot 10^{-3}$	m
Exit Mach number	3.92	
Expansion ratio	5.18	
Exit area	$3.91 \cdot 10^{-4}$	m^2
Exit diameter	$2.23 \cdot 10^{-2}$	m
Mass Data		
Fuel mass flow rate	0.019	kg s^{-1}
Oxidiser mass flow rate	0.144	kg s^{-1}
Fuel mass	0.119	kg
Total mass flux	306.713	$\text{kg s}^{-1}\text{m}^{-2}$
Sizing		
Initial Port Area	$2.10 \cdot 10^{-2}$	m^2
Port diameter	$2.56 \cdot 10^{-2}$	m
Fuel grain length	0.35	m
Final Port diameter Chamber	$3.03 \cdot 10^{-2}$	m
Post-Comb. Chamber length	$2.4 \cdot 10^{-2}$	m
Pre-Comb. Chamber length	$2.4 \cdot 10^{-2}$	m
From Simulations		
Characteristic velocity, C^*	5343.622	m s^{-1}
Chamber Cp/Cv	1.245	
Stabilized chamber temperature	3337.053	K

5.2.2 Injector

The main purpose of the injector is to inject and atomize the oxidiser flow into the combustion chamber. The amount of oxidiser flow required is the one that allows the O/F ratio of 7.6 to be maintained. The injector shall be able to create a shower of small droplets of liquid oxidizer, which would be vaporised into the combustion chamber and, with its high flow pressure, be able to erode the fuel grain and combust.

The final design of the injector is depicted in figure 5.5

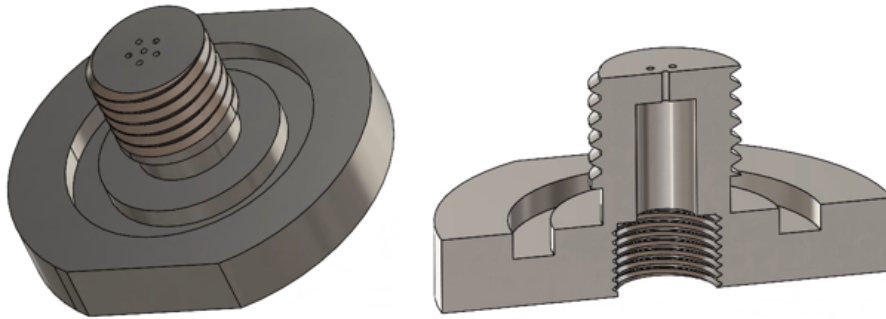


Figure 5.5: Designed Injector: Isometric View (left), Cross-Sectional View (right). Source: Own.

The main inputs to determine the design of the injectors are the properties of the oxidiser at the inlet of the injector (equal to the properties at the outlet of the feeding system), the pressure in the combustion chamber, and the mass flow of the oxidiser. And the outputs will be the number of holes and the diameter necessary to satisfy the requirements.

For simplicity's sake, the design of the injector follows a **showerhead axial injector** style. That means that the injector is a plate with several holes, all of them with the same diameter and drilled axially to the plate.

The diameter of each hole is set as 1 mm. This value is in accordance with the general rule to avoid diameters higher than 1.5 mm [4] while keeping a realistic view of its manufacturing.

The input values are shown in Table 5.2

Table 5.2: Input values to determine the number of holes on the injector plate.

Parameters	Values
Oxidiser mass flow rate	0.164 kg/s
Injector hole diameter	1.0 mm
Oxidiser density	822.2 kg/m ³

It is necessary to determine both the pressure drop across the injector and the discharge coefficient (C_d). The pressure drop can be regulated/adjusted by the feeding system reducing the pressure from its maximum value. As the discharge coefficient depends on the operational conditions and the quality of the manufactured holes, this value only can be estimated until the injector is physically tested. For the current case, it has been estimated to be 0.8. The values of the discharge coefficient follow the indications seen in [5].

It is observed that for a wide range of C_d values and pressure drops, the optimal number of holes is 6: 1 hole in the centre, while the other 5 holes are radially concentric to the centre in a PCD of 5 mm. The complete calculations have been developed and described in the next chapter's section 6.8.

The injector plate has been evaluated for structural performance through Finite Element Analysis (FEA). The resulting deformation and induced stress are indicated in figure 5.6. The analysis result showcases the maximum stress in the worst-case scenario of maximum thrust, with the worst temperature and vibrations modelled in the software.

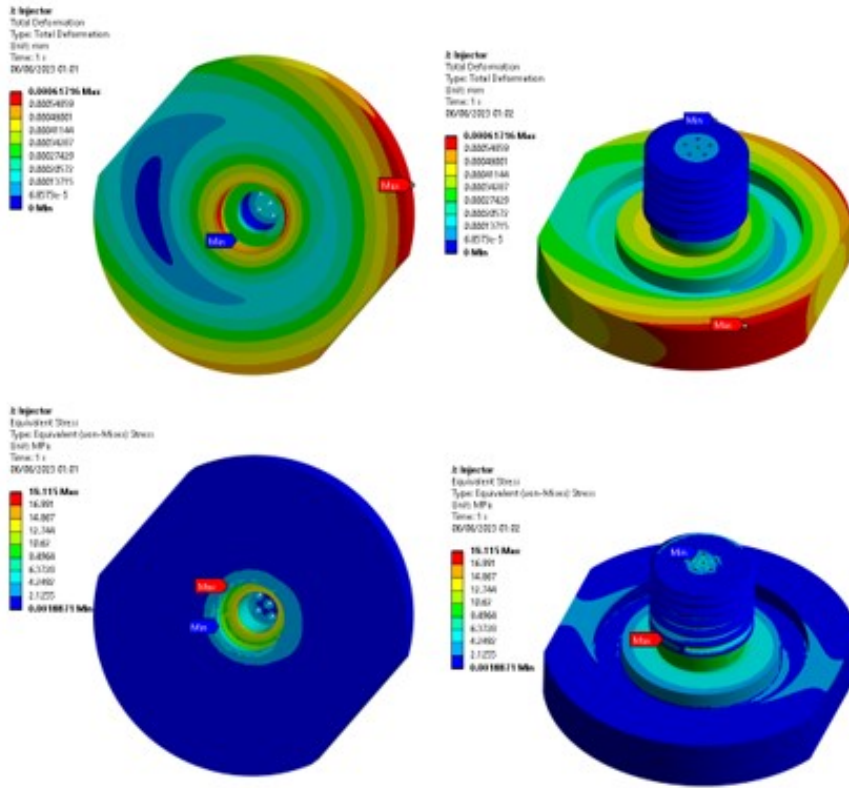


Figure 5.6: FEA results of injector plate of mild steel: Deformation: $0.6 \mu\text{m}$ (left); Max. Stress: 19.1 MPa (FOS: 13.1) (right). Source: Own.

A similar analysis was performed on the injector flange that holds the injector plate and makes up the injector sub-assembly. The results have been displayed in figure 5.7.

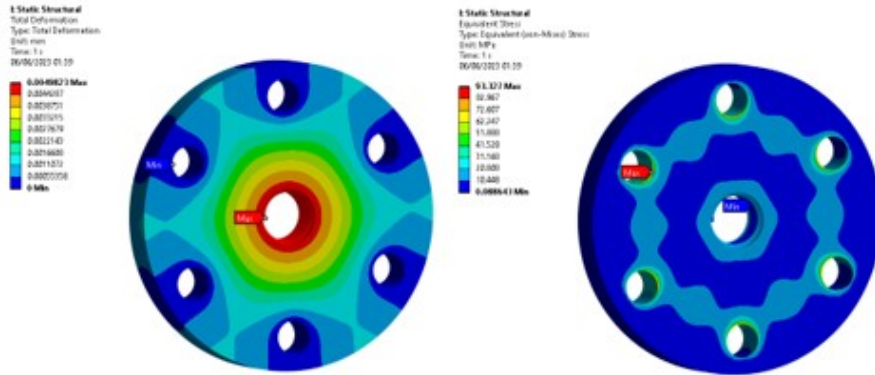


Figure 5.7: FEA results of injector flange of mild steel: Deformation: $4.9 \mu\text{m}$ (left); Max. Stress: 93.3 MPa (FOS: 2.7) (right). Source: Own.

5.2.3 Nozzle Design

This section outlines the design of the converging-diverging bell nozzle with a conical diverging section. The area ratio selected between the throat and the exit is 3.7. Based on the calculations shown in the section 6.5, the design for the nozzle was prepared, and the final design is depicted in figure 5.8.

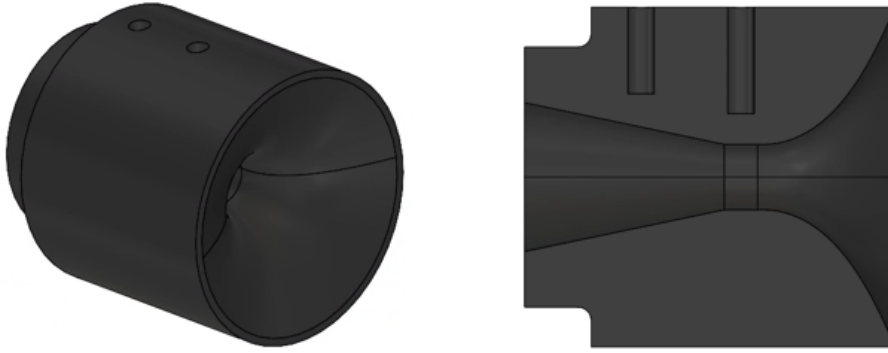


Figure 5.8: Graphite Nozzle Design: Isometric View (left), Cross-Sectional View (right; Short high curve edge is the convergent part facing the combustion chamber). Source: Own.

Note: The 2 holes in the cross-section view indicate the location for putting in the thermocouples.

The performance of graphite nozzles greatly increases with less oxidation (controlled manually). Graphite has moderate resistance to cracks generated due to thermal stresses. Fibre-reinforced plastic nozzles show less erosion but are costly to manufacture [1]. The datasheet for the graphite material used has been attached in appendix 11.3.1.

The conical nozzle is the oldest and perhaps the simplest configuration. It is relatively easy to fabricate and most suitable for small nozzles due to its simplicity. The half cone angle is taken at 15° with exit radius and throat radius calculated using isentropic relations.

Using the equation:

$$L_{cone} = \frac{r_2 - r_1}{\tan\alpha} \quad (5.2)$$

The Length of the cone is calculated to be **24.32 mm**.

The graphite nozzle and the nozzle casing have been evaluated for structural performance through Finite Element Analysis (FEA). The resulting deformation and induced stress are indicated in figure 5.9 for the graphite nozzle and in figure 5.10 for the steel nozzle casing. The analysis result showcases the maximum stress in the worst-case scenario of maximum thrust, with the worst temperature and vibrations modelled in the software.

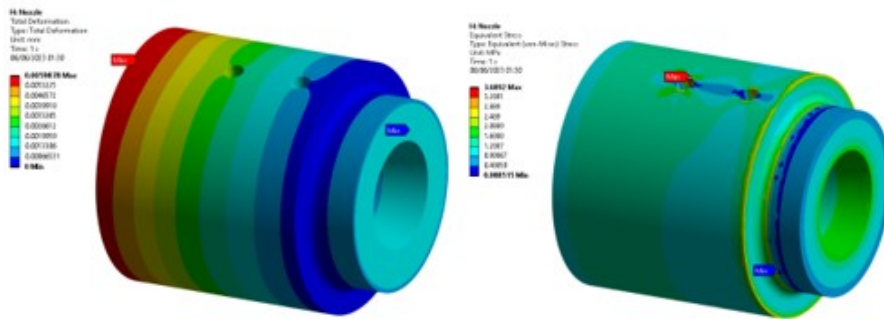


Figure 5.9: FEA results of the graphite bell nozzle: Deformation: $5.9 \mu\text{m}$ (left); Max. Stress: 3.6 MPa (FOS: 16.6) (right). Source: Own.

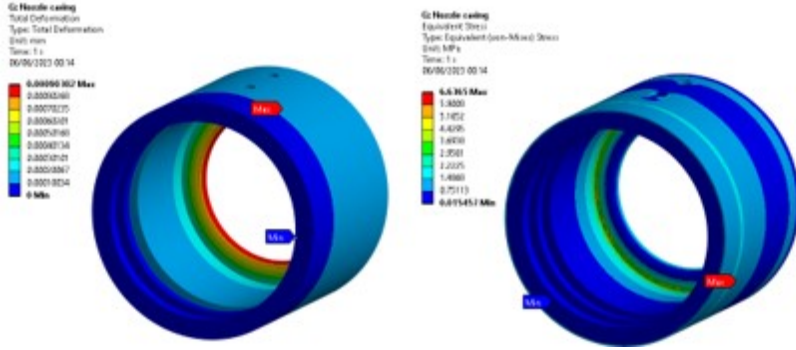


Figure 5.10: FEA results of steel nozzle casing: Deformation: $0.9 \mu\text{m}$ (left); Max. Stress: 6.6 MPa (FOS: 37.8) (right). Source: Own.

5.2.4 Ignition Mechanism

A 15 kV DC High Voltage Arc Ignitor ($\approx 100 \text{ cm}^2$) will be placed close to the nozzle next to the rocket stand. The arc will ignite a long fuse ($\approx 1 \text{ m}$), which will enter via the nozzle exit and go through the nozzle until it reaches the pre-combustor chamber. The fuse will be lighted wirelessly from a safe distance via the arc ignitor using an Arduino circuit. A rough schematic for this system is depicted in figure 5.11 [1].

The spark is assumed to be hot enough to ignite the fuel-air mixture. The fuse shall be able to carry the spark successfully up to the point of ignition. The electric arc generated shall ignite the fuse.

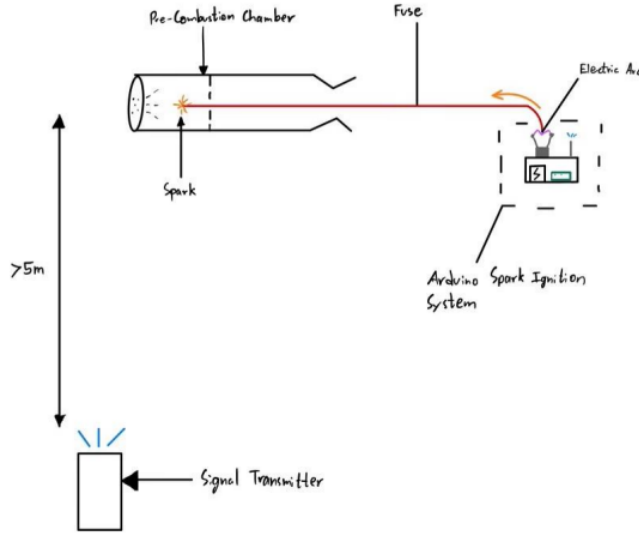


Figure 5.11: Schematic of Ignition System. Source: Own. [1]

5.2.5 Thrust Adapter Assembly

The purpose of the thrust adapter is to transfer the thrust force to the load cell. This adapter is needed to provide a central port for supplying the liquid propellants into the injector plate while still providing axial support and strength. The assembly has 2 end plates, one connected to the chamber flange and the other connected to the load cell. These plates are attached by 4 tie rods. The material for this whole assembly is Mild Steel.

The critical buckling of the struts is given by Euler's Buckling formula: [1]

$$P_{cr} = \frac{\pi^2 \cdot E \cdot I}{L_e^2} \quad (5.3)$$

where L_e is the effective length, equal to half the length of the strut, E is the elastic modulus of steel, and I is the Moment of Inertia.

The cross-sectional moment of inertia for rods with a circular cross-section is given by:

$$I = \frac{\pi \cdot d^4}{64} \quad (5.4)$$

Using this method, the critical buckling load is calculated to be 2337 kN. The maximum load each strut is expected to experience is $1500/5 = 300$ N. Each strut will experience maximum stress of 9.4 MPa. Mild steel with a yield strength of 250 MPa provides a high factor of safety.

The circular plate is directly bolted to the load cell and thus has the highest risk of bending. An appropriate thickness for the plate is determined to be 3 mm by performing structural analyses.

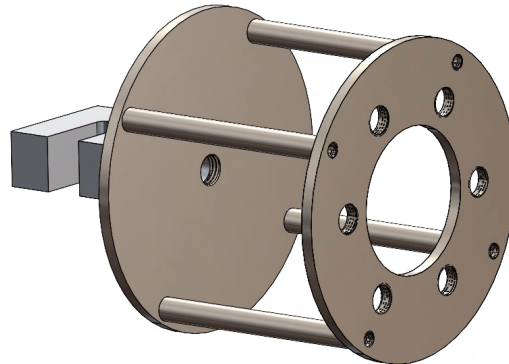


Figure 5.12: Thruster Assembly (The rectangular section in the back is the S-type Load cell). Source: Own.

The thrust assembly and all its constituent parts have been evaluated for structural performance through Finite Element Analysis (FEA). The resulting deformation and induced stress are indicated in figures 5.13, 5.14, and 5.15. The analysis result showcases the maximum stress in the worst-case scenario of maximum thrust, with the worst temperature and vibrations modelled in the software.

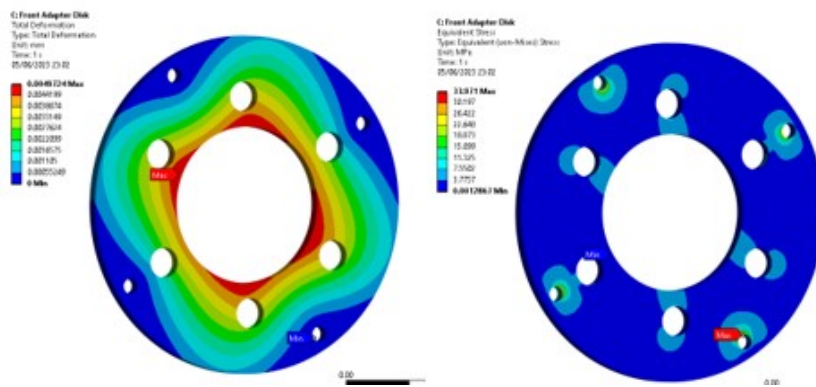


Figure 5.13: FEA results of the thrust adapter's front plate: Deformation: $5 \mu\text{m}$ (left); Max. Stress: 33.9 MPa (FOS: 7.3) (right). Source: Own.

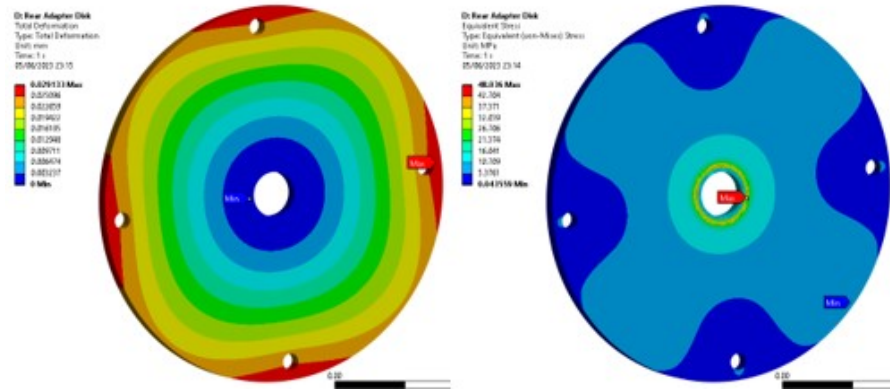


Figure 5.14: FEA results of the thrust adapter's rear plate: Deformation: 0.03 mm (left); Max. Stress: 48.04 MPa (FOS: 5.2) (right). Source: Own.

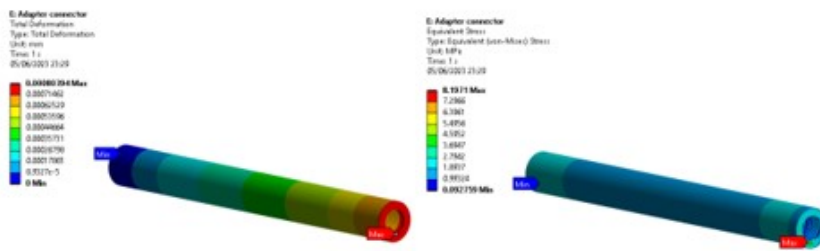


Figure 5.15: FEA results of the thrust adapter's connector: Deformation: 0.8 μm (left); Max. Stress: 8.2 MPa (FOS: 30) (right). Source: Own.

The resulting geometry had a minor fluke during the manufacturing of the rear plate, due to which the central hole was drilled up to 14 mm. This meant the design required employing a bushing, which was 3D printed using ASA (acrylonitrile styrene acrylate) material, with a yield strength of 32.7 MPa. The resulting FEA showcasing its structural integrity through the worst loading case of the test firing is shown in figure 5.16.

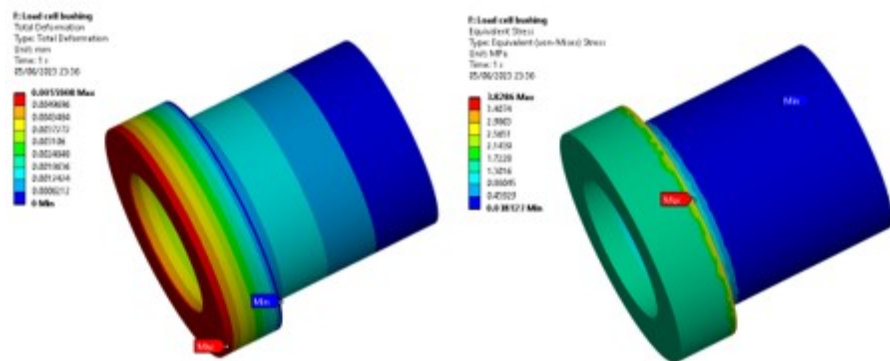


Figure 5.16: FEA results of the thrust adapter's 3D printed bushing (ASA material): Deformation: 5.5 μm (left); Max. Stress: 3.8 MPa (FOS: 8.6) (right). Source: Own.

5.3 Feed System Design

The feed system designed for the hybrid engine is simple in comparison to a Liquid bipropellant engine. There are 3 components for which the feed line system needs to be developed.

For the Hybrid engine, we need only one propellant to be supplied by the feed line, which is Nitrous

Oxide from a pressurized tank to the injector plate of the combustion chamber.

However, in real test firing, Nitrous oxide does not ignite easily at lower temperatures due to its low affinity to break down to its constituent species and release oxygen which will combust the compound. Therefore, a small amount of oxygen is required as a precharge to create an oxygen-rich environment for a fast pace ignition. Once ignited, nitrous oxide at the already high temperature is able to break down to release oxygen and sustain the combustion for its entirety without any more aid from the oxygen source.

For clearing out the feed line and the combustion chamber line before the pre-charge or ignition and after the end of the firing, the system needs to be purged with a non-reactive gas that will flush out any group of particles that haven't been fully combusted and are in the chamber, which may stand as a hazard afterwards. For this purpose, we use Nitrogen gas from a highly pressurized tank. As this purge gas acts as a safety net for the whole system that can flush out the other 2 gases in case of a leak or emergency failure, the pressure for nitrogen is kept the highest.

A schematic for the feed system was prepared by the team and verified by the on-site technicians for the design's viability and safety. This has been depicted in figure 5.17.

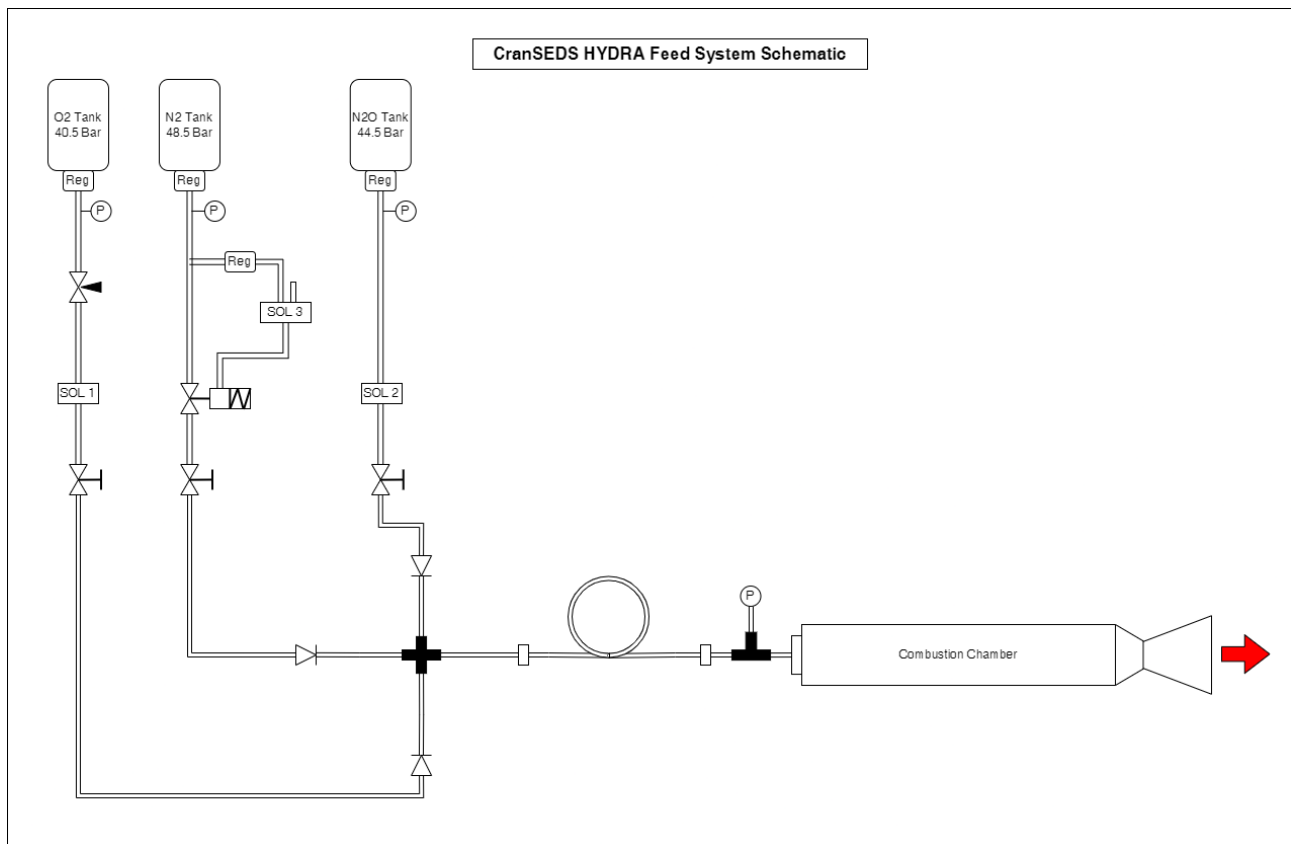


Figure 5.17: Feed System Schematic. Source: Own.

Note: The circular loop represents a bendable pipeline taking all the deformation loads from the chamber firing and saving the metal pipes and other feed components.

- The feed line sub-system consists of 3 lines from the Nitrous oxide tank, Nitrogen tank and Oxygen tank.
- As to fulfil the need for a flame restrictor on the nitrous oxide line, the design was updated after talks with BOC Ltd. (British-based multinational industrial gas company) and the university technicians to incorporate a separate run tank between the main nitrous oxide tank and the combustion chamber.

- So, the main nitrous oxide tank is regulated to let about 1.2 litres in the run tank. This connection is manual and performed before commencing the test firing.
- This run tank is directly connected to the combustion chamber using pressure actuated valve, which is triggered by a separate line of nitrogen gas with a solenoid valve to trigger the pressure-actuated valve. The valve on this line is normally closed.
- A similar configuration is used for the Nitrogen purge line as well. The pressure-actuated valve is triggered by flowing nitrogen gas through it. This valve is normally open to purge the whole system in case anything goes sideways and the power supply is cut off.
- The oxygen line is at low pressure, just for recharging, and hence incorporates only a normally closed solenoid valve.
- The nitrous oxide tank, run tank, and oxygen tank also have a burst valve for safety reasons.
- The 3 gas lines merge onto a 4-way connector, feeding into the combustion chamber through the outside of the injector plate. The connection has been designed according to the specifications given in the ICD document ([6]) by the Race to Space competition.

5.3.1 Valves

As can be observed from the schematic shown above, each feed line has 3 separate valve configurations, that is,

- **Manual stop valves** to control the flow of the pressurant inside the feed line (Note that this valve is separate from the regulator used just after the tank).
- **Solenoid valves**, which will be actuated using the control system from the control room to regulate and initiate the chemical flow when required.
Note that the solenoid valve used for Nitrogen gas is Normally open configuration, while the other 2 are Normally closed configuration. This ensures in the case of electrical failure; the valves will close off the Oxygen and Nitrous oxide while purging the whole system with Nitrogen gas.
- **Non-return valves**, as the pressure flow of Nitrogen is higher than the other 2, we need to avoid any backflow in the feed lines, and all the component gases flow into the combustion chamber.
- Nitrogen being at very high pressure is sought out to be employed using 2 feed valves, one of which is a **3-way solenoid valve**, and the other is a **2-way solenoid valve**. This valve configuration reduces the load on a single valve and strengthens the system from any imminent failure.
- As for the feed lines, the team made a design choice for using a 3/8 inch steel pipe, which can be employed for highly pressured liquids which will be used in the coming years by the team. And they provide ample performance for the current design case.
- The feed system needs to be validated by a physical leak test, which is planned to be performed before the competition. Further details regarding the same can be found in the Manufacturing section.

5.3.2 Controls and DAQ Electronics

The controls encompass the electronic circuit inside a control box, controlling the feed line sub-system to perform the hot fire testing, and the data acquisition system on-board the test stand.

The control box is sub-divided into 2 separate circuits, controlled using a toggle switch. The 1st switch activates manual control, where all the control inputs for the feed system, including oxidiser feed, purging, pre-charge, ignition and run-through, are performed annually by the personnel from the control room. The 2nd switch initiates a circuit which automates the complete fire sequence. And this circuit uses an Arduino board which will be used to control the sensors and actuators remotely from a safe distance of the control room, monitor the pressure in the oxidiser tank and combustion chamber, measure thrust output via load cells in the thrust adapter and provide data used for validation of the CFD simulations. The control box circuit is described in figures 5.18 and 5.19, while the integration is discussed in the engine setup chapter 9.

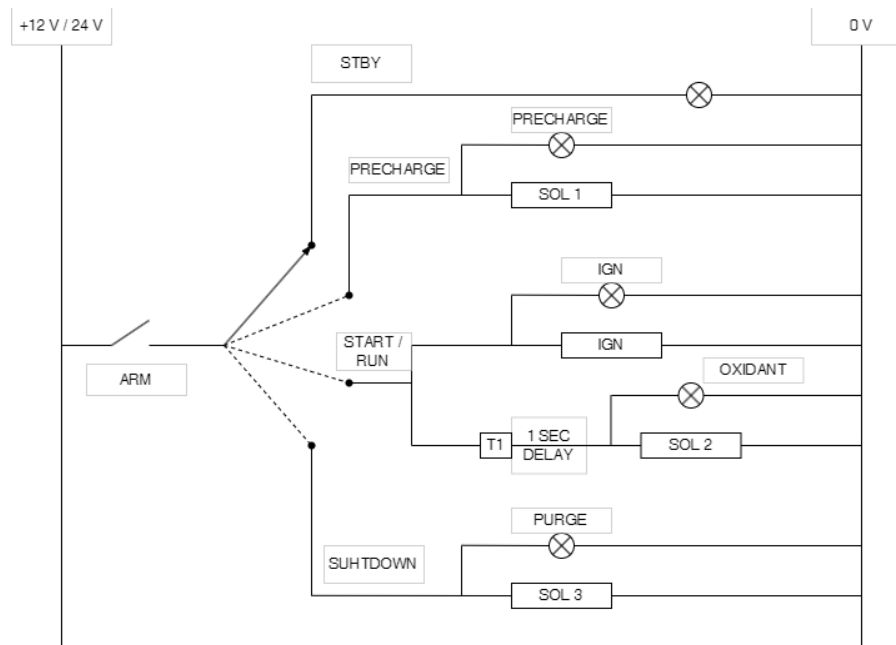


Figure 5.18: Control Box setup schematic. Source: Own.

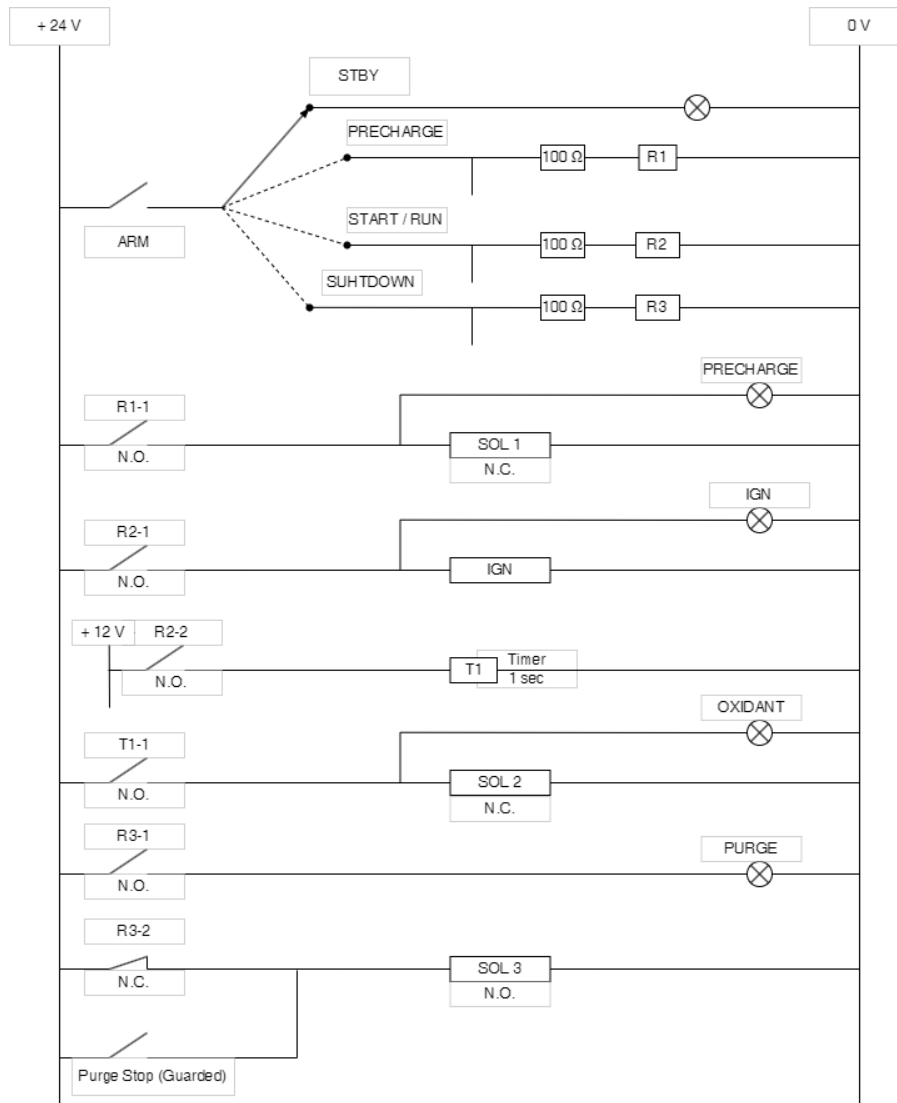


Figure 5.19: Control Box setup schematic. Source: Own.

The Data acquisition system consists of the sensors employed over the engine test stand to measure the performance and characteristics of the test firing. The sensors used, and the parameter measured within this sub-system are:

- Engine Thrust: S block Load cell
- Internal combustion chamber pressure: Pressure transducer
- Fuel line pressure: Pressure transducer
- Temperature of the nozzle and combustion chamber casing: K-type thermocouple

There are 3 thermocouples on the casing and 2 on the nozzle, which sits in a groove which is not through. That means the internal environment of the system is preserved, and the readings of the thermocouples are the measurement of internal temperature after conduction through the steel casing and graphite nozzle, respectively. The depth of their placements on the setup is shown in figure 5.20.

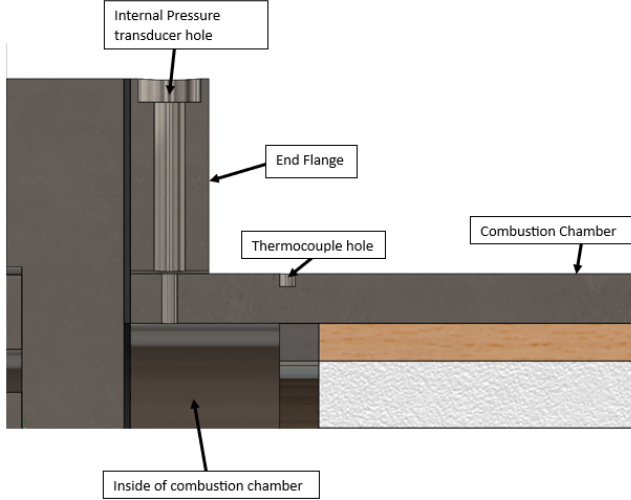


Figure 5.20: Sensor placement on the combustion chamber. Source: Own.

The thermocouples have their independent readers, which will be used for the testing. The thermocouples draw power from the LiPo battery.

The pressure transducer used to measure the feed line pressure is directly connected to the line using a tee connector, which is then passed through the injector inside the combustion chamber.

While the pressure transducer for measuring the internal combustion chamber pressure is mounted on top of the end flange on the combustion chamber next to the injector flange, the initial design was supposed to have it mounted on the casing. However, due to the small clearance between the welded connector and the welded end flange, the design was updated to incorporate the adapter on top of the flange, which covers a through hole going inside the combustion chamber. This hole will help in measuring the internal chamber pressure throughout the firing, depicted in figure 5.20.

The pressure transducers have independent connections with their readers and draw power from the AC voltage regulator.

The load cell measures the thrust produced during the firing. The S block load cell used is Tedea Huntleigh 615, with a capacity of 100 kg measurement. However, the readings obtained in terms of mV are very small, which cannot be read by Arduino. For that, a load cell amplifier needs to be used. It was decided to use HX711, as it is the most reliable, most commonly used, and industrially acceptable amplifier for load cells. This helps the Arduino board to read the signals and plot the thrust graph for the firing.

The Arduino board, load cell circuit, and thermocouples draw power from the LiPo battery. Based on the power budget (Appendix 11.7.3), the battery to be used was selected as an 11.1 V 1500 mAh LiPo battery. However, the Arduino operates at 5 V, which requires a step-down voltage converter to be placed between the battery and the Arduino Uno. LM 2596 was selected to be used as the step-down converter, owing to the previous experience of using it and its performance. The complete data acquisition circuit is presented in figure 5.21. The code for the load cell Arduino circuit is attached in appendix 11.6.

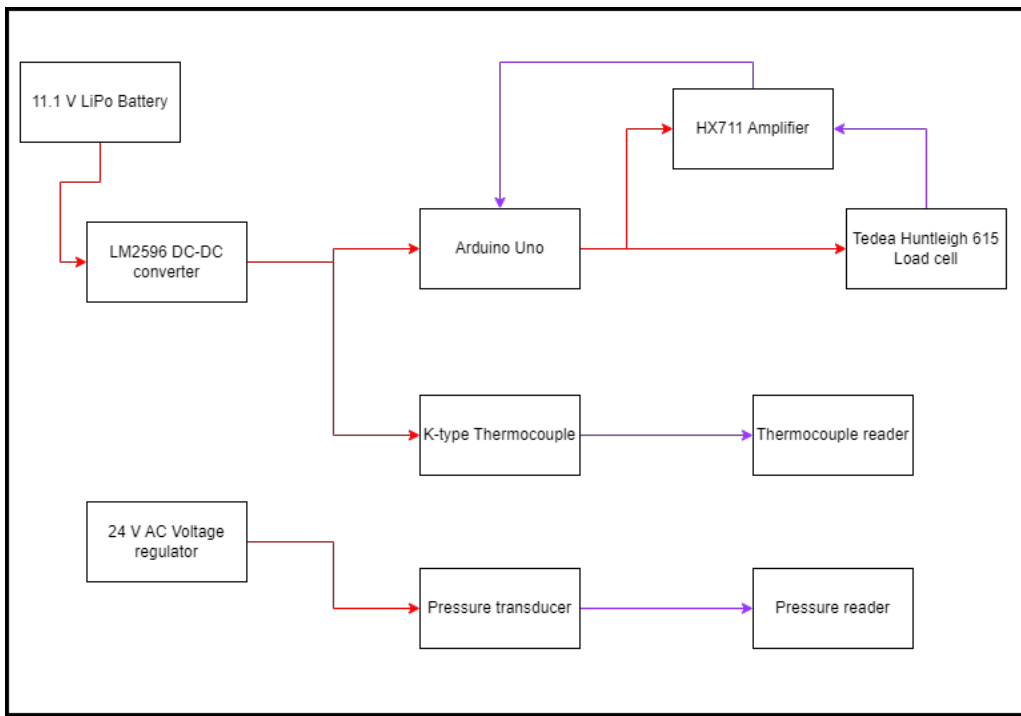


Figure 5.21: Data acquisition sub-system circuit schematic diagram. Source: Own.

An image of the load cell DAQ setup is shown in chapter 8, in figure 8.9.

5.4 Engine Mount

5.4.1 Test Stand

The objective of the Engine mount is to provide support and fixture capability to the main combustion chamber and carry the loads transmitted from the engine firing without any failure-causing deformation. The final design for the engine mount has been shown in figure 5.22.

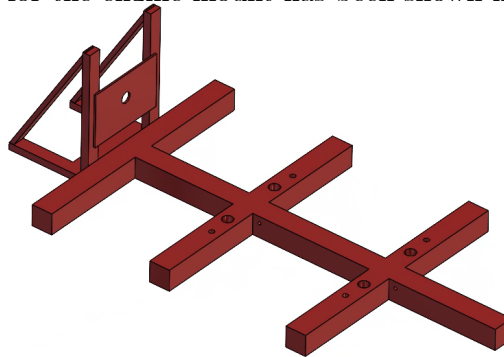


Figure 5.22: Test Stand. Source: Own.

For this, the design began with an L-shape configuration, where a thrust assembly provides axial support to the combustion chamber and carries the transmitted loads from the firing to the structure mount.

While the lower end, horizontal to the ground, ran across the length of the combustion chamber and provided mounting points for support plates, on which the chamber rests and attains a horizontal alignment with the bench.

From these interface criteria, the mount needs to connect to the steel bench as described in the ICD document ([6]). This has been depicted in figure 5.23. The loads transmitted from the chamber firing and due to gravity are to be carried by the Engine mount and passed on to the Test house bench provided by the competition. According to the ICD, the connection will be accomplished using M10 bolts with standard pitch. Therefore, the Engine mount has been designed with boreholes of 10 mm diameter. For the estimation of the number of bolt holes, the bolts should be in pairs so as to avoid any Yaw movement of the structure after assembly.

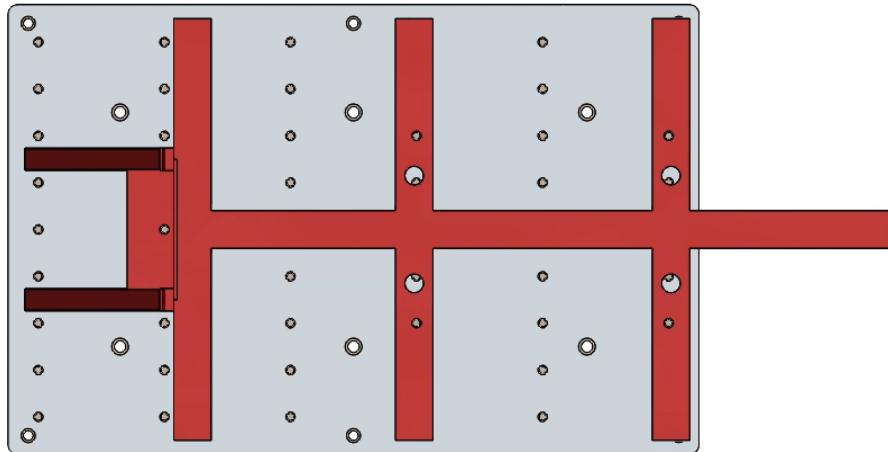


Figure 5.23: Test Stand on the ICD Bench. Source: Own.

Note: The Image of the Test Stand (figure 5.23) has 4 bigger holes (M20) which do not align with the holes of the ICD bench. Those are the bolt holes we have used for the test bench available at our university's test facility. This will be modified to adapt to the interface as provided in the ICD document.

The mount has bars in the lateral direction to provide roll stability, and the bolt holes are drilled at the sides of the chamber length symmetrically.

The cross-sectional shape used for the mount is square with a 3 mm thickness. The material used for the mount is stainless steel. The team was able to manufacture the engine mount and successfully tested it for another engine of 1.5 kN, justifying that the structure and design for the engine mount are safe and have sufficient structural strength.

The test bench has been evaluated for structural performance through Finite Element Analysis (FEA). The resulting deformation and induced stress are indicated in figure 5.24. The analysis result showcases the maximum stress in the worst-case scenario of maximum thrust, with the worst temperature and vibrations modelled in the software. The iterations for FEA started with 2 bolts and for the worst loading scenario. Although safe, the team decided to add 3 more bolts for additional safety. Hence, a 5-bolt configuration was selected, with 4 bolt holes on the side arms and 1 bolt behind the L-bracket plate.

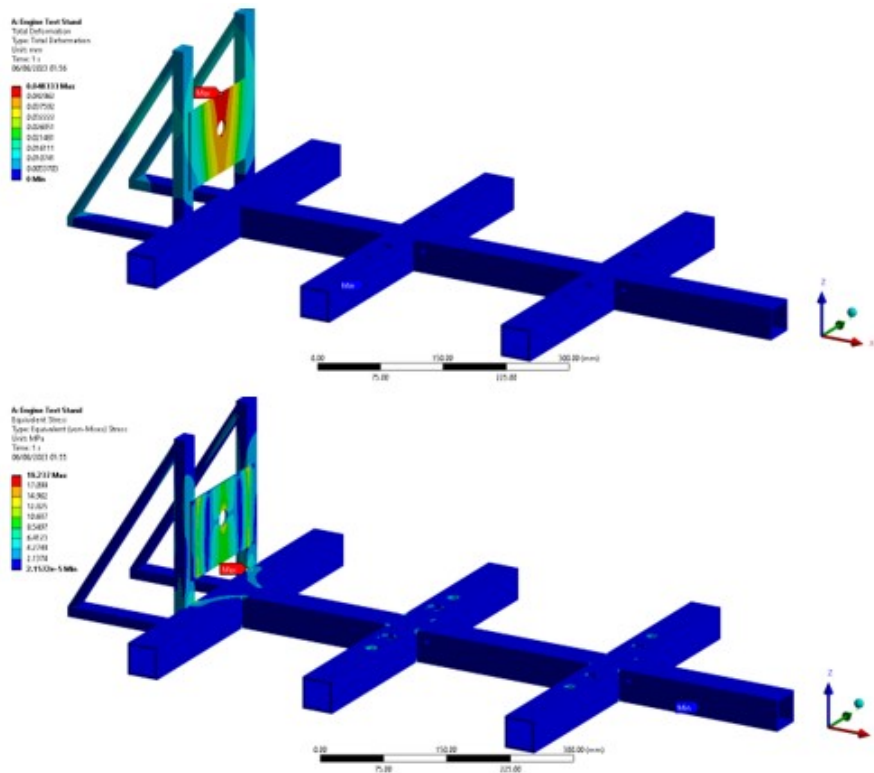


Figure 5.24: FEA results of the engine test stand: Deformation: 0.05 mm (left); Max. Stress: 19.23 MPa (FOS: 13) (right). Source: Own.

5.4.2 Support sub-assembly

The ring clamp system, which holds the combustion chamber over the engine mount, has 2 parts: A ring clamp and a metal plate which sits on the mount. As the load from the engine firing is bored by the L-bracket mount, the ring clamp system will carry the gravitational load for the chamber assembly, for which they have been analysed and are deemed safe for our use. The design is depicted in figure 5.25.



Figure 5.25: Ring Clamp System. Source: Own.

The manufacturing of the lower steel bend plate has been performed by the team and described in chapter 8. At the same time, the support plate has been evaluated for structural performance through Finite Element Analysis (FEA). The resulting deformation and induced stress are indicated in figure 5.26. The analysis result showcases the maximum stress in the worst-case scenario of maximum thrust, with the worst temperature and vibrations modelled in the software.

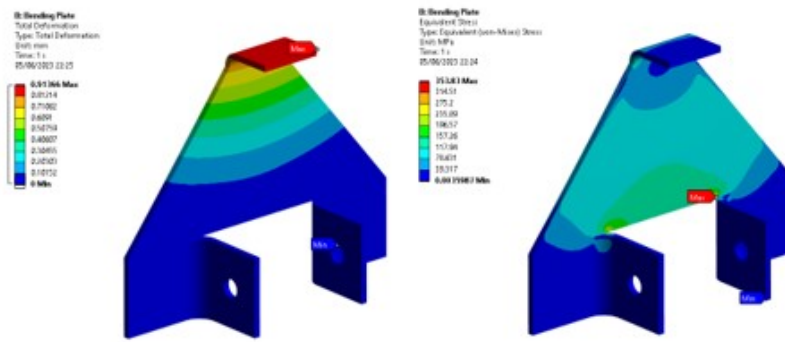


Figure 5.26: FEA results of the steel support plate: Deformation: 0.91 mm (left); Max. Stress: 176.91 MPa (FOS: 1.4) (right). Source: Own.

5.5 Material Selection

The material selected for the combustion chamber and all its parts is Mild Steel due to its high enough material strength, low cost and easy machining. Mild Steel, however, poses the risk of corrosion, which could have been resolved by using Stainless steel. Plus, Stainless steel has a higher yield strength, providing a better factor of safety. On the downside, the cost of stainless steel is higher than mild steel. So the team made a design choice to use mild steel instead of stainless steel. And to tackle the corrosion issue, the components will be protected by using paint.

For the nozzle, which will experience peak temperatures (enough to melt steel), graphite material (DuraGraph, appendix 11.3.1) was selected.

While for the insulation between the fuel grain and steel casing is a 5 mm thick layer of cork Tufnol with very low thermal conductivity, ease in manufacturing and lightweight.

5.6 Cooling Plan and Thermal Analyses

As it stands, the design incorporates a 5mm thick insulating layer of Tufnol to isolate the internal combustion chamber and grain case from the steel cylinder casing and the external environment. The insulating material has very low thermal conductivity and, thus, for a burn time of 6-7 seconds, will not conduct high enough heat to melt the steel casing.

However, this needs to be validated and correctly estimated. For this reason, the team used RPA software to study the thermal response of the developed engine. The results are indicative of the stable state when the temperature and flow stabilize, not for 6 seconds, and thus the values obtained are extremely higher than the ones which will be experienced in the actual testing of the engine. The results showed that the maximum temperature occurs at the nozzle throat, as expected, while the average combustion chamber temperature at the stabilized state will be about 2100 K. These results, being at the stabilized state, do not include thermal insulation from the tufnol layer between the fuel grain and steel casing. Hence, a better model needs to be developed to estimate an accurate temperature profile for the engine. The team is working on this front and will elaborate on the research work in the final Engine document.

The melting point of mild steel is 1620 K, which makes the material unsuitable to be used.

However, the current scenario runs for less than 7 seconds, and the repetitive tests are planned to be performed with enough time intervals for the system to cool down. This consideration, along with the cost consideration, led the team to select Mild Steel for the design.

However, the material will be subjected to high loads from thermal cycling, which needs to be assessed and analysed. For this, thermos-structural analyses were performed to simulate the material component for the worst thermal cycling and loading altogether to see if the Mild steel can hold or not.

Chapter 6

Design Calculations

6.1 Engine Sizing

Using RPA (Rocket Propulsion Analysis) software (in Appendix 11.4), the following parameters were found to be optimum:

- Chamber Pressure: 3.35 MPa
- O/F: 7.6

This resulted in a C* of 1546.22 m s^{-1} . Using a nozzle with a throat diameter of 9.8mm and an expansion ratio of 5.18, this produced an Isp of 2251.4 m s^{-1} .

To achieve a mean thrust of 350 N ($\sim 1.2x$ higher than the minimum thrust of 300 N), the required mass flow rate is, therefore, accounting for nozzle efficiency:

$$\dot{m} = \frac{\text{Thrust}}{\epsilon \cdot \text{Isp}} = \frac{350}{0.95 \cdot 2251.4} = 0.164 \text{ kg s}^{-1} \quad (6.1)$$

From this, the expected oxidiser mass flow rate and fuel mass flow rate can be calculated, assuming an O/F ratio of 7.6:

$$\dot{m}_{ox} = \dot{m} \cdot \frac{7.6}{8.6} = 0.145 \text{ kg s}^{-1} \quad (6.2)$$

$$\dot{m}_f = \dot{m} \cdot \frac{1}{8.6} = 0.019 \text{ kg s}^{-1} \quad (6.3)$$

The target burn time (t) is 6.3 seconds. To achieve this burn time, the total volume of fuel required is,

$$V_f = \frac{\dot{m}_f \cdot t}{\rho} = 1.28 \cdot 10^{-4} \text{ m}^3 \quad (6.4)$$

The fuel grain must be sized appropriately to achieve the required optimum average O/F ratio specified by RPA. The optimum O/F ratio is a function of the length-to-diameter ratio of the fuel port, the fuel density, the oxidiser mass flux, and the properties of the fuel oxidiser pair being used,

$$O : F = \frac{G_{ox}^{1-n}}{4 \cdot a_o \cdot \rho \cdot L/D} \quad (6.5)$$

For N_2O and HDPE, $n = 0.605$ and $a_o = 0.0000236$. Here, it is important to use the average L/D to achieve optimum performance.

The fuel grain geometry has been developed in section 6.2, providing the inner and outer diameter for the fuel grain block.

The average L/D can then be calculated as,

$$L/D = \frac{h}{\frac{d_i+d_o}{2}} = \frac{350}{\frac{31+38}{2}} = 10.145 \quad (6.6)$$

where d_i and d_o represent the inner and outer port diameters of the fuel grain block. Using the average port area, the average oxidiser flux is,

$$G_{ox,avg} = \frac{m_{ox} \cdot}{0.25 \cdot \pi \cdot \frac{d_i^2+d_o^2}{2}} \quad (6.7)$$

This average L/D ratio and G_{ox} can then be used to verify that the correct average O:F ratio is reached, using the equation 6.5.

$$O : F = \frac{G_{ox}^{1-n}}{4 \cdot a_o \cdot \rho \cdot L/D} = \frac{274^{1-0.605}}{4 \cdot 2.36 \cdot 10^{-5} \cdot 935 \cdot 10.145} = 7.6 \quad (6.8)$$

6.2 Fuel Grain Geometry

Mass of Fuel, $m_f = 0.119 \text{ kg}$ Volume of Fuel, $V_f = 1.274 \cdot 10^5 \text{ mm}^3$ Let's assume the inner and outer diameters of the fuel grain are d_i and d_o . So, the volume expression can be written as,

$$\frac{\pi \cdot (d_o^2 - d_i^2) \cdot h}{4} = V_f \quad (6.9)$$

where h is the length of the fuel grain (350 mm).

The inner diameter of the steel casing from the available steel billet is 47.6 mm. And considering insulation of about 4 - 5 mm of cork liner, we can put in a design choice of the outer diameter for the fuel grain to be **38 mm**.

Thus, the inner diameter from the equation 6.9 can be calculated to be about **31 mm**.

6.3 Regression Rate

Average Oxidiser Flux, $\phi_{ox} = 271.048 \text{ kg m}^{-2} \text{ s}^{-1}$

Regression rate coefficient, $a_0 = 1.039 \cdot 10^{-5}$

First Regression rate exponent, $n = 0.763$

Second Regression rate exponent, $m = -0.148$

The distance down the port (only for fuel grain), $x \in [0 \text{ mm}, 350 \text{ mm}]$

So, Average Regression Rate using modified St. Robert's Law, [7]

$$r = a_0 \cdot \phi_{ox}^n \cdot x^m = \epsilon [0, 8.719 \cdot 10^{-4}] \text{ mm s}^{-1} \quad (6.10)$$

This portrays that the regression rate varies along the length of the combustion chamber and will be highest at the end of the grain close to the nozzle, where the burn rate will be **0.872 grams/sec.**

Now, to calculate the burn rate, Fuel Volume consumption can be achieved from the regression rate, which gives $Q_f = \frac{r}{\rho_f} = 932.62 \text{ mm}^3 \text{ s}^{-1}$

From this volumetric rate, keeping the length constant, we can measure the rate of change of the grain diameter and thus the burn rate,

$$2 \cdot 350 \text{ mm} \cdot \frac{\pi \cdot d}{2} \text{ mm} \cdot r = 932.62 \text{ mm}^3 \text{ s}^{-1} \quad (6.11)$$

This provides the burn rate as, $r_b = 1.842 \text{ mm s}^{-1}$.

And, Average O:F Ratio,

$$O : F_{avg} = \frac{\phi_{ox}^{1-n}}{4 \cdot a_0 \cdot \rho_f \cdot \frac{L}{D}} = 7.32 \quad (6.12)$$

6.4 Combustion Chamber Length

For the Steel Casing available with us, Outer Diameter, $OD_{cc} = 60 \text{ mm}$

Inner Diameter, $ID_{cc} = 48 \text{ mm}$

Thickness, $t_{cc} = 6 \text{ mm}$

Post Combustion Chamber length, $L_{postcc} = ID_{cc}/2 = 24 \text{ mm}$

Pre Combustion Chamber Length, $L_{precc} = L_{postcc} = 24 \text{ mm}$

Minimum Required Combustion Chamber Length, $L_{req.cc} = L_f + L_{precc} + L_{postcc} = 398 \text{ mm} \sim 400 \text{ mm}$

6.5 Nozzle Shape

Characteristic Velocity, $C^* = 1546.22 \text{ m s}^{-1}$

Throat Area,

$$A_t = \frac{m \cdot C^*}{T_m} = 7.553 \cdot 10^{-5} \text{ m}^2 \quad (6.13)$$

Throat Diameter, $d_t = \sqrt{\frac{4 \cdot A_t}{\pi}} = 9.81 \text{ mm}$

Expansion Ratio, $\epsilon = 5.18$

Exit Area, $A_e = \epsilon \cdot A_t = 3.91 \cdot 10^{-4} \text{ m}^2$

Exit Diameter, $d_e = \sqrt{\frac{4 \cdot A_e}{\pi}} = 22.32 \text{ mm}$

Heat Capacity Ratio at Nozzle Exit, $\gamma_e = 1.2413$

So, Exit Mach Number,

$$M_e = \sqrt{\frac{2}{\gamma - 1}} \cdot \frac{P_{cc}}{P_{atm}}^{\frac{\gamma}{\gamma - 1}} = 3.92 \quad (6.14)$$

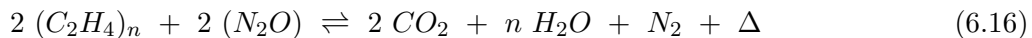
Throat to Exit Nozzle Length, $L_{n_{te}} = 30\text{mm}$

And Nozzle Divergence Angle,

$$\theta_{n_{te}} = \tan^{-1}\left(\frac{d_e - d_t}{L_{n_{te}}}\right) = 11.8\text{deg} \quad (6.15)$$

6.6 Thermochemistry for combustion reaction

The combustion reaction occurring between liquid nitrous oxide and solid HDPE fuel results in 3 products from 100% combustion, carbon dioxide, water vapour and nitrogen. This has been represented in the reaction given in equation 6.16.



The "n" in the reaction signifies the number of molecules in a single polymer chain of HDPE.

The initial reaction mass of HDPE is 119.118 grams, and N_2O is 905.3 grams.

HDPE is a polynomial of carbon and hydrogen molecule monomers. So, the molecular mass of HDPE can be calculated from the available data of its constituent components, i.e., carbon and hydrogen. Carbon has 12 grams/mol, and hydrogen has 1 gram/mol. Calculating for HDPE's molecular mass,

$$m_{HDPE} = n \cdot [2(12) + 4(1)] \text{ grams/mol} = 28n \text{ grams/mol} \quad (6.17)$$

Similarly, molecular mass for N_2O is,

$$m_{N_2O} = 14 \cdot 2 + 16 \text{ grams/mol} = 44 \text{ grams/mol} \quad (6.18)$$

Now, to calculate the moles consumed in the chemical reaction,

$$Moles_{N_2O} = N_{N_2O} = \frac{905.3}{44} = 20.575\text{mol} \quad (6.19)$$

This provides the number of moles that are produced in the reaction when it is 100% complete. The number of moles produced per species are:

- Carbon dioxide: 20.58 mol
- Water vapour: 8.50 mol
- Nitrogen: 10.29 mol

Now, to calculate the enthalpy of all the reactants and products, Enthalpy of formation of carbon dioxide at 298.15 K, $\Delta H_f(CO_2) = -393.5 \text{ kJ/mol}$ Enthalpy of formation of water vapour at 298.15 K, $\Delta H_f(H_2O) = -285.82 \text{ kJ/mol}$ Enthalpy of formation of nitrogen at 298.15 K, $\Delta H_f(N_2) = 0 \text{ kJ/mol}$ Enthalpy of reduction of nitrous oxide at 298.15 K, $\Delta H_{red}(N_2O) = -82.05 \text{ kJ/mol}$ Enthalpy of combustion of HDPE is a 2-part enthalpy, enthalpy of polymerization and enthalpy of combustion of a single monomer. This is described in equation 6.20.

$$\Delta H_{comb}(HDPE) = \Delta H_{poly}(HDPE) + \Delta H_{comb}(C_2H_4) \quad (6.20)$$

$$\Delta H_{comb}(HDPE) = (-100 \text{ kJ/mol}) + (-651.28 \text{ kJ/mol}) = -751.28 \text{ kJ/mol} \quad (6.21)$$

The above enthalpies will be used to calculate the overall enthalpy of the reaction as follows,

$$\Delta H_{reaction} = 2 \Delta H_f(CO_2) + n \Delta H_f(H_2O) + \Delta H_f(N_2) - 2 \Delta H_{comb}(HDPE) - 2 \Delta H_{red}(N_2O) \quad (6.22)$$

$$\Delta H_{reaction} = 308.02 \text{ kJ/mol} \quad (6.23)$$

Now, using the enthalpy values and number of moles, we can calculate the dissipated heat using the formula,

$$Q_{reaction} = \Delta H_{reaction} \cdot N_{HDPE} \quad (6.24)$$

This dissipated heat can be equated to the amount of heat carried by the 3 reaction products with the formula,

$$Q_{reaction} = n \cdot C_{p,eq.} \cdot dT \quad (6.25)$$

Here, $C_{p,eq.}$ represents the equivalent specific heat of the reaction products at constant pressure. This can be calculated as,

$$C_{p,eq.} = \frac{N_{CO_2} \cdot C_{p,CO_2} + N_{H_2O} \cdot C_{p,H_2O} + N_{N_2} \cdot C_{p,N_2}}{N_{CO_2} + N_{H_2O} + N_{N_2}} \quad (6.26)$$

Putting in the values,

$$C_{p,eq.} = \frac{N_{CO_2} \cdot 0.849 \text{ J/gK} + N_{H_2O} \cdot 4.186 \text{ J/gK} + N_{N_2} \cdot 1.04 \text{ J/gK}}{N_{CO_2} + N_{H_2O} + N_{N_2}} = 1.72 \text{ J/gK} \quad (6.27)$$

Now equating both the equations of dissipative heat, the temperature gradient can be calculated as,

$$dT_{reaction} = \frac{Q_{reaction}}{C_{p,eq.}} = \frac{\Delta H_{reaction} \cdot N_{HDPE}}{C_{p,eq.}} = 761.039 \text{ K} \quad (6.28)$$

Considering the initial ambient temperature is 298.15 K, the final temperature when the reaction is exhausted can be calculated as

$$T_{f_{reaction}} = dT_{reaction} - T_{ambient} = 1059.19 \text{ K} \quad (6.29)$$

Now, the temperature within the combustion chamber increases exponentially, which can be represented as

$$T_{CC} = T_A \cdot e^{B \cdot t} \quad (6.30)$$

where T_A is the temperature constant, B is the temperature exponential rate constant, and t is the time in seconds.

And the regression rate calculated in section 6.3 is 0.872 grams/sec.

The calculation made in the previous section for the time until complete exhaustion of the HDPE solid fuel is 6.25 seconds, and the final temperature calculation made in this section aids in estimating the values for the constants of equation 6.30.

The exponential rate constant has the inverse value to the oxidizer flux rate constant used for the regression rate, representing the exact same combustion property of fuel material exhaustion but with an increment factor rather than a reduction (regression).

From this, T_A can be calculated by integrating equation 6.30 as

$$dT_{CC} = T_A \cdot e^{\frac{t}{0.763}} \cdot dt \quad (6.31)$$

$$\int_{298.15}^{1059.19} dT_{CC} = T_A \cdot \int_0^{6.25} e^{\frac{t}{0.763}} dt \quad (6.32)$$

$$761.04K = \frac{T_A \cdot [e^{\frac{6.25}{0.763}} - e^{\frac{0}{0.763}}]}{0.763} = T_A \cdot 4729.478 \quad (6.33)$$

The value of T_A obtained is 0.161 K. The obtained graph of the exponential rise in temperature is displayed in figure 6.1. The graph has been developed using the Matlab tool, and the code is attached in appendix 11.5.

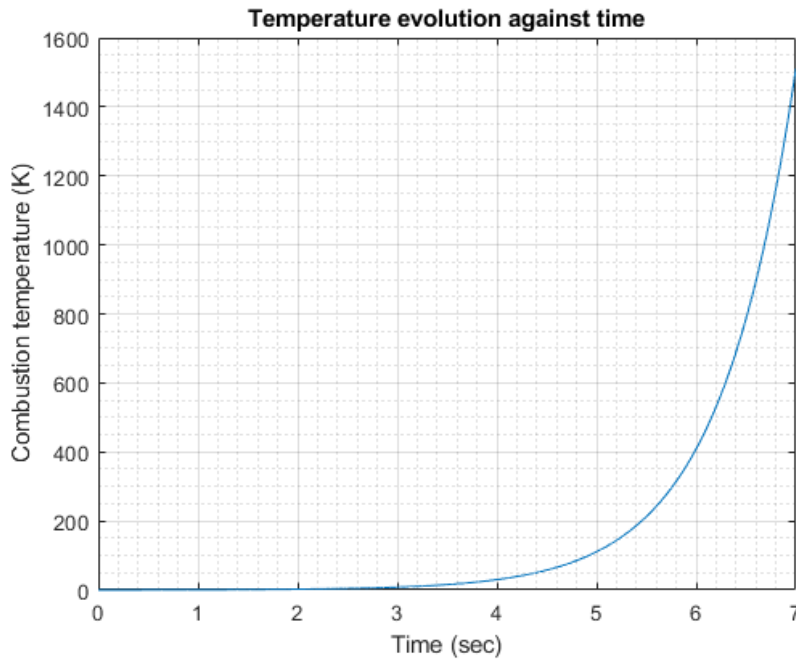


Figure 6.1: Exponential rate graph for temperature with time

6.7 Pressure Drop

6.7.1 Feed Line Pressure Drop

Oxidiser mass flow rate, $\dot{m} = 0.144 \text{ kgs}^{-2}$

Oxidiser Density, $\rho_{ox} = 822.2 \text{ kgm}^{-3}$

Dynamic Viscosity of Nitrous Oxide of Saturated Gas at 15°C , $\nu = 0.016 \text{ mNs/m}^2$

Flow Velocity,

$$v = \frac{\dot{m}_{ox}}{\rho_{ox} \cdot A_{pipe}} = 2.6 \text{ ms}^{-1} \quad (6.34)$$

Reynold's Number,

$$R = \frac{\rho_{ox} \cdot v \cdot ID_{pipe}}{\nu} = 1648 \quad (6.35)$$

Darcy Friction Factor, $f_{darcy} = 0.04$

Feed Pipe maximum estimated length, $l_{pipe} = 2 \text{ m}$

A quarter-inch pipe is planned to be used for the feed system.

Combustion Chamber Pipe Inner Diameter, $OD_{pipe} = 13.7 \text{ mm}$ [8]

And, thickness for standard pipe, $t_{pipe} = 2.24mm$ [8]

So, Combustion Chamber Pipe Inner Diameter, $ID_{pipe} = OD_{pipe} - 2xt_{pipe} = 9.26mm$

Frictional Pressure Drop,

$$dP_{feed} = f_{darcy} \cdot \frac{l_{pipe}}{ID_{pipe}} \cdot \rho_{ox} \cdot \frac{v^2}{2} = 1.78 \cdot 10^{-7} bars \quad (6.36)$$

6.7.2 Injector Pressure Drop

Mass flow rate, $m' = 0.1636 kgs^{-2}$

The general value of the Coefficient of Discharge for Nitrous Oxide, $C_d = 0.8$

(Historical Data) Diameter of Injector, $d_{inj} = 1mm$

Area of Injector, $A_{inj} = 7.854 \cdot 10^{-7} m^2$

Density of Nitrous Oxide, $\rho_{ox} = 822.2 kgm^{-3}$

Number of Injector holes, $n = 6$.

Using the modified Bernoulli's equation for a single-phase incompressible fluid, we have [9] [10]

$$m' = Q \cdot \rho = C_d \cdot A_{inj} \cdot \sqrt{\frac{2 \cdot dP_{inj} \cdot \rho_{ox}}{1 - \left(\frac{A_{inj}}{A_1}\right)^2}} \quad (6.37)$$

where A_1 is the upstream cross-sectional area, i.e., the area of the inlet side of the injector, which is $A_1 = 5.026 \cdot 10^{-5}$. Also, $A << A_1$. Rearranging the equation above and substituting the values, we get the value of pressure drop for total $n = 6$ holes as

$$0.1636 = 0.8 \cdot 6 \cdot 7.854 \cdot 10^{-7} \cdot \sqrt{\frac{2 \cdot dP_{inj} \cdot 822.2}{1 - \left(\frac{7.854 \cdot 10^{-7}}{5.026 \cdot 10^{-5}}\right)^2}} \quad (6.38)$$

And so, the Overall Injector Pressure Drop, $dP_{overall,inj} = 1.1097 MPa = 10.952 bars$

From the above 2 sections, we get the overall pressure drop as,

$$dP_{overall} = dP_{overall,inj} + dP_{feed} = 10.952 bars \quad (6.39)$$

The target chamber pressure is 33.5 bars. Therefore, the pressure regulator on top of the Nitrous oxide tank shall regulate the flow at $P = 33.5 + dP_{overall} = 44.452 bars$.

As can be seen in the feed system diagram (figure 5.17), the pressure for the Nitrous oxide tank is taken as 44.5 bars.

Hence, the pressure drop calculations correlate with the set chamber pressure and tank pressure.

6.8 Injector Design

6.8.1 Injector Sizing

To calculate the injector size, the basic design shall be defined.

The injector is a single bolt configuration with injector holes in the configuration of showerhead injection.

The values used from other sections for determining injector sizing are, Maximum operating pressure of combustion chamber, $CC_{max.op.} = 44.5 \text{ MPa}$, Number of injector bolts, $n_i = 1$, The inner diameter of the combustion chamber, $CC_{ID} = 0.048 \text{ m}$.

These can be used to calculate the maximum axial force on the combustion chamber as,

$$F_{A,max.op.} = CC_{max.op.} \cdot \frac{\pi \cdot CC_{ID}^2}{4} = 8056.37 \text{ N} \quad (6.40)$$

The selected material is Mild steel with a proof load of 580 MPa. This will be used to calculate the maximum applicable axial force on the injector. And for this, an iterative approach was undertaken with an injector outer diameter varying from 14 mm to 28 mm.

The maximum applicable axial force was calculated as,

$$\text{Axial force} = 580 \cdot 10^6 \text{ Pa} \cdot \frac{\pi \cdot 0.02^2}{4} \text{ m}^2 = 1.82 \cdot 10^5 \text{ N} \quad (6.41)$$

And the factor of safety is calculated as,

$$FoS = \frac{\text{Axial force}}{F_{A,max.op.}} = \frac{1.82 \cdot 10^5 \text{ N}}{8056.37 \text{ N}} = 22.617 > 20 \quad (6.42)$$

And so, the selection for 20 mm diameter was selected, pertaining to safety factors, and enough clearance for the injector holes and external thread for interfacing with the injector flange.

The M20 thread used has the following attributes, obtained from [11]:

- ISO Metric coarse threads
- Outer diameter = 20 mm
- Pitch = 2.50 mm
- Depth = 1.5336 mm
- Tapping drill = 17.50 mm
- Clearance drill = 202.25 mm

The butting piece is sized with a 50 mm outer diameter and 10 mm thickness.

The butting flange tolerance is 2 mm.

This derives the cut length, which is the part of the injector inside the butting flange, as 5 mm.

The injector has a total length of 20 mm, which leads to about 8 mm of injector inside the combustion chamber.

6.8.2 Injector holes

To calculate the number of holes, we use the equation presented in injector pressure drop in section 6.7.2, i.e.,

$$\dot{m}_{ox} = C_d \cdot N_{inj} \cdot A_{inj} \cdot \sqrt{2 \cdot \rho_{ox} \cdot \Delta P_{inj}} \quad (6.43)$$

From the literature, for N_2O , we have the value for the coefficient of discharge as,

$$C_d = \sqrt{\frac{1}{C}} = \sqrt{\frac{1}{1.56}} \equiv 0.8 \quad (6.44)$$

From the previous sections, we accumulate, Oxidiser mass flow rate, $\dot{m}_{ox} = 0.1446 \text{ kg sec}^{-1}$, Oxidiser density, $\rho_{ox} = 823 \text{ kg m}^{-3}$, Injector hole diameter, $d_{inj} = 1 \text{ mm}$, Injector hole area, $A_{inj} = \frac{\pi \cdot d_{inj}^2}{4} \text{ mm}^2$, and the injector pressure drop, $\Delta P_{inj} = 9.3 \text{ bars} = 0.93 \text{ MPa}$.

This provides the required cross-section area of injector hole/s as,

$$\text{Required Area, } A = \frac{\dot{m}_{ox}}{C_d \cdot \sqrt{2 \cdot \rho_{ox} \cdot \Delta P_{inj}}} = 5.227 \cdot 10^{-6} \text{ m}^2 \quad (6.45)$$

Now this area can be used to estimate the number of holes as,

$$N = \frac{A}{A_{inj}} = \frac{A}{\frac{\pi \cdot d_{inj}^2}{4}} = 6.655 \rightarrow 6 \quad (6.46)$$

1 hole shall be in the central axis concentric to the injector, while the other 5 holes shall be in a pitch circle of 5 mm pitch diameter around the central hole.

6.9 Flange Sizing

From the previous sections, we know the values for:

outer diameter of combustion chamber = 60 mm,

bolt size = M10,

bolt head diameter = 18.9 mm.

Assuming weld pool clearance of 1 mm, we get the flange inner diameter as,

$$\text{Flange inner diameter, } ID_f = CC_{OD} + 2(\text{weld pool clearance}) = 62 \text{ mm} \quad (6.47)$$

The bolt-hole clearance is 2 mm. This gives us the bolt hole diameter with clearance as 12 mm.

While the bolt-hole side clearance is 6 mm.

Now, the flange outer diameter can be calculated as,

$$OD_f = ID_f + 2(\text{bolt hole diameter with clearance}) + 4(\text{bolt hole side clearance}) \quad (6.48)$$

$$OD_f = 62 + 2(12) + 4(6) = 110 \text{ mm} \quad (6.49)$$

The number of bolts used is 6. This leads to an equal hole spacing as,

$$\text{Hole spacing} = \frac{360^\circ}{6} = 60^\circ \quad (6.50)$$

6.10 Chamber thin wall stress calculations

Circumferential / Hoop Stress:

$$\sigma_c = \frac{P \cdot d}{2 \cdot t} = 13.4 \text{ MPa} \quad (6.51)$$

Longitudinal Stress:

$$\sigma_L = \frac{P \cdot d}{4 \cdot t} = 6.7 \text{ MPa} \quad (6.52)$$

Shear Stress: Shear Stress occurs as In-plane stress and Out-of-plane stress. The value for the current case, however, remains the same.

$$\sigma_s = \frac{P \cdot d}{8 \cdot t} = 3.35 \text{ MPa} \quad (6.53)$$

Overall Stress and FOS: Calculating the overall stress from the above 3 defined stresses, we get,

$$\sigma_{total} = \sqrt{\sigma_c^2 + \sigma_L^2 + \sigma_s^2} = 15.713 \text{ MPa} \quad (6.54)$$

The Yield Strength of Mild Steel is 250 MPa, which gives a Factor of Safety value as, FOS = 15.9

Chapter 7

CFD Simulations

This chapter describes the CFD simulations performed on the nozzle and the combustion chamber, simulating the high temperature and pressure multi-phase flow in the hybrid engine. The target set for the simulations is to model the solver as close to the real world with multiple phases of the propellants, with varying pressure and temperatures for the first 6.5 seconds of the burn. The flow is steady state showcasing the evolution of combustion and engine characteristics for the 6.5 seconds burn for the developed engine.

The following sections describe the overall procedure/ methodology for performing the CFD simulation for the hybrid engine setup. It is followed by the obtained results and the future work that can be undertaken to develop the CFD model further in accuracy and correlation to real-world testing.

7.1 Methodology

As part of its computational fluid dynamics (CFD) software, Ansys has the ability to solve Navier-Stokes' equations in order to analyze complex fluid dynamics problems with a high degree of accuracy. The software was utilized to determine the performance aspects of the nozzle under various flow and boundary conditions, in addition to providing a variety of turbulence models to compute turbulent flow.

7.1.1 Step 1: Modelling the geometry

In Solidworks 2022, the nozzle was designed in two dimensions and then imported into Ansys Fluent Design for editing. The geometry was designed using simple tools such as sketching and plane surface creation. To facilitate the meshing process, after the geometry has been transferred to the Design modeller, it is divided into different sections. After importing the geometry to the ANSYS design modeller, the further process of named selection is performed. As shown in figure 7.1, the geometry is divided in half so that it will be easier to compute and because the other half which will produce similar results.

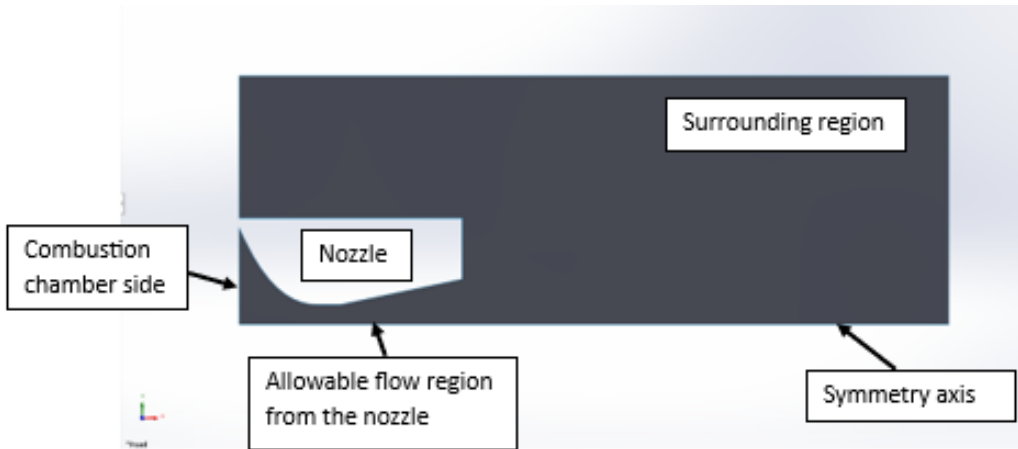


Figure 7.1: Model geometry for CFD simulation of the engine nozzle. Source: Own.

7.1.2 Step 2: Meshing

Among the most important process is meshing the developed geometry. A mesh refers to a discretization of geometry into small elements, which can be either structured or non-structured. The significance of performing this process lies in computing the flow equations at the nodes of each equation. In order to achieve close to accurate simulation results, we have used high-quality structured meshes. It was especially important to divide the nozzle curve part into a number of sections before meshing to ensure a structured mesh along the curve while maintaining orthogonality, skewness, and aspect ratio. The following subsections show the meshing operations performed, the overall meshing visual, and the meshing along the nozzle curve.

Skewness

Based on ideal element-type angles, Skewness is a measure of element quality. A minimum angle may also be defined as the angle between the vectors from each node and the opposing mid-side, as well as the angle between the two adjacent mid-sides of each element's nodes. As one of the primary properties of the Measures of finite element mesh, skewness is determined by the degree of closeness a face or cell is to ideal (i.e., equilateral or equiangular). The closer it is to zero, the better it is.

Aspect Ratio

As the name suggests, the aspect ratio describes the relationship between an element's largest and smallest characteristic dimensions. As a result of large aspect ratios, the finite element representation becomes more inaccurate, and the convergence of Finite Element Solutions suffers. A one-value aspect ratio is ideal but cannot always be maintained.

Orthogonal Quality

In terms of Orthogonal Quality, it refers to the angle between the vector that connects two mesh nodes (or control volumes) (s) and the normal vector for each integration point surface (n) associated with those nodes.

Figure 7.2 shows the final meshing and a zoomed-in view of the allowable nozzle flow region.

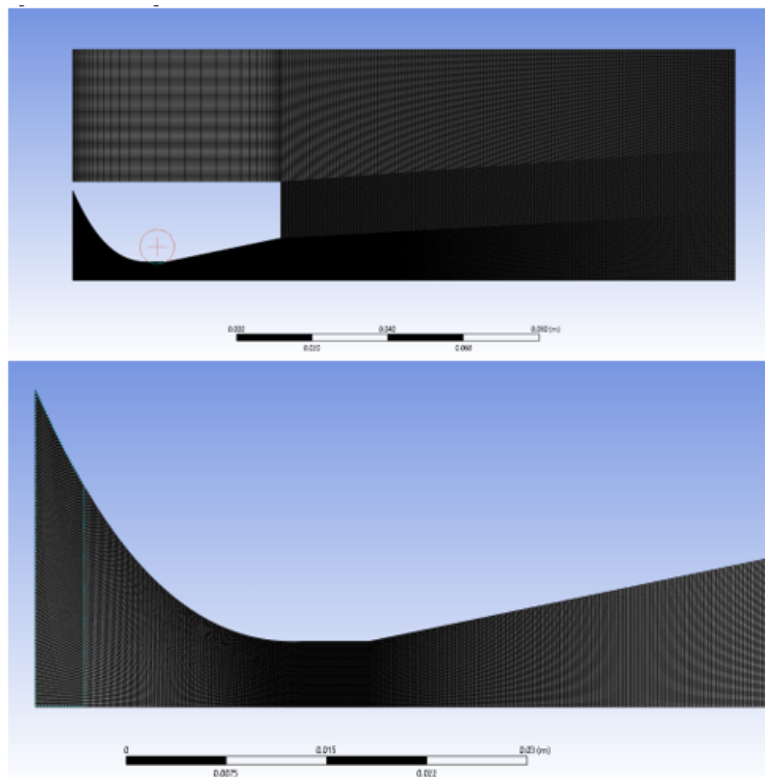


Figure 7.2: Meshed geometry for CFD simulation of the engine nozzle. Source: Own.

7.1.3 Step 3: Setting boundary conditions

The boundary conditions were set to the domain according to the preferences. They are enlisted below:

1. Far-field
2. Inlet
3. Nozzle wall
4. Outlet
5. Symmetry axis

7.1.4 Step 4: Solver pre-processing (Setup)

We proceed with setting the solvent parameters after setting the boundary conditions. This involves setting the parameters in such a way that we can obtain the required solution for our problem statement. In addition to general settings, there are physics models, material properties, boundary conditions, reference values, solution methods, solution controls, and solution initialization settings.

- To achieve accurate results, 2D double precision has been chosen to run simulations since it provides higher accuracy in the simulations.
- A steady state simulation is characterized by characteristics that do not change with time and are assumed to have been reached after a long period of time; therefore, real-time information does not need to be provided to describe these simulations.

- Since the mesh created was 2D, the axisymmetric option was chosen in 2D space settings. The central axis has been created in a C-D nozzle geometry. This method only requires simulating fluid behaviour in one two-dimensional plane, thereby saving time and computational power.
- In addition, since most of the domain does not rotate, the velocity formulation has been chosen to be absolute.
- During simulations, the energy equation was activated in order to allow heat transfer to occur.
- Model for turbulent viscosity: The realizable k model contains an alternative formulation for turbulent viscosity. An exact equation for the transport of mean-square vorticity fluctuation has been derived from a modified transport equation.
- As a flow material, N_2O has been selected. For density settings, the ideal gas has been chosen. Furthermore, a constant viscosity has been set for the compressible flow.
- Later, the pressure inlet, far field, and pressure outlet boundary conditions were determined. To calculate the selected oxidizer flow, the cell zone was made into nitrous oxide material. The pressure inlet was initially given conditions from the combustion chamber, such as temperature and pressure, while the pressure outlet was set to atmospheric conditions. The symmetric boundary was chosen as the axis since it defines the partition between the other half of the nozzle.
- Initial solution methods: include the Roe-FDS flux type, which splits the fluxes in accordance with their corresponding flux method eigenvalues. In spatial discretization, the initial gradient setting is set to be Least Square Cells Based, and the flow and modified turbulent viscosity are set to be Second Order Upwind. It is recommended that users use this flux type for most simulations.
- A standard initialization method has been selected for initialization, as well as the initial values have been computed from the inlet of the nozzle before initialization. Solution Initialization With the applied settings, the simulations have been set to run for 300-500 iterations in total, with constant monitoring if any adjustments are required.

7.2 Results

The obtained results are tabulated with pressure, velocity, and temperature values, taken from the report definitions, in table 7.1. The values are recorded for every 100 iterations.

Table 7.1: Tabulated results obtained from CFD simulation of the C-D nozzle

Index	Pressure (Pa)	Velocity (m/s)	Temperature (K)
1	2026446.62	279.38	3362.8
2	2523305.05	326.84	3235.1
3	2442082.61	325.18	3216.06
4	2478314.35	320.96	3221.7
5	2359351.15	325.59	3211.04
6	2150061.75	327.10	3180.92
7	1972831.63	320.96	3154.62
8	1735808.30	312.03	3110.44
9	1534459.99	316.00	3048.85
10	1473334.80	309.500	3033.23

Table 7.1 continued from previous page

Index	Pressure (Pa)	Velocity (m/s)	Temperature (K)
11	1413435.80	309.587	3023.07
12	1351686.12	307.45	3001.02
13	1310041.59	305.60	2988.82
14	1272710.41	305.80	2967.21
15	1244469.82	302.06	2959.77
16	1210935.38	305.64	2945.90
17	1186591.078	304.33	2936.15
18	1161872.52	301.72	2927.84
19	1139993.65	301.19	2913.28
20	1117990.96	300.28	2896.52
21	1104191.60	302.08	2883.78
22	1093393.083	303.78	2868.62
23	1086618.83	306.84	2855.26
24	1078542.34	306.99	2842.18
25	1071715.71	295.51	2832.46
26	1066128.48	278.31	2825.18
27	1061876.48	262.86	2819.709
28	1058921.40	248.45	2823.15
29	1058081.91	236.39	2829.25
30	1058758.61	201.30	2815.21

The contour results obtained for the nozzle flow for a 2D centre planar flow are highlighted in figures 7.3 for density contour, 7.4 for pressure contour, 7.6 for velocity contour, and 7.5 for temperature contour.

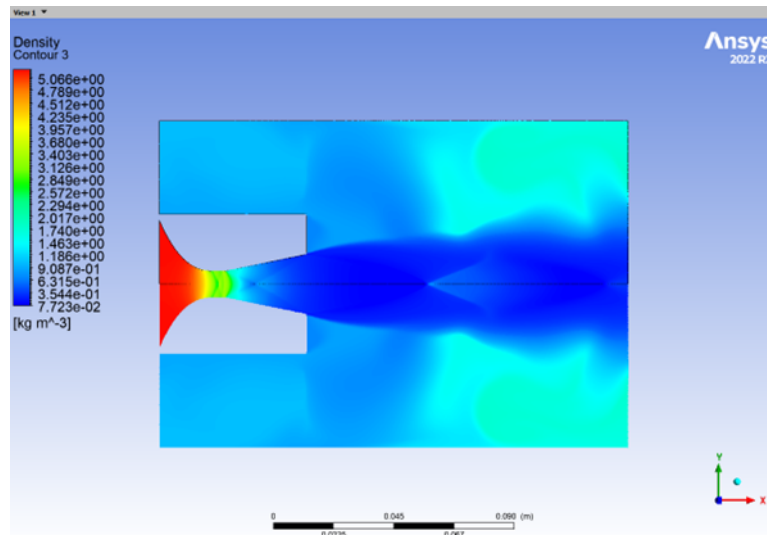


Figure 7.3: Obtained results for CFD simulation of the engine nozzle: Density contour. Source: Own.

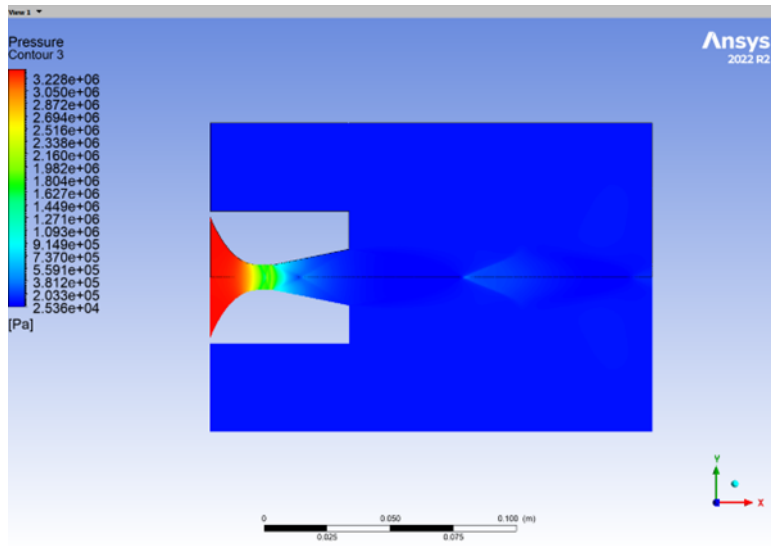


Figure 7.4: Obtained results for CFD simulation of the engine nozzle: Pressure contour. Source: Own.

The temperature and pressure both increase at first and then start decreasing after the throat section in the nozzle. The pressure shows a drastic change in the value after the combustion crosses the throat part.

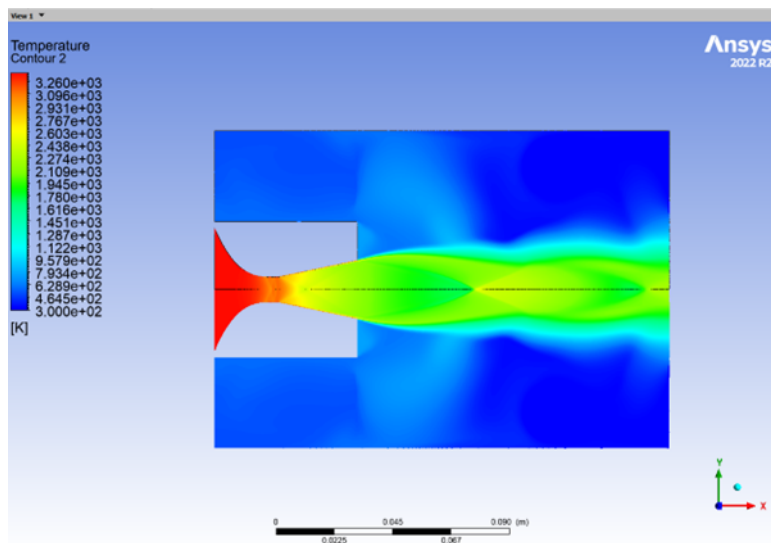


Figure 7.5: Obtained results for CFD simulation of the engine nozzle: Temperature contour. Source: Own.

On the other side, the velocity starts from a lower value and reaches a higher value after going through the throat of the nozzle.

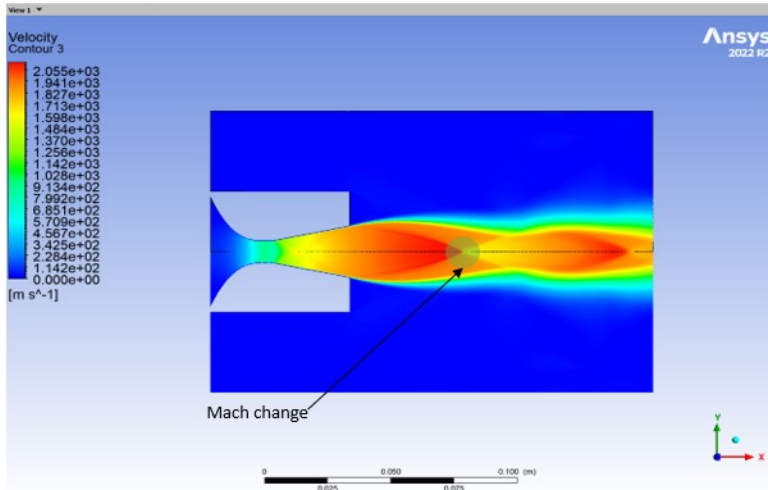


Figure 7.6: Obtained results for CFD simulation of the engine nozzle: Velocity contour. Source: Own.

7.3 Future Work

Further work requires performing a computation of the combustion chamber. Due to the need to use species transport models, which require the selection of premixed combustion options, it is difficult to compute the combustion chamber in two dimensions. To select the fuel and oxidizer for the hybrid rocket motor, a three-dimensional model must be used. For a proper understanding of the combustion distribution within the chamber, it is necessary to conduct a 3-D simulation of the combustion chamber, which will provide us with the necessary values to compare with the theoretical and experimental values derived from the computation. We are currently working on 3-D modelling of the combustion chamber and injector assembly. The next step should be the assembly of the injector and nozzle. Future work can also focus on simulating a transient (time-varying) model to achieve a better correlation with real-world testing. The transient response will aid in correctly determining the evolution of temperature, pressure, chemical reaction, and flow characteristics of the hybrid engine.

Chapter 8

Manufacturing

8.1 Timeline and lead time overview

1. **Procurement of steel:** Based on the verified engineering drawings, the manufacturing team was able to place an order for the required billets with the help of the test facility team. The procured material was cleaned, de-rusted, and the outer layers chipped off. These billets are not ready to be machined to the desired components.
2. **Test stand:** The Test Stand has already been manufactured by the team with M20 bolt holes. However, the stand needs to be updated according to the requirement from the ICD employing M10 bolts as the interface to the test bench at the competition.



Figure 8.1: Manufactured test stand. Source: Own.

3. **Combustion chamber:** The manufacturing of the combustion chamber is completed. The end flanges are welded onto the casing, and the chamber is pressure tested (8.3.1).



Figure 8.2: Manufactured combustion chamber. Source: Own.

- 4. Injector plate and flange:** The Injector plate with the tapped hole for fitting in the feed line end and the 1 mm holes for injection of oxidiser into the combustion chamber is manufactured, along with its flange, onto which the main injector plate will be fastened using external male threads on the injector plate.

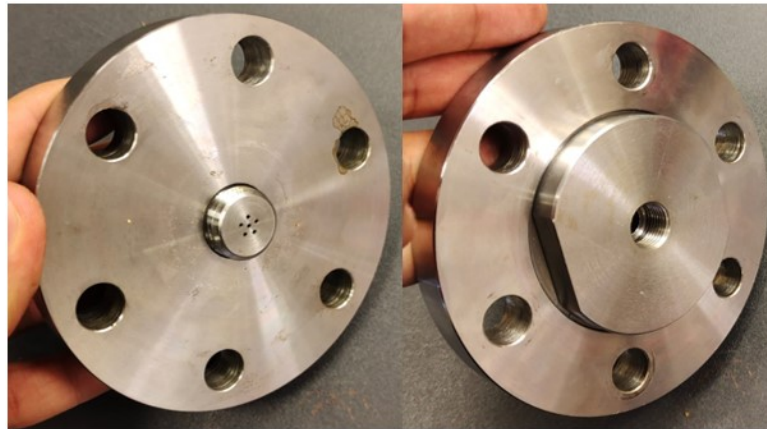


Figure 8.3: Manufactured and assembled injector plate. Source: Own.

- 5. Fuel grain block and cork liner sub-assembly:** The fuel grain block is machined on a lathe to the required outer and inner diameter. The fuel grain is divided into 2 equal parts for ease of machining.

The cork liner is a little more than 1 mm thick, allowing to use of 3 cork liner sheets overlapped on the fuel grain that fits inside the combustion chamber. The size of these sheets was carefully cut and wrapped around the fuel grain.

The bond adhesive will be spread out between the fuel grain and the cork liner sheets. To hold it in position until the adhesive is cured, 3D printed fixtures will be used for this purpose, as shown in figure 8.4.

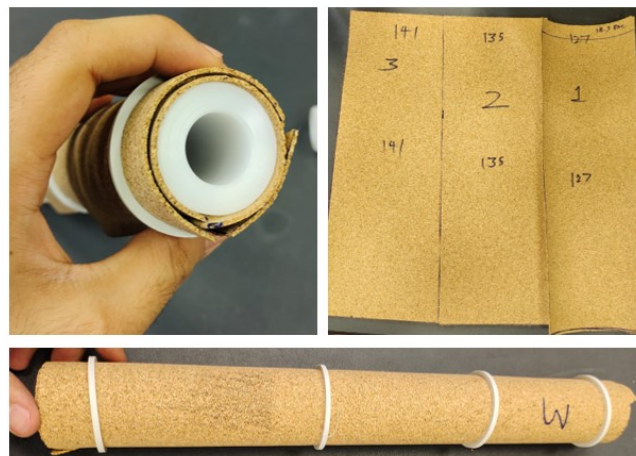


Figure 8.4: Manufactured and assembled fuel grain and liner sub-assembly. Source: Own.

- 6. Thruster assembly:** The thruster assembly with its front and back plate and the 4 mid connectors have been manufactured by the test facility manufacturing team based on the team's design. The design for the threads was updated to address the inevitable gap during the fastening of components using bolts and optimized to remove any unwanted gaps between the threads of the components. A separate connector bushing was designed, analyzed, and 3D printed to provide fitting to the bolt connection between the thruster assembly and the load cell. The material has been tested through brute force of pulling.

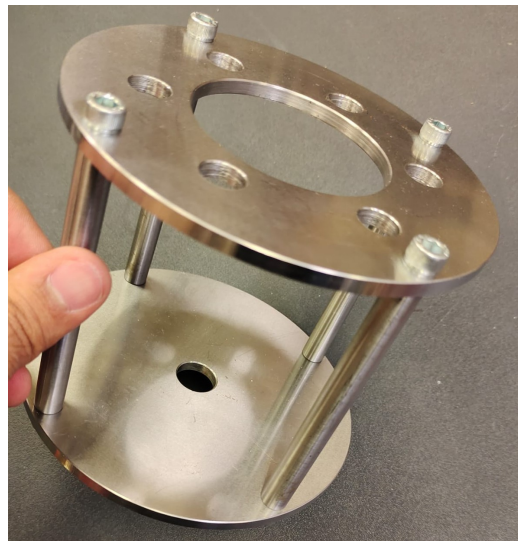


Figure 8.5: Manufactured and assembled thruster assembly. Source: Own.

7. **Support assembly:** The Support plates consist of 2 parts - Ring clamps and bend support plates. To conserve the cost of manufacturing, the mild steel sheet was procured separately, and the sheet metal machining, including cutting, bending, drilling, and fitting, was performed completely by the team.



Figure 8.6: Manufactured bend support plate. Source: Own.

This setup was tested with the combustion chamber for correct alignment through the length of the combustion chamber and tested with brute pull force.

8. **Graphite nozzle:** The graphite nozzle is manufactured and delivered to the team from external manufacturers. It has been verified for correct dimensions and has been used for correcting the fitting for the nozzle and the steel nozzle casing.
9. **Nozzle casing:** The nozzle casing is manufactured and modified for correct fitting with the manufactured and procured graphite nozzle. The 2 radial O-rings are also put and considered in the fitting so as to satisfy their 20% compression criteria.

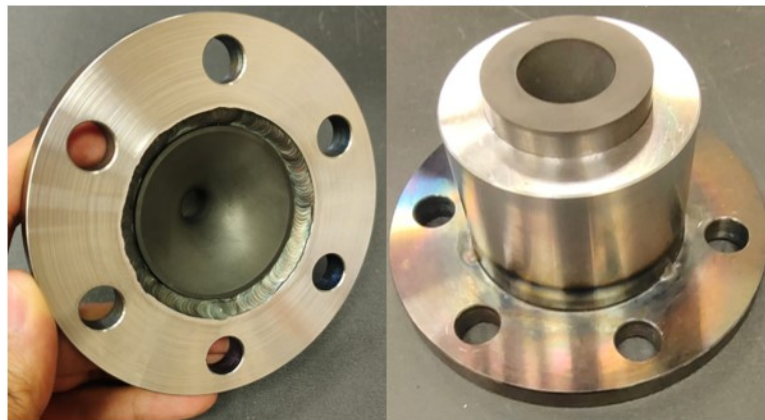


Figure 8.7: Manufactured and assembled nozzle sub-assembly. Source: Own.

10. **Feed line system:** The components for the feed system have been procured, and the cutting of steel pipes, joining with the adapters and valves, and the overall fitting has been initiated and is planned to be completed by the next week. This includes the connection to the 3 different tanks to the combustion chamber, the connection between the main oxidiser tank and the run tank, and the safety nets for the system. This will be tested thoroughly with the help of cold flow testing for the whole feed line system to check for any leaks or potential failures that will be reinforced.
11. **Controls and data acquisition system:** The Control Box has been assembled, integrated and tested by the test facility's supervision team and the student team. The control box will be in the safe operating room in the test house. This will be connected with a long tether for the power supply in the facility.

The Data Acquisition system has been developed and tested in 3 separate circuits by the student team separately that are, Load cell circuit, Thermocouple circuit, and Pressure transducer circuit. The connections are made and soldered to the component electronics, which will be housed inside a 3D-printed box fixed onto the nearby test bed tower. This sub-system will be assembled with the rest of the whole ensemble during the final assembly and integration of the system in the test house. This is further discussed in the next chapter on Engine Setup [9](#).

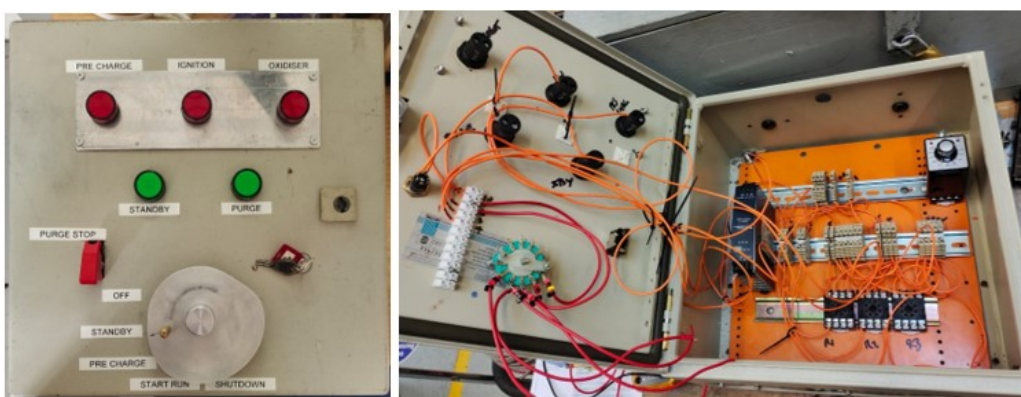


Figure 8.8: Assembled control box. Source: Own.

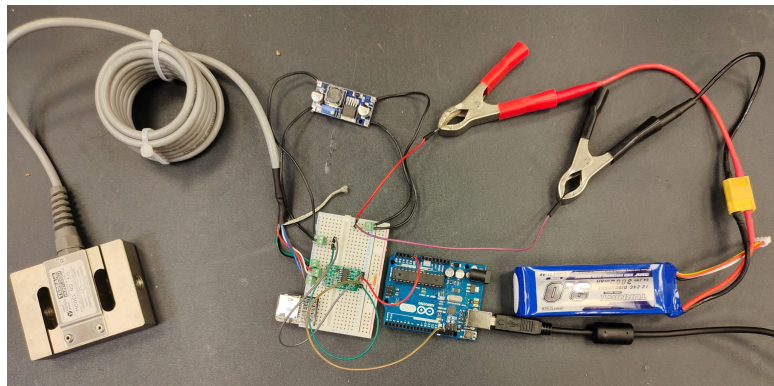


Figure 8.9: Assembled data acquisition system for the load cell. Source: Own.

12. Off-the-shelf components used: The team decided to use some components directly as OEM parts. They are –

- O-rings
- Engine liner
- Gasket
- Bolts and fasteners
- Electronics and Feed system (except for length cut of pipes)

13. Assembly and integration: The assembly will be performed by the members and the test facility supervision team. The team was able to manufacture all parts as depicted in figures 8.1 to 8.9. The assembly and integration is a long process that starts with the manufacturing phase for interface compatibility of the designed components and checking for the tolerance relations for the interacting components. This has been covered in-depth in the next chapter on Engine setup 9.

8.2 Manufacturers used

The manufacturing for the main combustion chamber assembly is primarily conducted by the manufacturing department and workers of the Cranfield University Test facility, with the guidance of the design team.

The structural assembly of the engine and the fuel sub-assembly is conducted in a separate area. The final assembly and integration of the test stand, controls and electronics, and the feed line system are being performed at the Test house by the team.

For the nozzle, Erodex Ltd. firm has been employed for the CNC machining of the graphite C-D bell nozzle. The graphite was integrated with the engine in the initial phase during the fitting of the nozzle in the steel nozzle casing for the structure sub-assembly integration. The fitting was performed by the university's manufacturing team by varying the tolerance of the nozzle casing to ensure tolerance fit for the nozzle sub-assembly.

The fuel blocks of 350 mm in length have been divided into 2 halves for ease of machining for boring through the billet on a lathe machine. At the same time, the assembly of fuel blocks, cork liner, and adhesive has been conducted by the team themselves.

The Test stand was initially manufactured by the test facility manufacturing team last year. However, it has been modified for this year to make it compatible with the Race to Space ICD document specified interface by the team.

The feed line pipe cutting, joining and assembling are being carried out by both the team with the assistance of the supervision team at Cranfield's Test facility.

8.3 Assembly overview and Sub-assembly testing

The final assembly shall be performed in the Test facility of Cranfield University, which has a dedicated control room with an integrated blast window. The image attached below shows the test house assigned for our team's use.

For assembling sub-systems of feed and controls, and subsequent separate testing shall be performed in the CranSEDS Lab under the CranSEDS club.

The overall engine set-up, assembly and testing are described in depth in the next chapter [9](#).



Figure 8.10: Test House for Assembly and Fire Testing. Source: Own.

8.3.1 Hydrostatic Pressure Testing

Hydrostatic pressure testing was conducted to ensure the high-pressure value of 50 bars can be endured by the combustion chamber without any leakage. To perform this test, a separate pair of end flanges were designed and manufactured. These flanges were specially developed for the chamber's pressure testing. The flange on the nozzle side is completely sealed. While the flange on the injector side incorporates a tapped hole for connecting the pressure feed line. This will be used to push water into the closed combustion chamber, and the pressure will be raised up to 50 bars. This will be held for a while at 50 bars to observe for any leakage or dripping. The manual pressure testing machine used is displayed in figure [8.11](#) and in appendix [11.8](#). The setup connected this machine with the fixed chamber in an upright position. The pressure testing was successful.



Figure 8.11: Pressure testing on the combustion chamber. Source: Own.

The pressure-tested combustion chamber has been etched as shown in figure 8.12, and the cold flow test will be completed before the competition. It is further discussed in the next section.



Figure 8.12: Pressure tested combustion chamber. Source: Own.

A detailed testing procedure planned by the team has been attached in the next chapter's section 9.2.

8.3.2 Cold Flow Testing

A separate sub-assembly testing needs to be performed in this phase. This test aims to test the feed line system and the flow of the oxidiser through the injector plate into the combustion chamber. For this, the whole feed line system is set up, and the thruster assembly and the injector plate are connected to the test stand.

Since it is a test and to avoid any wastage of the oxidizer, pressurized water is used instead of nitrous oxide. This setup simulates and checks the flow of the oxidiser through the injector plate. This test aids in observing the showerhead flow, properties and the force exerted by the flow itself (if any). The setup for this test is in the progress of its development and will be tested out by the end of June 2023.

Chapter 9

Engine Setup and Hot-Fire Sequence

9.1 Engine Integration

The assembly, integration and testing (AIT) phase of the project began in May 2023, with the successful assembly of the engine combustion chamber and thruster assembly. This temporary assembly aids in aligning the self-manufactured bending support plates onto the test stand. Once performed, the structural part of the test stand is complete. The images taken during the setup phase have been attached in Appendix 11.8. The section is sub-divided into 3 categories:

9.1.1 Engine Structure

- The injector houses an axial O-ring creating a seal between the injector and the injector flange. The graphite nozzle is pushed inside the nozzle casing with 2 radial O-rings.
- The combustion chamber sub-assembly consists of 2 end flanges welded on the ends of the combustion chamber casing and the solid fuel with its lining inside the casing.
- The liner is of cork, hardened by a special cork adhesive and hardener solvent. This mixture is spread out on one side of the liner, which is folded on the solid fuel bars. This is put in place using 3D-printed fixtures to hold it in place until the adhesive is cured. Once cured, the fuel block sub-assembly is ready to be assembled with the system.
- The nozzle sub-assembly and the injector sub-assembly is connected to the combustion chamber sub-assembly with solid fuel and liner inside of it.



Figure 9.1: Engine test stand structure assembly. Source: Own.

9.1.2 Feed Line System

- The feed line sub-system consists of 3 lines coming from the Nitrous oxide tank, Nitrogen tank and Oxygen tank.
- As to fulfil the need for a flame restrictor on the nitrous oxide line, the design was updated after talks with BOC and the university technicians to incorporate a separate run tank between the main nitrous oxide tank and the combustion chamber.
- So, the main nitrous oxide tank is regulated to let about 1.2 litres in the run tank. This connection is manual and performed before commencing the test firing.
- This run tank is directly connected to the combustion chamber using pressure actuated valve, which is triggered by a separate line of nitrogen gas with a solenoid valve to trigger the pressure-actuated valve. The valve on this line is normally closed.
- A similar configuration is used for the Nitrogen purge line as well. The pressure-actuated valve is triggered by flowing nitrogen gas through it. This valve is normally open to purge the whole system in case anything goes sideways and the power supply is cut off.
- The oxygen line is at low pressure, just for recharging, and hence incorporates only a normally closed solenoid valve.
- The nitrous oxide tank, run tank, and oxygen tank also have a burst valve for safety reasons.
- The 3 gas lines merge onto a 4-way connector, feeding into the combustion chamber through the outside of the injector plate. The connection has been designed according to the specifications given in the ICD document ([6]) by the Race to Space competition.
- The feed system overview schematic is described in figure [5.17](#).

9.1.3 Controls and DAQ System

- The control box is one of the most crucial components for the test firing, and its assembly of it shall adhere to strict and precise arrangements.
- The electrical parts are put in the available big control box connected to the electrical AC supply regulator. These are, in turn, connected to the switches mounted on the top face of the box, with their connecting ports below the box lid to make internal connections. It shall be ensured that the wiring is done, keeping frequent opening and closing of the box lid.
- The control box has a 4-way switch to actuate one of the 4 sub-circuits according to the test firing sequence. These phases are: Standby, Pre-charge, Start/Run, and Shutdown. They will, in turn, allow their respective circuit to be operational, and the firing sequence can be correctly continued.
- The schematics of the control box are shown in figures [5.18](#) and [5.19](#). The assembled control box is displayed in figure [9.2](#).

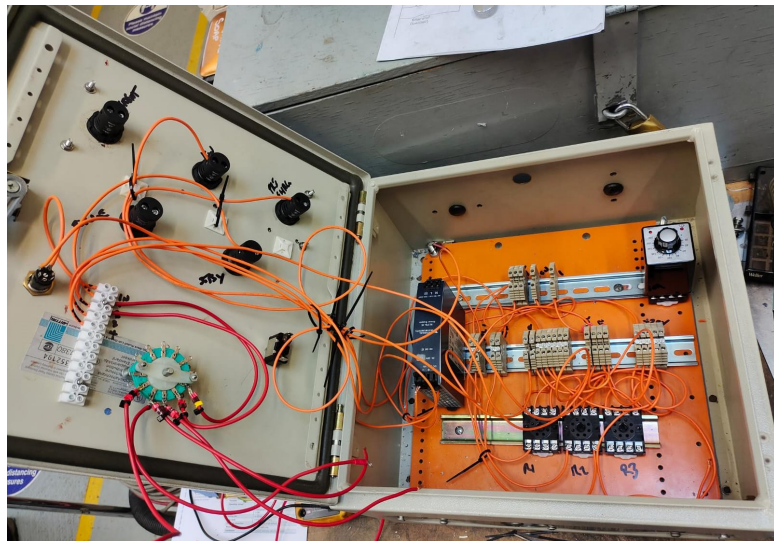


Figure 9.2: Assembled Control Box. Source: Own.

- For the data acquisition system, the red-designed slots and positions are correctly manufactured and ready to be placed.
- The load cell is fastened and acts as the connection between the combustion chamber assembly and test stand, acting as the thrust carrier.
- The thermocouples are sealed inside their respective slots using high-grade silicone sealant.
- The pressure transducers are screwed down to the tee connector for the feed line and the adapter on top of the combustion chamber's end flange.
- Although the electrical connections were made separately for testing the circuit, it is rewired with long wires to mount the data loggers and Arduino board on the adjacent tower. This process took a little bit of on-site work with long wires cutting into place.

9.2 Manufacturing: Test-Firing Procedure and Operations

A preliminary procedure for the hot test-firing was developed so the operators follow the correct procedure in a checklist manner, and safety is ensured.

9.2.1 Combustion Sequence Overview

The combustion chamber casing is separated from the bottom injector plate attached using bolts. The combustion chamber is closed and properly sealed with different components (Injector coin, nozzle, ceramic coating inside) intact using retainer rings, gasket, and sealants. The whole assembly is then fixed to the test table. The following subsections discuss the assembly, maintenance, safety, and test preparations.

9.2.2 Assembly and maintenance

Fuel Preparation

Procedure:

1. Take the 2 part machined solid blocks of HDPE, both of which are 175 mm long, and the cork liner.
2. The cork liner is 1 mm thick, so at least 4 layers will be required to fix the fuel inside the combustion chamber. Cut the cork such that it only completes one whole revolution around the fuel blocks.
3. The cork liners will be 375 mm long, encompassing the solid fuel part of 350 mm and the pre and post-combustion chamber lengths.
4. The liner and the fuel blocks will be fixed into position using industrial-grade adhesive mixed with a hardener. This will fix the blocks relative to the liner sheets and fix the liner sheets with each other. This also aids in hardening the soft cork liner to provide structural rigidity.
5. Wait until the adhesive in this liner and fuel block assembly is cured.
6. Now spread a very small amount of adhesive into the combustion chamber when starting to put the fuel block in the chamber.
7. While fastening the injector plate on one side of the combustion chamber, pass on the fuel and liner block through the nozzle side. The adhesive layer will bind the cork liner to the combustion chamber, thus fixing its position.

Chamber Assembly

Prerequisites: Fuel Preparation Procedure [9.2.2](#).

Procedure:

1. Ensure the horizontally stable position of the combustion chamber.
2. Attach the nozzle sub-assembly to the end of the combustion chamber.
3. Once the prerequisites are fulfilled, and the combustion chamber is assembled, connect it with the thruster assembly and the load cell, which will then complete the single-line assembly.
4. Put the 2 ring clamps around the combustion chamber and tighten them until the chamber is fixed and collinear with the lower straight bar of the test stand.
5. Now take this to the site and the test bench, where the stand needs to be bolted down tightly.
6. Place the screws two by two in opposite positions. Tighten without reaching the stop. Once they are all positioned and tightened, give the last torque adjustment to all of them two by two in opposite positions.
7. Connect the 1/2 inch BSP parallel connection between the feed line output and the injector mouth.
8. From the assembled circuit for the load cell, connect the 6 wires from the load cell to the board and secure the electronics in position on the tower.
9. Screw in both the pressure transducers and plug their output into their respective data loggers.
10. Use silicone sealant to fix the 5 thermocouples on the combustion chamber and the nozzle. Wait until it's cured. (Do this step earlier so there will not be a need to wait at the test site. Possibly 8 hours prior.)
11. With the assembly completed, the safety and inspection phase can be initiated.

9.2.3 Safety Checks

Prerequisites: None; can be done at any time.

Procedure:

1. Ensure N₂O Tank charged to > ((min pressure))
2. Check N₂ Tank charged to > ((min pressure & 5 bar > N₂O tank pressure))
3. Check PI and PX coherent
4. With Feed Sys Manual Isolation Vv SHUT, set Feed Sys EAV to OPEN and check OPEN; SHUT EAV and check SHUT
5. With Purge Sys Manual Isolation Vv SHUT, set EAV to OPEN and check OPEN; SHUT EAV and check SHUT

9.2.4 Run System

Prerequisites:

1. PXX Safety Checks
2. PXX Fuel Preparation
3. Suitably qualified and experienced personnel on hand at the firing site
4. University Fire Safety notified
5. Area cleared and marked to reduce risk to bystanders
6. All teams give the OK on their systems to the Run Coordinator
7. Fire extinguishers on hand

Procedure:

1. Ensure Feed Sys EAV SHUT and Purge Sys EAV SHUT
2. Ensure N₂O tank Feed Vv SHUT
3. Check N₂O tank pressure ((ok))
4. Check N₂ tank pressure ((ok))
5. Assemble Arduino circuit with arc-ignitor
6. Insert SIM Card in the circuit board
7. Mount the Assembly adjacent to the pre-combustion chamber
8. Place the wire fuse inside the arc ignitor
9. OPEN N₂O tank Manual Isolation Vv and OPEN N₂ tank Manual Isolation Vv
10. Evacuate firing chamber
11. Initiate ignition via Text Message: “Fire”

12. OPEN Feed Sys EAV
motor runs
13. SHUT Feed Sys EAV
14. OPEN Purge Sys EAV
run purge
15. SHUT Purge Sys EAV
16. Check fire out
17. Ventilate firing chamber (if indoors; open doors); safe to re-enter
18. SHUT Purge Sys and Feed Sys Manual Isolation Vvs
19. Remove the SD card from Arduino and disassemble the circuit.
20. Note down final N₂O and N₂ tank pressures

Chapter 10

Knowledge Transfer Plan

The knowledge transfer plan for the team is absolutely crucial, which is engraved by the student's situation of being enrolled in the University for only 1 year as a graduate student. A lot of members apply and enrol for external internships after 6 months of coursework, which makes it difficult for the team to keep the project rolling with a correct procedural plan for the upcoming students next year. The team is dependent upon the new members' interest in pursuing to keep the team alive.

However, the current team has discussed and set out some essential plans to deal with this scenario for the betterment of the project, team, and team members, both old and new. The new students are inducted and steered to join the team with the help of open days, introductory sessions, social events, and intra-university activities for the students.

Once in, the following methodology will be used to transfer essential materials and skills so that the students can take up the big role of designing, manufacturing and testing a scaled-up hybrid engine in the university, and participate in the Race to Space UK competition within a span of less than 1 year.

1. The new members will be provided with all the official documents, team meeting minutes, progress reports, essential emails, post-event reports, videos, and literature with important sections marked that will be directly beneficial for them during designing and manufacturing.
2. At the start of the team induction, the old team will hold a 2-day workshop for the new team members to provide them with an overview of the work done last year and the information that may be essential for them to start working.
3. The team cannot summarize everything in just 2 days, especially if the team will manufacture after 5-6 months. For this, the team members have individually decided to assist the new team by making themselves available for monthly or bimonthly progress and doubt clearance sessions.
4. IN the documents and videos provided to the new team, a separate document of lessons learnt at every stage of the project, since inception, through design, updates, manufacturing, procurement, testing, competition, management, and running the team will be compiled in this document comprehensively, to train the new team to avoid them repeating the same mistakes, or facing the same issues and wasting their crucial time and effort.
5. Through our initiative of keeping in contact to the new team, we act purely as team mentors and aid them through inevitable problems they will face throughout the year, including designing, manufacturing, testing, procurement, sponsorships, dealing with administration, and in general managing their coursework with the team.

The team strive for a proper and adequate balance so that everyone in the team and the project can grow simultaneously. As the current team has gone through the same struggle managing the team, and other aspects, we become the prime source for the new team to learn from, grow, and start working themselves.

The knowledge transfer documents are in the process of development and will be completed sometime after the event, including the complete cycle of the project, and everything related to the team shall be passed to the members for their disposal and reference.

Bibliography

- [1] CranSEDS Hybrid Rocket Motor and Test Stand Team. Cranseds - critical design review: Hybrid rocket motor test stand, 2021.
- [2] Guobiao Cai, Hao Zhu, Dalin Rao, and Hui Tian. Optimal design of hybrid rocket motor powered vehicle for suborbital flight. *Aerospace Science and Technology*, Volume 25, 2013.
- [3] Francesca Heeg, Lukas Kilzer, Robin Seitz, and Enrico Stoll. Design and test of a student hybrid rocket engine with an external carbon fiber composite structure. *Aerospace*, Volume 7, 2020.
- [4] Richard M. Newland. *The science and design of the hybrid rocket*. Lulu.com, 2017.
- [5] Jungpyo Lee, Artur Elias De Moraes Bertoldi, Artem Andrianov, Renato Alves Borges, Carlos Alberto Gurgel Veras, Simone Battistini, Takakazu Morita, and Patrick Hendrick. Role of pre-combustion chamber design in feed-system coupled instabilities of hybrid rockets. *Journal of Propulsion and Power (JPP)*, Volume 36, Issue 6, 2020.
- [6] Race to Space (R2S) UK. Ail j1 nirous oxide test rig, 2023.
- [7] Ronald W.Humble, Gary N. Henry, and Wiley J. larson. *Space Propulsion Analysis and Design*. Space Technology. The McGraw Hill Companies, Inc. Primis Custom Publishing, 1995.
- [8] Engineering Toolbox. Pipes - nominal wall thickness, 2008.
- [9] Benjamin S. Waxman, Jonah E. Zimmerman, Brian J. Cantwell, and Gregory G. Zilliac. Mass flow rate and isolation characteristics of injectors for use with self-pressurizing oxidizers in hybrid rockets. *American Institute of Aeronautics and Astronautics*, 2013.
- [10] RIT Launch Initiative Hybrid Rocket. Injector design process, injector, propulsion, engine specifications, 2018.
- [11] Roebuck. Zeus precision data charts and reference tables for drawing office toolroom & workshop, 2021.

Chapter 11

Appendices

11.1 Sub-System Requirements

11.1.1 Structures

Figure 11.1: Sub-System Requirements: Structures (HY-2XXX)

ID	Requirement	Description
Structures – General (2000)		
2001	Movability	The structure shall be movable from an indoor storage facility to an outdoor test site.
2002	Dimensions	Maximum dimensions shall not exceed medium-size facility; L=5 m, l=2 m, h=2 m.
2003	Safety	A protective structure shall be provided between the motor and feeding system.
2004	Structures cost	All material decisions shall consider a cost minimising parameter, ensuring the remaining drivers are kept within acceptable ranges.
Structures – Test Stand (2100)		
2101	Horizontal test	The test stand shall be designed for horizontal static fire tests.
2102	Thrust measurement	The test stand shall include a mechanism to ensure safety of thrust measuring device while it measures the thrust.
2103	Max. thrust	The test stand shall withstand a maximum load of 1.5 kN of thrust.
Structures – Combustion Chamber (2200)		
2201	Safety factor	Structural strength of the combustion chamber shall include a safety factor, a minimum value of FOS = 1.5.
2202	Insulation	Structure of the combustion chamber shall include internal insulation.
2203	Sensor placement	The Combustion Chamber shall include specific safe places for sensors and control systems.
2204	Temperature	The Nozzle and combustion chamber must be able to accommodate the temperature and pressure during the burn stage without failing.
Structures – Oxidiser Tank (2300)		
2301	Safety	The oxidiser tank shall be safe to operate, compatible with the oxidiser and approved by Cranfield University safety rules and UK legislation.
2302	Oxidiser tank independency	The oxidiser tank shall not be part of the structure to allow for easier mobility.
2303	Oxidiser control	The oxidiser tank shall have an internal independent system of control and regulation.

11.1.2 Propulsion

Table 11.1: Sub-System Requirements: Propulsion (HY-3XXX)

ID	Requirement	Description
Propulsion – General (HY-3000)		
3001	Thrust	The motor shall provide 300 N of thrust.
3002	Burn time	The burn time of each test shall be at least 5 sec.
3003	Thrust monitoring	The thrust of the motor shall be monitored during the testing.
Propulsion – Feeding System (HY-3100)		
3101	Feeding system	The propellant flow in the feeding system into the motor shall be adjustable.
3102	Ignition	The motor ignition system shall be safe through the complete assembly, testing, firing, and post fire phases.
3103	Multiple ignition	The ignition system shall be able to be restarted / reignited.
Propulsion – Propellants (HY-3200)		
3201	Safety of propellant	The propellants shall be environmentally and sanitary safe.
3202	Compliance	The selected propellants shall be compliant to the standards of the test facility, Cranfield University and of the UK Government.
3203	Propellant selection	The propellant choice shall consider a cost minimising parameter, ensuring all the other parameters are within acceptable ranges.

11.1.3 Controls

Table 11.2: Sub-System Requirements: Controls (HY-4XXX)

ID	Requirement	Description
Control – Electronics Design (HY-4000)		
4001	Digital signals	The control of the rocket motor shall be provided by means of digital signals.
4002	Control interface	The control interface shall include an easy to access emergency, shut-off button.
4003	Oxidiser mass flow rate	The oxidiser flow rate shall be measured.
4004	Combustion chamber temperature	The combustion chamber temperature shall be measured.
4005	Combustion chamber pressure	The internal pressure in the combustion chamber shall be measured or derived from alternative measurements.
4006	Measured thrust	The thrust output shall be measured. (linked to req. HY-2102)
4007	Computer safe distance	The control computer shall be located at a safe distance of 5 m from the test stand, inside the control room.
Control – Software Design (HY-4100)		
4101	Controller	The controller input signal(s) shall not exceed actuator physical limitations.
4102	Live data	The acquired data shall be stored and fed back directly to compute live graphical data.
Control – Avionics Design (HY-4200)		
4201	Oxidiser flow	The oxidiser flow to the main chamber shall be electrically controlled by an independent control mechanism.
4202	Inert components	All avionic components in contact with the oxidiser or the combustion flow shall be inert.
4203	Fire suppression	The avionics circuit shall include a fire suppression system to ensure the motor can be shut down in case of an emergency.

11.2 Engineering Drawings

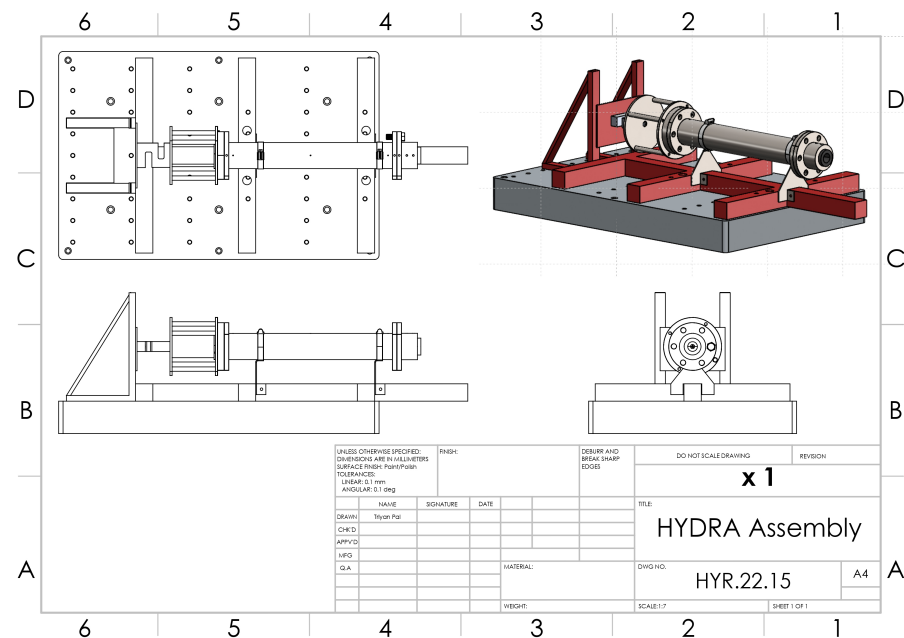


Figure 11.2: Hybrid Engine Assembly on Test Stand. Source: Own.

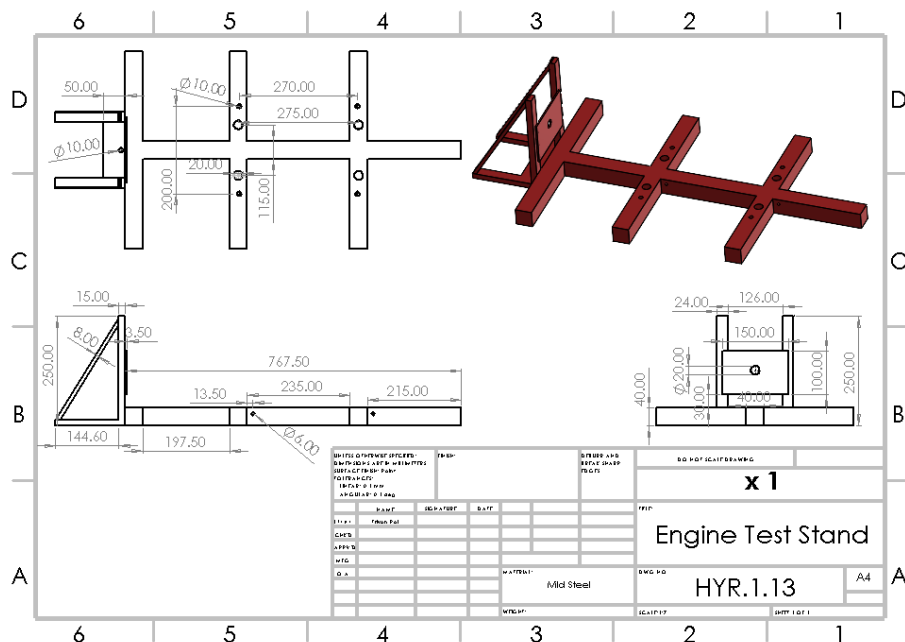


Figure 11.3: Engine Test Stand. Source: Own.

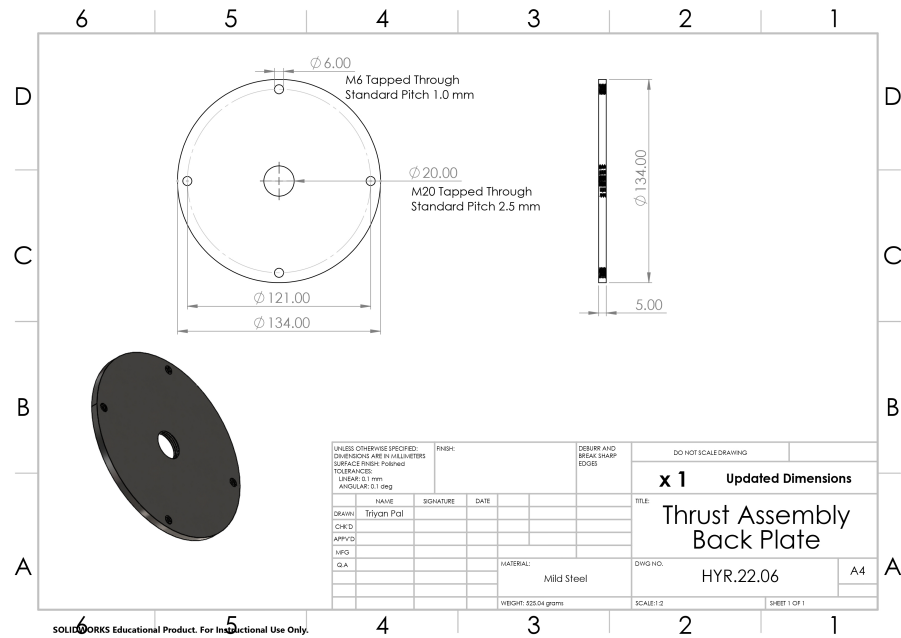


Figure 11.4: Thrust Adapter Rear Plate. Source: Own.

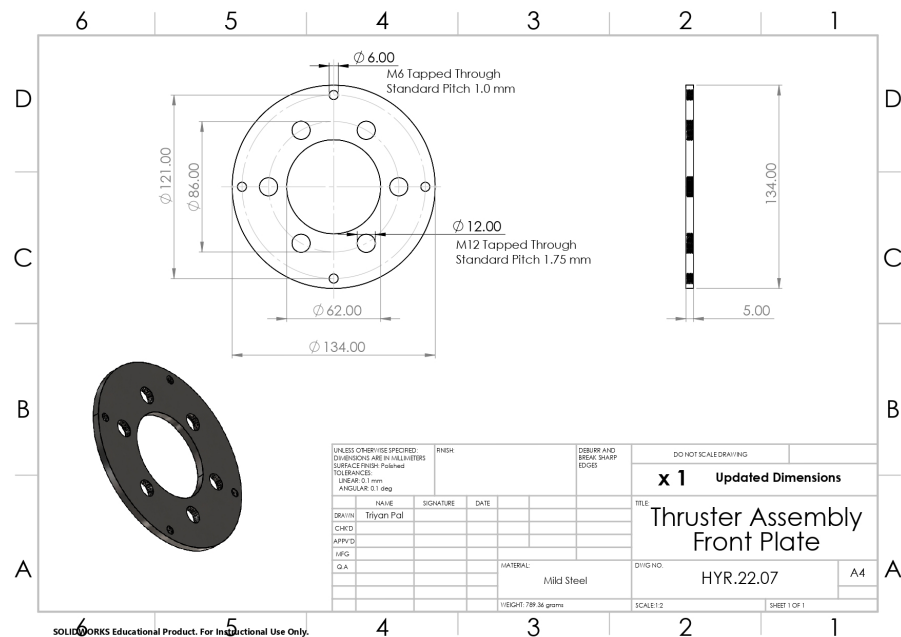


Figure 11.5: Thrust Adapter Front Plate. Source: Own.

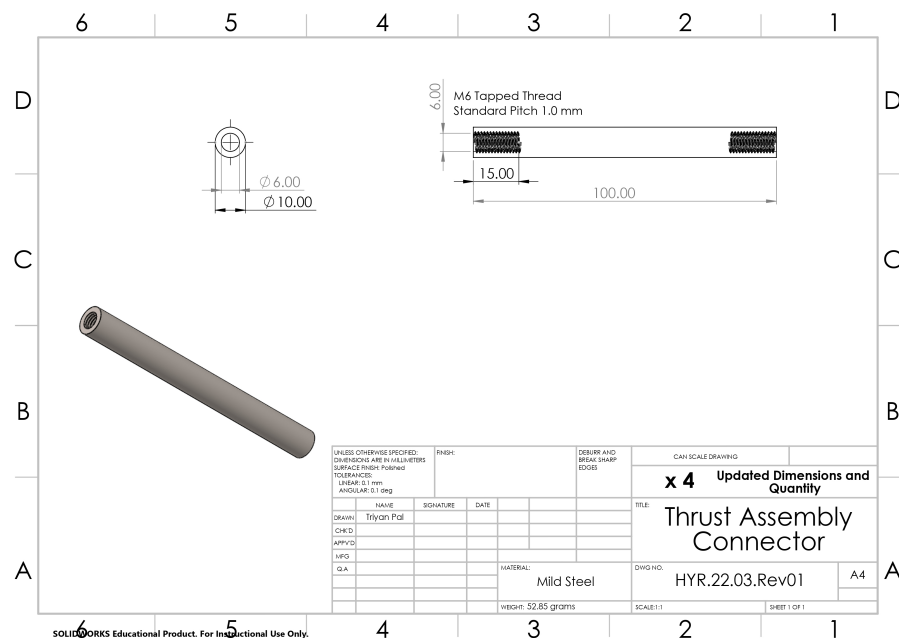


Figure 11.6: Thrust Adapter Connecting Tie rods. Source: Own.

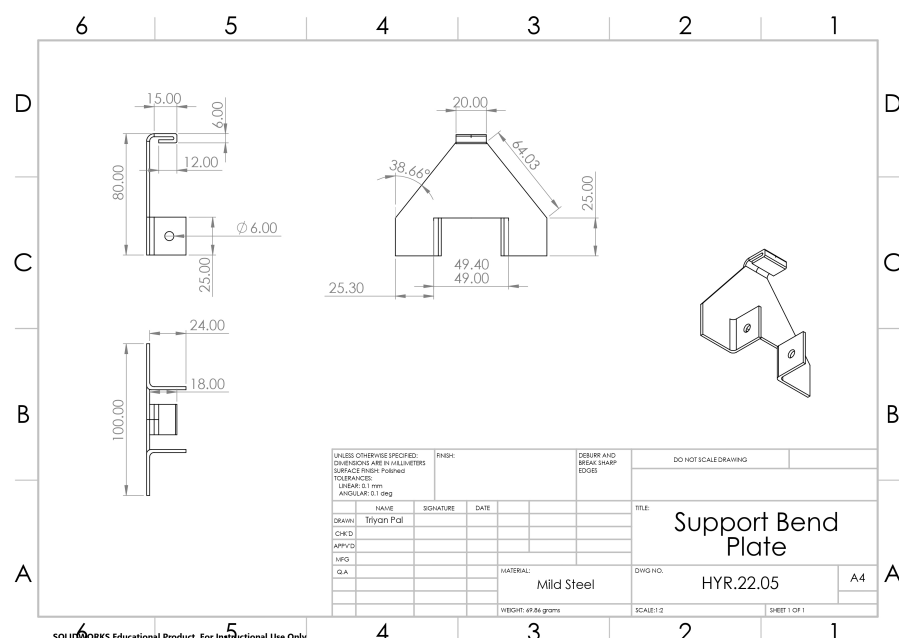


Figure 11.7: Engine Chamber Ring Clamp System Support Plates. Source: Own.

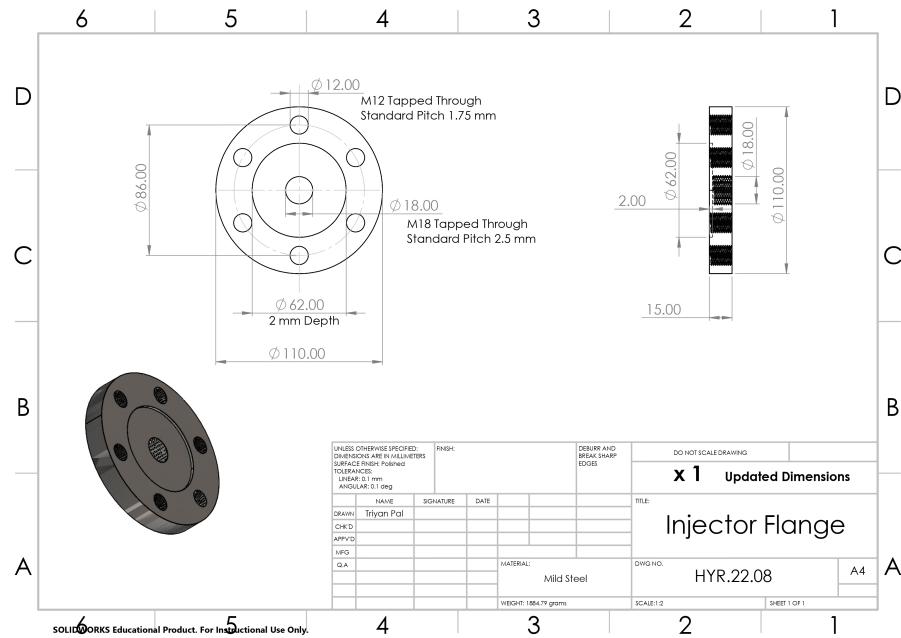


Figure 11.8: Engine Injector Flange. Source: Own.

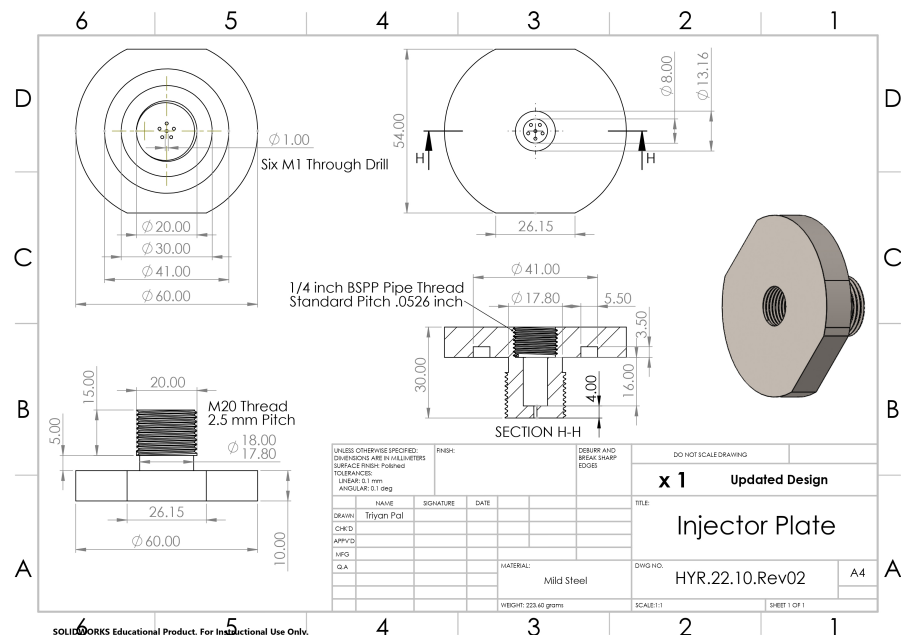


Figure 11.9: Engine Injector Plate. Source: Own.

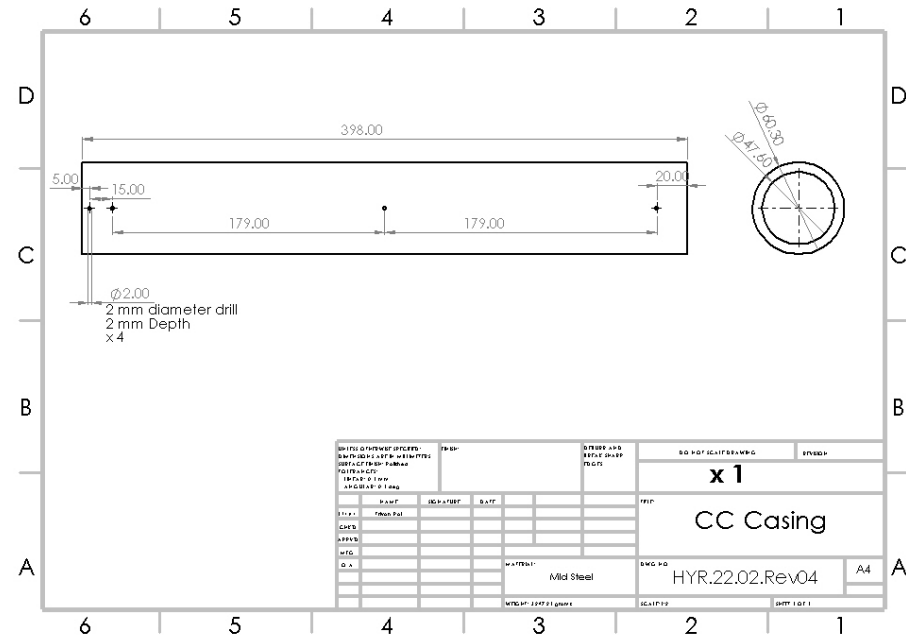


Figure 11.10: Combustion Chamber Casing. Source: Own.

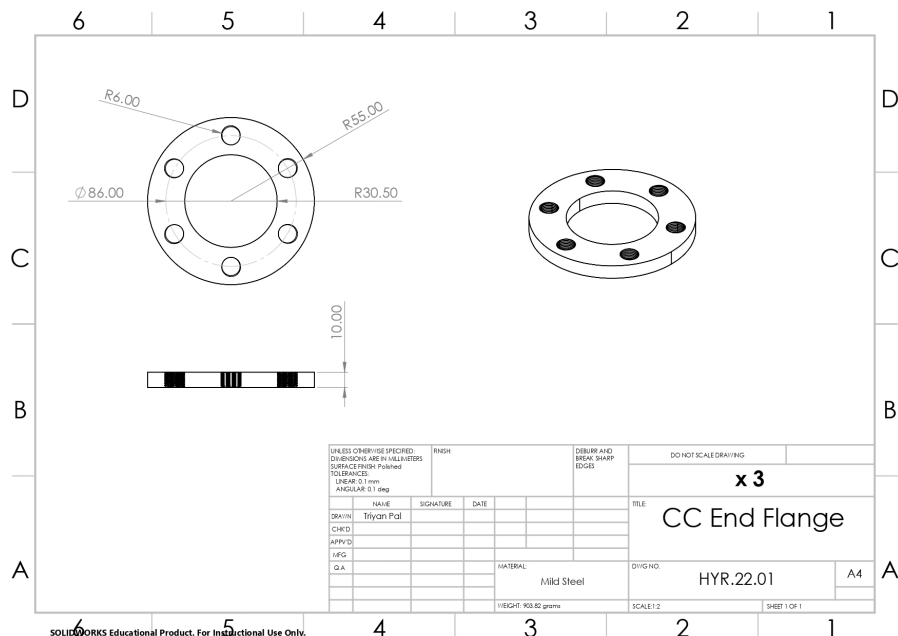


Figure 11.11: Combustion Chamber Casing End Flanges. Source: Own.

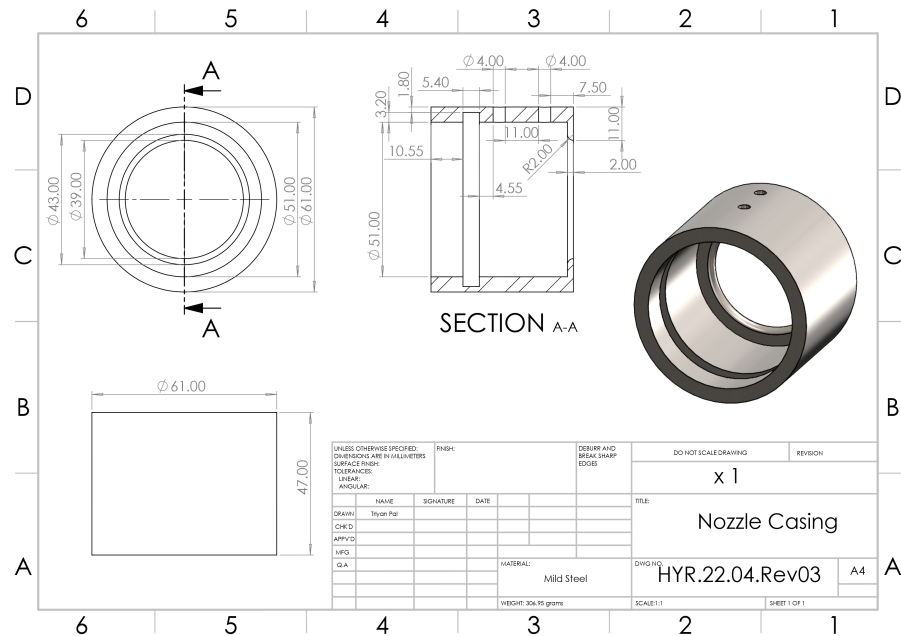


Figure 11.12: Metal Nozzle Casing. Source: Own.

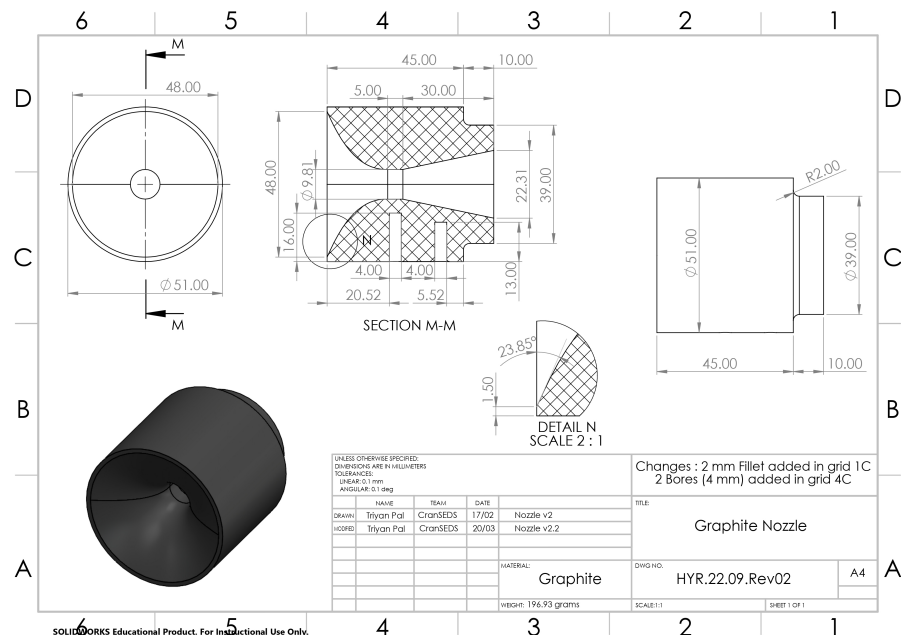


Figure 11.13: Graphite Nozzle. Source: Own.

11.3 Material Datasheets

11.3.1 Graphite Datasheet

Typical Property	Test Standard	Unit	Value
Average Grain Size	ISO 13320	µm	10
Bulk Density	DIN IEC 60413 / 204	g/cm³	1.83
Open Porosity	DIN 66133	Vol.%	10
Medium Pore Size	DIN 66133	µm	1.8
Permeability (Air at 20°C)	DIN 51935	cm²/s	0.06
Rockwell Hardness HR _{10/100}	DIN IEC 60413 / 303		90
Specific Electrical Resistivity	DIN IEC 60413 / 402	µΩm	13
Flexural Strength	DIN IEC 60413 / 501	MPa	60
Compressive Strength	DIN 51910	MPa	130
Young's Modulus	DIN 51915	MPa	11.5 x 10³
Thermal Expansion (20- 200°C)	DIN 51909	K⁻¹	4.2 x 10⁻⁶
Thermal Conductivity (20°C)	DIN 51908	Wm⁻¹K⁻¹	105
Ash Content	DIN 51903	ppm	20

*Value might be changed due to material size

11.4 Simulation Output

11.4.1 ProPEP3

Isp*	206.3573
C*	5329.005
Density	0.0626778
Molecular Wt.	26.58859
Chamber CP/CV	1.238274
Chamber Temp.	3553.142

Figure 11.14: Simulation Outputs. Source: Own.

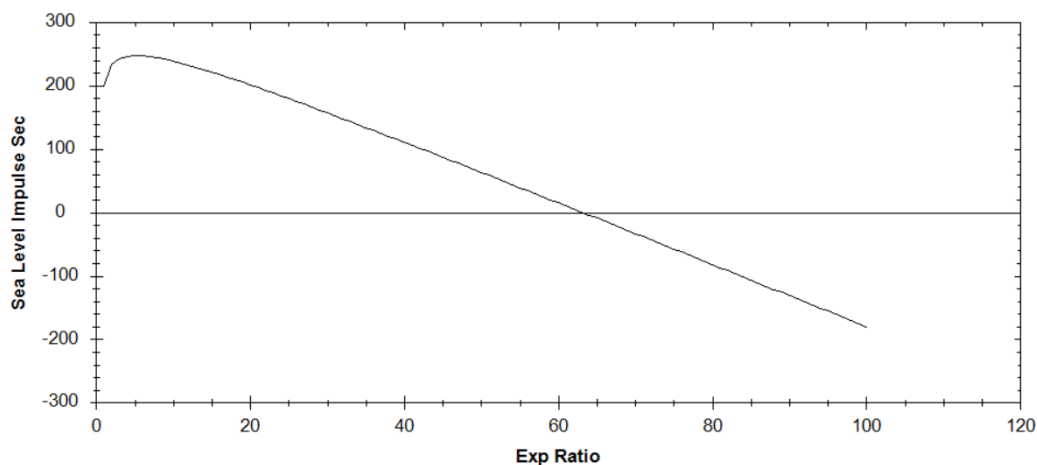


Figure 11.15: Nozzle Impulse vs Expansion Ratio response curve. Source: Own.

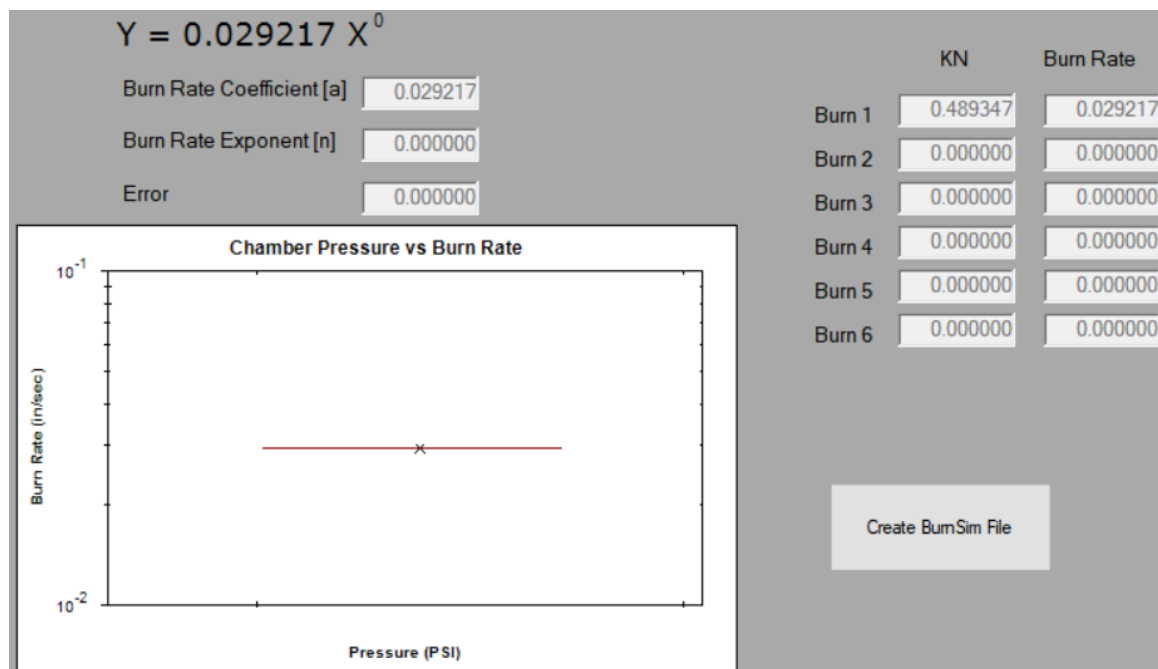


Figure 11.16: Chamber Pressure vs Burn Rate Results. Source: Own.

ProPEP 3 Simulation Output File: CranSEDS HYDRA

Code	WEIGHT	D-H	DENS	COMPOSITION
O NITROUS OXIDE	905.300	443	0.07140	2 N 1 O
O POLYETHYLENE	119.100	-453	0.03250	2 C 4 H

THE PROPELLANT DENSITY IS 0.06268 LB/CU-IN OR 1.7349 GM/CC

THE TOTAL PROPELLANT WEIGHT IS 1024.4000 GRAMS

NUMBER OF GRAM ATOMS OF EACH ELEMENT PRESENT IN INGREDIENTS

16.981540 H
8.490768 C
41.135040 N
20.567520 O

*****CHAMBER RESULTS FOLLOW *****

T(K)	T(F)	P(ATM)	P(PSI)	ENTHALPY	ENTROPY	CP/CV	GAS	RT/V
3553	5936	330.53	4859.00	347.10	2264.20	1.2383	38.528	8.579

SPECIFIC HEAT (MOLAR) OF GAS AND TOTAL = 10.323 10.327

NUMBER MOLS GAS AND CONDENSED = 38.528 0.000

2.034992e+001 N2	6.859846e+000 H2O	4.905532e+000 CO	3.584138e+000 CO2
1.152519e+000 H2	7.077605e-001 HO	4.317968e-001 NO	2.439777e-001 H
2.005943e-001 O2	8.610791e-002 O	1.944782e-003 HO2	6.537487e-004 NHO
4.852437e-004 CHO	4.420799e-004 NO2	4.368680e-004 N	3.348320e-004 N2O
2.501592e-004 NH3	1.902374e-004 NH2	1.574555e-004 NH	7.884222e-005 NHO2
7.091595e-005 NHO2	6.391459e-005 CNHO	6.111898e-005 CNH	2.700755e-005 CH2O

THE MOLECULAR WEIGHT OF THE MIXTURE IS 26.589

*****EXHAUST RESULTS FOLLOW *****

T(K)	T(F)	P(ATM)	P(PSI)	ENTHALPY	ENTROPY	CP/CV	GAS	RT/V
1280	1845	1.00	14.70	-665.47	2264.20	1.2690	37.549	0.027

SPECIFIC HEAT (MOLAR) OF GAS AND TOTAL = 9.375 9.375

NUMBER MOLS GAS AND CONDENSED = 37.549 0.000

2.056727e+001 N2	6.487546e+000 H2O	5.589150e+000 CO2	2.901117e+000 CO
2.0029 H2	2.0029 H2		

THE MOLECULAR WEIGHT OF THE MIXTURE IS 27.282

*****PERFORMANCE: FROZEN ON FIRST LINE, SHIFTING ON SECOND LINE*****

IMPULSE	IS EX	T*	P*	C*	ISP*	OPT-EX	D-ISP	A*M	EX-T
281.9	1.2590	3146	182.86	5202.0	25.41	489.1	0.03328	1077	
293.3	1.1887	3265	187.31	5329.0	206.4	27.61	508.8	0.03410	1280

BOOST VELOCITIES FOR PROPELLANT DENSITY OF 0.06268 (S.G. OF 1.735)

10/ 23316	15/ 19880	25/ 15796	30/ 14422	55/ 10270	60/ 9734
69/ 8906	71/ 8743	88/ 7572	100/ 6925	150/ 5129	175/ 4546
200/ 4084	300/ 2909	1000/ 970	3000/ 335	5000/ 202	5000/ 202

EXP. EXIT EXIT EXIT OPTIMUM OPTIMUM VACUUM VACUUM SEA LV SEA LV

	RATIO	PRESS	PRESS	TEMP	IMPULSE	IMPULSE	IMPULS	IMPULS	IMPULS	IMPULS
	ATM	SI	K	SEC	SI	SEC	SI	SEC	SI	SI
1	187.300	18973.5	3265	112.5	1103	206.4	2024	205.9	2039	
2	62.433	6324.5	2773	184.7	1811	247.3	2425	246.3	2440	
3	21.953	2223.8	2359	226.6	2222	259.6	2545	258.1	2557	
4	14.288	1447.3	2167	239.8	2352	268.5	2633	266.5	2640	
5	10.341	1047.5	2033	248.7	2438	274.6	2693	272.1	2695	
6	7.978	808.2	1931	255.2	2502	279.1	2737	276.1	2736	
7	6.424	650.8	1850	260.2	2552	282.7	2773	279.2	2766	
8	5.334	540.3	1783	264.3	2592	285.7	2802	281.7	2790	
9	4.532	459.1	1727	267.7	2625	288.2	2826	283.7	2810	
10	3.921	397.2	1678	270.6	2654	290.3	2847	285.3	2826	
11	3.442	348.7	1635	273.2	2679	292.1	2865	286.6	2839	
12	3.057	309.7	1597	275.4	2701	293.8	2881	287.8	2851	
13	2.742	277.8	1563	277.4	2720	295.2	2895	288.7	2860	
14	2.480	251.3	1533	279.1	2737	296.5	2908	289.5	2868	
15	2.260	228.9	1505	280.8	2753	297.7	2920	290.2	2875	
16	2.072	209.8	1479	282.2	2768	298.8	2930	290.8	2881	
17	1.909	193.4	1455	283.6	2781	299.8	2940	291.3	2886	
18	1.768	179.1	1433	284.8	2793	300.8	2949	291.7	2890	
19	1.645	166.6	1413	286.0	2804	301.6	2958	292.1	2894	
20	1.536	155.6	1394	287.0	2815	302.4	2966	292.4	2897	
21	1.439	145.8	1376	288.0	2824	303.2	2973	292.6	2899	
22	1.352	137.0	1359	289.0	2834	303.9	2980	292.8	2901	
23	1.275	129.1	1343	289.8	2842	304.5	2986	293.0	2903	
24	1.205	122.0	1329	290.7	2850	305.2	2992	293.1	2904	
25	1.141	115.6	1314	291.5	2858	305.7	2998	293.2	2905	

	EXP.	EXIT	EXIT	EXIT	OPTIMUM	OPTIMUM	VACUUM	VACUUM	SEA LV	SEA LV
	RATIO	PRESS	PRESS	TEMP	IMPULSE	IMPULSE	IMPULS	IMPULS	IMPULS	IMPULS
	ATM	SI	K	SEC	SI	SEC	SI	SEC	SI	SI
26	1.083	109.7	1301	292.2	2865	306.3	3004	293.3	2905	
27	1.030	104.4	1288	292.9	2872	306.8	3009	293.3	2906	
28	0.982	99.4	1276	293.6	2879	307.3	3014	293.3	2906	
29	0.937	94.9	1264	294.2	2885	307.8	3019	293.3	2905	
30	0.896	90.8	1253	294.8	2891	308.3	3023	293.3	2905	
31	0.858	86.9	1242	295.4	2897	308.7	3027	293.2	2904	
32	0.823	83.3	1232	296.0	2902	309.2	3032	293.1	2904	
33	0.790	80.0	1222	296.5	2907	309.6	3036	293.0	2903	
34	0.760	76.9	1213	297.0	2913	309.9	3039	292.9	2902	
35	0.731	74.1	1204	297.5	2917	310.3	3043	292.8	2900	
36	0.704	71.4	1195	298.0	2922	310.7	3047	292.6	2899	
37	0.679	68.8	1186	298.4	2927	311.0	3050	292.5	2897	
38	0.656	66.5	1178	298.9	2931	311.4	3053	292.3	2896	
39	0.634	64.2	1170	299.3	2935	311.7	3057	292.2	2894	
40	0.613	62.1	1162	299.7	2939	312.0	3060	292.0	2892	
41	0.594	60.1	1155	300.1	2943	312.3	3063	291.8	2890	
42	0.575	58.3	1148	300.5	2947	312.6	3065	291.6	2888	
43	0.558	56.5	1141	300.9	2950	312.9	3068	291.3	2886	
44	0.541	54.8	1134	301.2	2954	313.2	3071	291.1	2884	
45	0.525	53.2	1127	301.6	2957	313.4	3074	290.9	2882	
46	0.511	51.7	1121	301.9	2961	313.7	3076	290.6	2879	
47	0.496	50.3	1115	302.3	2964	314.0	3079	290.4	2877	
48	0.483	48.9	1109	302.6	2967	314.2	3081	290.1	2874	
49	0.470	47.6	1103	302.9	2970	314.4	3083	289.9	2872	
50	0.458	46.4	1097	303.2	2973	314.7	3086	289.6	2869	
51	0.446	45.2	1091	303.5	2976	314.9	3088	289.3	2866	
52	0.435	44.0	1086	303.8	2979	315.1	3090	289.1	2864	

53	0.424	43.0	1081	304.1	2982	315.3	3092	288.8	2861
54	0.414	41.9	1075	304.3	2985	315.5	3094	288.5	2858
55	0.404	40.9	1070	304.6	2987	315.8	3096	288.2	2855
56	0.395	40.0	1065	304.9	2990	316.0	3098	287.9	2852
57	0.386	39.1	1061	305.1	2992	316.2	3100	287.6	2849
58	0.377	38.2	1056	305.4	2995	316.3	3102	287.3	2846
59	0.369	37.3	1051	305.6	2997	316.5	3104	287.0	2843
60	0.361	36.5	1047	305.9	2999	316.7	3106	286.6	2840
61	0.353	35.8	1042	306.1	3002	316.9	3108	286.3	2836
62	0.346	35.0	1038	306.3	3004	317.1	3109	286.0	2833
63	0.338	34.3	1034	306.6	3006	317.2	3111	285.7	2830
64	0.332	33.6	1029	306.8	3008	317.4	3113	285.3	2827
65	0.325	32.9	1025	307.0	3010	317.6	3114	285.0	2823

EXP. EXIT EXIT EXIT OPTIMUM OPTIMUM VACUUM VACUUM SEA LV SEA LV
RATIO PRESS PRESS TEMP IMPULSE IMPULSE IMPULS IMPULS IMPULS IMPULS

	ATM	SI	K	SEC	SI	SEC	SI	SEC	SI
66	0.319	32.3	1021	307.2	3012	317.7	3116	284.7	2820
67	0.312	31.6	1017	307.4	3015	317.9	3117	284.3	2817
68	0.306	31.0	1013	307.6	3017	318.1	3119	284.0	2813
69	0.301	30.5	1010	307.8	3018	318.2	3120	283.6	2810
70	0.295	29.9	1006	308.0	3020	318.4	3122	283.3	2806
71	0.290	29.3	1002	308.2	3022	318.5	3123	282.9	2803
72	0.284	28.8	999	308.4	3024	318.6	3125	282.6	2799
73	0.279	28.3	995	308.6	3026	318.8	3126	282.2	2796
74	0.274	27.8	992	308.8	3028	318.9	3127	281.8	2792
75	0.270	27.3	988	308.9	3029	319.1	3129	281.5	2788
76	0.265	26.9	985	309.1	3031	319.2	3130	281.1	2785
77	0.261	26.4	981	309.3	3033	319.3	3131	280.7	2781
78	0.256	26.0	978	309.4	3034	319.5	3133	280.4	2777
79	0.252	25.5	975	309.6	3036	319.6	3134	280.0	2774
80	0.248	25.1	972	309.8	3038	319.7	3135	279.6	2770
81	0.244	24.7	969	309.9	3039	319.8	3136	279.3	2766
82	0.240	24.3	966	310.1	3041	320.0	3138	278.9	2763
83	0.236	24.0	963	310.2	3042	320.1	3139	278.5	2759
84	0.233	23.6	960	310.4	3044	320.2	3140	278.1	2755
85	0.229	23.2	957	310.6	3045	320.3	3141	277.7	2751
86	0.226	22.9	954	310.7	3047	320.4	3142	277.3	2747
87	0.222	22.5	951	310.8	3048	320.5	3143	276.9	2744
88	0.219	22.2	948	311.0	3050	320.7	3144	276.6	2740
89	0.216	21.9	946	311.1	3051	320.8	3145	276.2	2736
90	0.213	21.6	943	311.3	3052	320.9	3147	275.8	2732
91	0.210	21.3	940	311.4	3054	321.0	3148	275.4	2728
92	0.207	21.0	938	311.5	3055	321.1	3149	275.0	2724
93	0.204	20.7	935	311.7	3056	321.2	3150	274.6	2720
94	0.201	20.4	932	311.8	3058	321.3	3151	274.2	2716
95	0.198	20.1	930	311.9	3059	321.4	3152	273.8	2712
96	0.196	19.8	927	312.1	3060	321.5	3153	273.4	2708
97	0.193	19.6	925	312.2	3061	321.6	3154	273.0	2704
98	0.191	19.3	923	312.3	3063	321.7	3155	272.6	2700
99	0.188	19.1	920	312.4	3064	321.8	3155	272.2	2696
100	0.186	18.8	918	312.6	3065	321.9	3156	271.8	2692

11.4.2 RPA

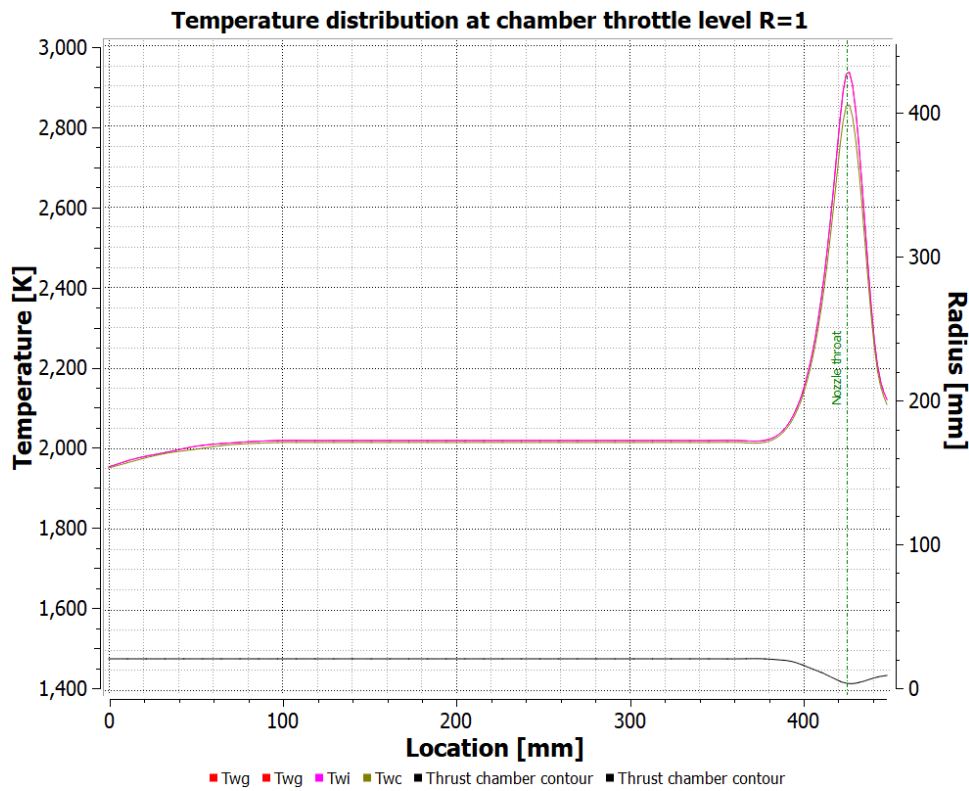


Figure 11.17: Combustion Chamber and Nozzle Stabilized Temperature Curve. Source: Own.

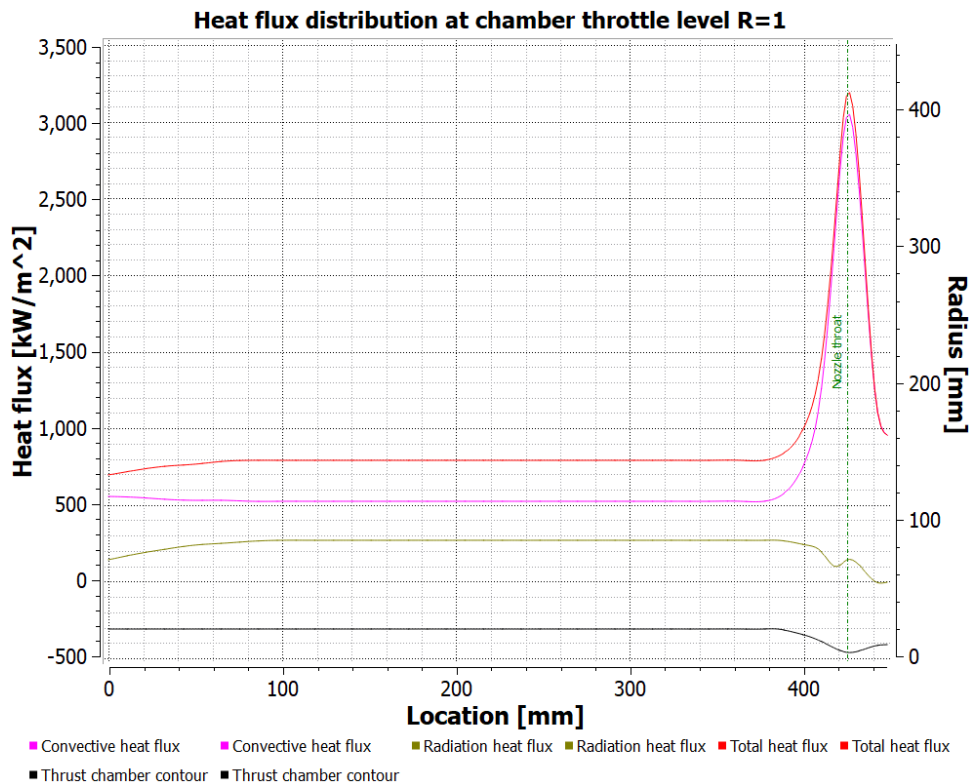


Figure 11.18: Combustion Chamber and Nozzle Stabilized Wall Heat Flux Curve. Source: Own.

RPA Simulation Output File: CranSEDS HYDRA

Results of thermal analysis												
Location , mm	Radius , mm	Conv. heat coeff., k, W/m^2-K	Conv. heat flux, kW/m^2	Rad. heat flux, kW/m^2	Total heat flux, kW/m^2	Twg, K	Twi, K	Twc, K	Tc, K	pc, MPa	wc, m/s	rho, kg/m^3
0	21.63	0.3951	557.2931	140.3894	697.6825	1953.56	1953.56	1950.55	0	0	0	0
16.53	21.63	0.3935	546.812	179.8476	726.6596	1974.48	1974.48	1970.49	0	0	0	0
33.06	21.63	0.3923	538.6516	211.8869	750.5385	1990.91	1990.91	1986.49	0	0	0	0
49.59	21.63	0.3913	532.433	235.3909	767.824	2003.36	2003.36	1997.83	0	0	0	0
66.12	21.63	0.3907	528.3251	253.3255	781.6506	2011.8	2011.8	2006.76	0	0	0	0
82.65	21.63	0.3904	525.8704	264.8663	790.7367	2016.9	2016.9	2012.57	0	0	0	0
99.18	21.63	0.3902	525.0137	267.7489	792.7626	2018.59	2018.59	2013.85	0	0	0	0
115.7	21.63	0.3902	525.0137	267.7489	792.7626	2018.59	2018.59	2013.85	0	0	0	0
132.23	21.63	0.3902	525.0137	267.7489	792.7626	2018.59	2018.59	2013.85	0	0	0	0
148.76	21.63	0.3902	525.0137	267.7489	792.7626	2018.59	2018.59	2013.85	0	0	0	0
165.29	21.63	0.3902	525.0137	267.7489	792.7626	2018.59	2018.59	2013.85	0	0	0	0
181.82	21.63	0.3902	525.0137	267.7489	792.7626	2018.59	2018.59	2013.85	0	0	0	0
198.35	21.63	0.3902	525.0137	267.7489	792.7626	2018.59	2018.59	2013.85	0	0	0	0
214.88	21.63	0.3902	525.0137	267.7489	792.7626	2018.59	2018.59	2013.85	0	0	0	0
231.41	21.63	0.3902	525.0137	267.7489	792.7626	2018.59	2018.59	2013.85	0	0	0	0
247.94	21.63	0.3902	525.0137	267.7489	792.7626	2018.59	2018.59	2013.85	0	0	0	0
264.47	21.63	0.3902	525.0137	267.7489	792.7626	2018.59	2018.59	2013.85	0	0	0	0
281	21.63	0.3902	525.0137	267.7489	792.7626	2018.59	2018.59	2013.85	0	0	0	0
297.53	21.63	0.3902	525.0137	267.7489	792.7626	2018.59	2018.59	2013.85	0	0	0	0
314.06	21.63	0.3902	525.0137	267.7489	792.7626	2018.59	2018.59	2013.85	0	0	0	0
330.58	21.63	0.3902	525.0137	267.7489	792.7626	2018.59	2018.59	2013.85	0	0	0	0
347.11	21.63	0.3902	525.0137	267.7489	792.7626	2018.59	2018.59	2013.85	0	0	0	0
363.64	21.63	0.3902	525.0137	267.7489	792.7626	2018.59	2018.59	2013.85	0	0	0	0
377.09	21.63	0.3902	525.0128	267.4498	792.4626	2018.57	2018.57	2013.66	0	0	0	0
385.35	21.07	0.4116	547.6955	267.7696	815.4651	2033.34	2033.34	2028.12	0	0	0	0
393.61	19.35	0.4915	631.7354	256.0525	887.7878	2078.76	2078.76	2071.67	0	0	0	0
401.88	16.36	0.6875	818.2915	236.5322	1054.8237	2173.71	2173.71	2162.9	0	0	0	0
410.14	11.97	1.2806	1272.8584	190.2449	1463.1033	2370.02	2370.02	2347.26	0	0	0	0
418.41	7.2	3.5035	2296.6816	98.6333	2395.315	2708.45	2708.45	2655.11	0	0	0	0
425	4.42	7.0171	3039.4448	144.4249	3183.8697	2930.84	2930.84	2850.89	0	0	0	0
441.53	8.98	1.0265	1162.5728	-1.7709	1160.8019	2231.46	2231.46	2215.3	0	0	0	0
447.96	10.06	0.7696	956.803	-1.4049	955.3981	2120.74	2120.74	2110.03	0	0	0	0
447.96	10.06	0.8391	1648.048	5.0339	1653.0819	1400	0	0	0	0	0	0

11.5 Temperature Graph Matlab Code

Listing 11.1: Temperature exponential graph calculation code. Source: Own.

```

1 % This code is a property of HRMTS CranSEDS 2022-2023 team.
2 % Author: Triyan Pal Arora
3 % Date: 3rd June 2023
4
5 % This line marks the start of the code for deriving the temperature
6 % evolution with respect to time using its exponential function derived
7 % in
8 % section 5.5: Thermochemistry in the final document report.
9
10 T_a = 0.161; % Temperature constant
11 e=2.71; % Napier's constant
12 t=0:0.001:7; % timestep definition
13 T_cc = T_a*(e.^((t/0.763))); % Exponential temperature evolution equation
14
15 % Plotting the temperature against time for the equation,
16 figure
17 plot(t,T_cc)
18 hold on
19 grid on
20 grid minor
21 xlabel('Time (sec)')
22 ylabel('Combustion temperature (K)')
23 title('Temperature evolution against time')
24 hold off
25
% This line marks the end of the code.

```

11.6 Load cell DAQ Arduino code

Listing 11.2: Load cell DAQ Arduino code. Source: Own.

```

1 // Tedea Huntleigh Load Cell Calibration
2 // Arduino Uno Pinout:
3 // E+ - 5V
4 // E- - GND
5 // S+ - A0
6 // S- - A1
7 // +S - A2
8 // -S - A3
9
10 // Calibration parameters
11 float LOADCELL_OFFSET = 0.0;      // Offset value
12 float LOADCELL_SCALE = 1.0;        // Scale value
13
14 // Known weight for calibration (replace with your own value)
15 const float KNOWN_WEIGHT = 2.779; // Known weight in kilograms
16
17 void setup() {
18     Serial.begin(9600);
19
20     // Print the calibration parameters
21     Serial.println("Load_Cell_Calibration_Parameters:");
22     Serial.print("Offset:_");
23     Serial.println(LOADCELL_OFFSET);
24     Serial.print("Scale:_");
25     Serial.println(LOADCELL_SCALE);
26
27     // Calibrate the load cell
28     calibrateLoadCell();
29 }
30
31 void loop() {
32     // Read the load cell value
33     long value = readLoadCell();
34
35     // Apply calibration
36     float calibratedValue = (value - LOADCELL_OFFSET) / LOADCELL_SCALE;
37
38     // Check if LOADCELL_SCALE is not zero or close to zero
39     if (LOADCELL_SCALE > 0.00001) {
40         // Convert calibrated value to load in kilograms
41         float load = calibratedValue * LOADCELL_SCALE;
42
43         // Print the load value
44         Serial.print("Load:_");
45         Serial.print(load);
46         Serial.println("_N");
47     } else {
48         // Print an error message if LOADCELL_SCALE is zero or close to zero
49         Serial.println("Error:_Load_cell_not_calibrated_properly.");

```

```
50    }
51
52    // Delay for stability
53    delay(1000);
54 }
55
56 void calibrateLoadCell() {
57     Serial.println("Calibrating_Load_Cell...");
58     Serial.println("Please_place_the_known_weight_on_the_load_cell.");
59     Serial.println("Press_any_key_to_start_calibration.");
60
61     // Wait for user input to start calibration
62     while (!Serial.available()) {
63         // Wait for user input
64     }
65     Serial.read(); // Clear the input buffer
66
67     // Read the load cell value with the known weight
68     long value = readLoadCell();
69
70     // Calculate the calibration parameters
71     LOADCELL_OFFSET = value;
72     LOADCELL_SCALE = KNOWN_WEIGHT / (value - LOADCELL_OFFSET);
73
74     // Print the calibration results
75     Serial.println("Calibration_completed!");
76     Serial.print("Offset:_");
77     Serial.println(LOADCELL_OFFSET);
78     Serial.print("Scale:_");
79     Serial.println(LOADCELL_SCALE);
80 }
81
82 long readLoadCell() {
83     // Read the voltage across the load cell
84     // int sensePositive = analogRead(A2);
85     // int senseNegative = analogRead(A3);
86     // int signalPositive = analogRead(A0);
87     int signalNegative = analogRead(A1);
88
89     // Serial.println(sensePositive);
90     // Serial.println(senseNegative);
91     // Serial.println(signalPositive);
92     Serial.println(signalNegative);
93
94
95
96
97
98     // // Calculate the differential voltage
99     // int differentialVoltage = sensePositive - senseNegative;
100
101    // // Adjust the voltage with the signal terminals
```

```
102 // int adjustedVoltage = differentialVoltage - (signalPositive -  
103 // signalNegative);  
104 // // Return the adjusted voltage  
105 // return adjustedVoltage;  
106 return 0;  
107 }
```

11.7 Project Budgets

11.7.1 Cost and Mass Budget

Table 11.3: Cost and Mass Budget

Components	Mass (grams)	Cost (GBP)	Quantity	Net Cost (GBP)	Net Mass (grams)
Adapter Disk 1	530.81	112.40	1	112.40	530.81
Adapter Disk 2	396.24	148.20	1	148.20	396.24
End Flange	900.60	102.16	3	306.48	2701.80
Injector Plate	440.21	402.80	1	402.80	440.21
Injector Flange	945.46	240.80	1	240.80	945.46
Bending Plate	91.15	10.00	2	20.00	182.30
Casing	3107.53	103.80	1	103.80	3107.53
Nozzle Casing	277.50	155.20	1	155.20	277.50
Pressure transducer adapter	20.00	0.00	1	0.00	20.00
Graphite Nozzle	196.93	307.18	1	307.18	196.93
Radial O rings	5.00	8.64	2	17.28	10.00
Axial O ring	4.00	0.00	1	0.00	4.00
HDPE fuel block	119.12	45.80	1	45.80	119.12
Liner Resin and Hardener	16.14	0.01	1	0.01	16.14
Liner Cork	20.00	9.99	1	9.99	20.00
Ring clamps	80.00	6.30	2	12.60	160.00
Load cell	580.00	0.00	1	0.00	580.00
Pressure Transducer	120.00	0.00	2	0.00	240.00
Thermocouples	5.00	0.00	5	0.00	25.00
HX711 Amplifier	10.00	0.00	1	0.00	10.00
Arduino Uno	31.75	0.00	1	0.00	31.75
LM2596 Step down converter	12.00	0.00	1	0.00	12.00
Adapter connectors	52.85	125.40	4	501.60	211.40
Test Stand	10006.28	143.20	1	143.20	10006.28
M6 bolts	0.71	0.00	10	0.00	7.10
M10 bolts	3.50	0.00	2	0.00	7.00
M12 bolts	5.47	0.00	12	0.00	65.64
Thruster assembly bushing	2.29	0.00	1	0.00	2.29
Nichrome wire	5.00	6.90	1	6.90	5.00
Gasket	7.03	0.00	2	0.00	14.06
Margin	20%			505.47	4065.30
Total				3039.71 GBP	24.41 kg

11.7.2 Propellant Budget

Table 11.4: Propellant Budget

Propellant	Physical state	Volume used (litres)	Storage pressure (bars)
Nitrous Oxide	Pressurized liquid	1.2	44.5
High density Polyethylene	Solid	0.13	1
Liquid Oxygen	Pressurized liquid	0.6	40
Nitrogen	Gas	5.5	50

11.7.3 Power Budget

Table 11.5: Electrical Power Budget

Component	Quan.	Operating voltage (V)	Operating current (mA)	Power (W)	Duration (sec)	Net power
Load cell	1	10.00	13.40	0.13	10.00	0.13
HX711	1	5.50	1.80	0.01	10.00	0.01
Arduino Uno	1	5.00	200.00	1.00	10.00	1.00
Step down transformer	1	5.00	0.00	0.00	10.00	0.00
Pressure transducer	2	10.00	20.00	0.20	10.00	0.40
Thermo-couple	3	0.06	5.00	0.00	10.00	0.00
Control box	1	24.00	5000.00	120.00	15.00	120.00
Margin		20%				24.31
Total						145.85

Power Source	Description	Net Voltage (V)	Nominal Current (A)	Delivered Power (W)	Required Capacity (mAh)
Battery	11.1 V 1500 mAh LiPo battery	11.10	2.35	26.09	6.53
AC supply	24 V voltage generator	24.00	5.00	120.00	20.83
Total		35.10		146.09	27.36

11.8 Engine Test Setup



Figure 11.19: Welding on the combustion chamber and end flange connection. Source: Own.

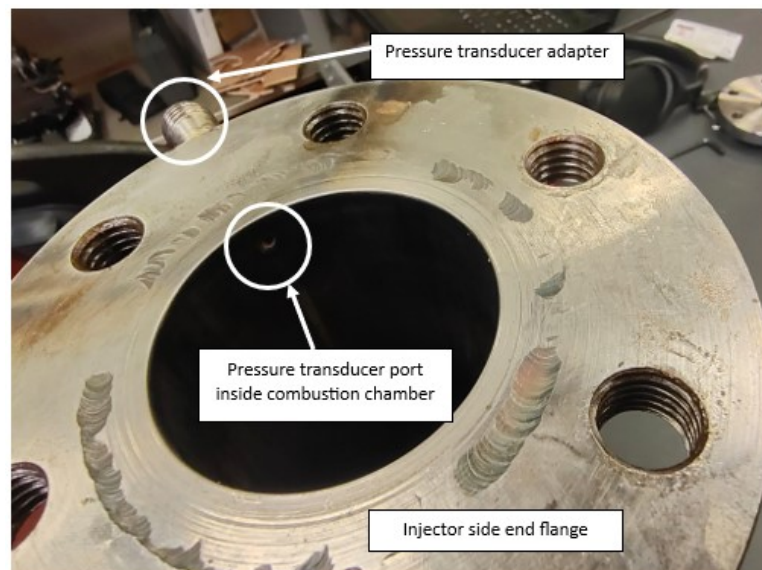


Figure 11.20: Internal hole for pressure transducer to measure internal combustion chamber pressure. Source: Own.

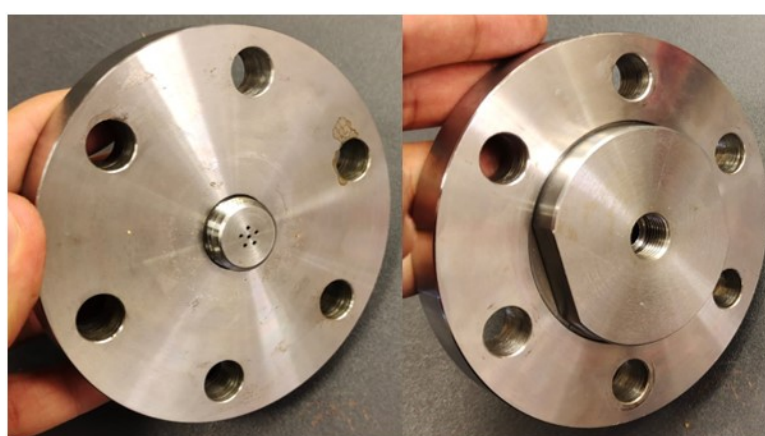


Figure 11.21: Injector plate assembly. Source: Own.



Figure 11.22: Line assembly of the combustion chamber. Source: Own.

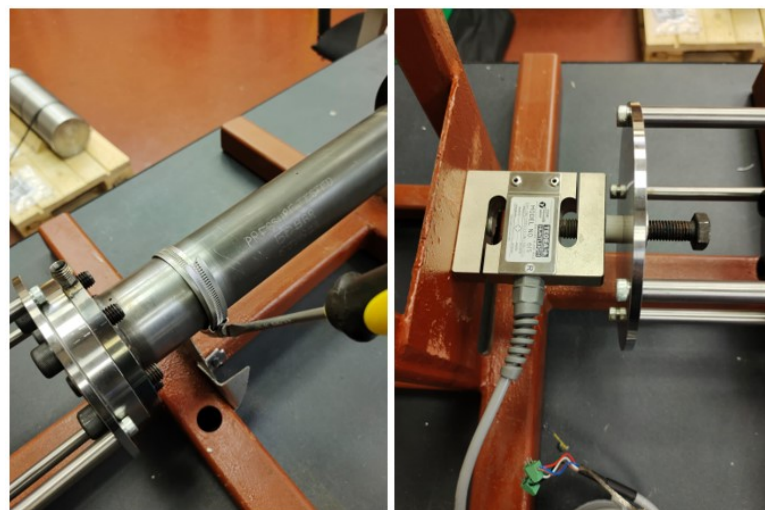


Figure 11.23: Structural assembly of the engine setup. Source: Own.



Figure 11.24: Pressure testing machine for the combustion chamber. Source: Own.

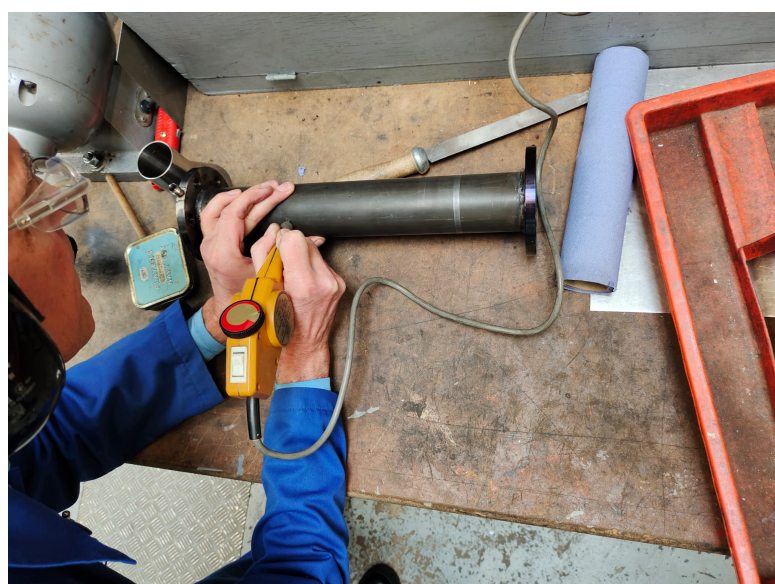


Figure 11.25: Etching on combustion chamber after passing the pressure test. Source: Own.

11.9 Risk Assessment

The table below displays all the identified risks for the project made initially at the PDR phase. The team is responsible,’/ and the current status of the action taken is updated at this stage. If the status is marked as “Closed”, then it is no longer considered an issue. If the status is marked as “Open”, then the risk mitigation action is still in effect and will carry on further on into the project.

The Pareto diagram illustrates the risks in order of their importance. The accumulated risk helps to show the most important tasks from the lesser ones. Typically, 80% and below are considered tasks of less importance. With this, more dedication was given to mitigating high-importance risks.

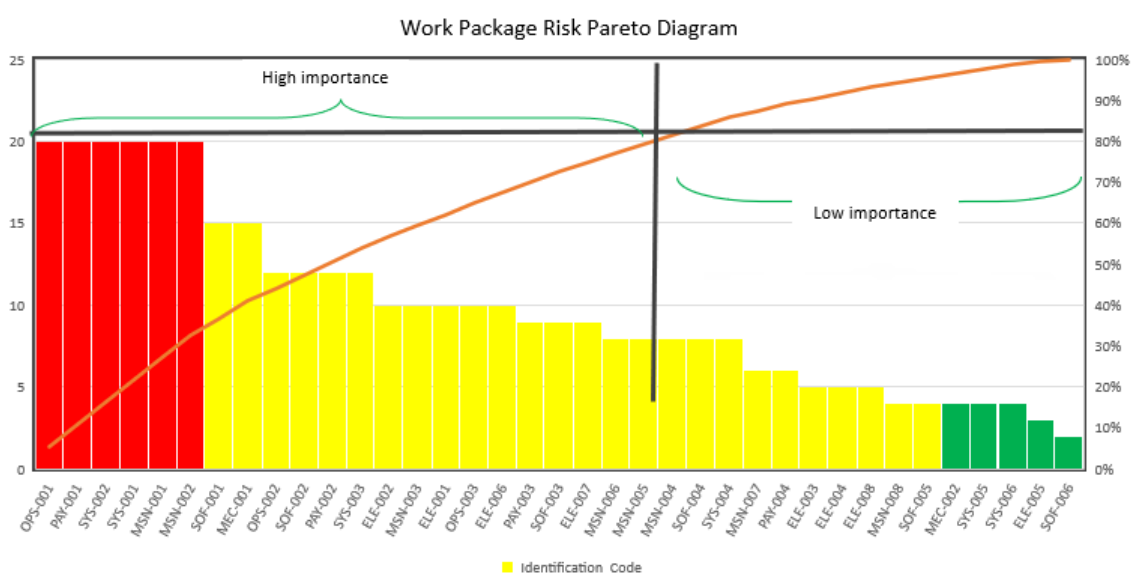


Figure 11.26: Pareto diagram. Source: Own.

11.9.1 Risk Assessment



Risk Assessment Form

CU-SHE-FORM-3.01

V4.0

Risk Assessment Number:	1 of 1	Title:	H.Y.D.R.A. Hybrid Rocket Engine, CranSEDS 2022-2023 v2.0		
Task/Activity assessed:	Hot Fire Rocket Engine Test				
Name/job role of people consulted during assessment:	Project Supervisor, Project Mentors, Test Site Manager, Health and Safety Officer	Date of Assessment	11 th June 2023		
Acknowledgements, Sign off and Authorisation					
	Acknowledgement	Name	Signature	Date	
Risk Assessor:	By signing this risk assessment, I acknowledge my responsibility as the Risk Assessor for conducting this risk assessment in accordance with CU-HAS-PROC-3.01, Risk Assessment Procedure.	Triyan Pal Arora, Project Manager		11 th June 2023	
Checked by:	By signing this risk assessment, I acknowledge my responsibility as the checker for this risk assessment in accordance with CU-HAS-PROC-3.01, Risk Assessment Procedure.	Dr Adam Baker, Visiting Fellow, Space Propulsion			
Authorising Person:	By signing the risk assessment, I acknowledge my responsibility as the Line manager/Supervisor for reviewing and approving this risk assessment and communicating controls and any additional controls to staff/students (as appropriate).	Scott Booden, Test Site Manager			

Tasks/Operational steps/Sub tasks/Events:	Significant hazards	Who is affected and how	What are your existing controls? (Reference all Safe Systems of Work (SSOW), Standard Operating Procedures (SOP) and Emergency Procedures)	Existing Risk Rating (Consequence x Likelihood = Total)			Are additional controls needed? Y/N (If Yes, RAMP required)		
				C	L	TOTAL			
1	Stored gas pressure vessel failure (e.g., where filling run-tanks with high pressurise fluids (Nitrous Oxide, Oxygen, and Nitrogen)).	The tank connector, feed line or the tanks themselves could either become disconnected or rupture due to over pressurisation.	Operators (student s/staff)	Minor injury due to filling line pipe disconnecting during filling. Possibility of tanks rupturing due to over pressurisation. Blast effects, possible - shrapnel.	<ul style="list-style-type: none"> The maximum expected operating pressure (MEOP) of the system is significantly less than the maximum allowable tank pressures (60 Bar maximum working pressure to be held within the 207 Bar rated run tanks – safety factor of 3.45x MEOP). To prevent the tanks from over pressurisation, each feed line shall contain a burst disk rated to 130 Bar. All tanks used during firing shall undergo a hydrostatic pressure test prior to use, alongside being new and certified for use. All feed system components are rated sufficiently in excess (227 Bar) of the 130 Bar burst disk setting. A nitrogen pressurisation leak test shall be conducted using soapy water to ensure all feed system connections are reliable and secure. Filling shall be done in a well-ventilated area. All stored gas cylinders to be secured when not being transferred to avoid unintentional shock loads. Eye protection must be worn during filling operations. The run tank employed shall have a maximum allowable pressure of 200 bars. The run tank shall incorporate dip tube and proper external connection to secure the gas in the tanks properly. 	5	1	5	N
2	Electrical Fire in test house 11 when preparing to test fire or during/after firing.	Control system short circuiting, cable melting or being exposed to extreme engine temperatures, causing an electrical fire.	Operators (student s/staff)	Could cause the generation of asphyxiate gas (e.g., CO/CO ₂). The fire could reach the propellant tanks which could heat	<ul style="list-style-type: none"> Ensure the test house is well ventilated. All operators shall wear fire protection lab coats and have water and CO₂ fire extinguishers readily available. A metal blast shield shall be mounted to the tank stand to deflect any excess heat from the engine. The tank stand, containing the electrical equipment shall be located besides the engine as opposed to 	3	2	6	Fire blankets (for an electrical fire) and multiple buckets of water (for a chemical

		Engine failure exposing tank stand to excess heat.		them to a sufficient temperature to cause over pressurisation and compromise their structural integrity.	<p>behind the engine, to reduce the risk of failure if the engine's injector were to fail.</p> <ul style="list-style-type: none"> All wires selected have been selected to withstand the maximum likely current expected, reducing the risk of wires melting. Tanks have burst disks rated to 130 Bar, so if the tank were to heat excessively and over pressurise, this would rupture first and release its contents, as opposed to rupturing the tanks. To reduce the risk of the tank contents encouraging the fire during such an event, the tanks shall only be filled to a maximum of 3 Litres. All test operations shall be conducted 10 m away from the engine, behind a blast-proof shield, in a well-ventilated room. If the fire becomes uncontrollable, all operators shall evacuate the test site and gather in the test site car park. Calling the fire brigade for assistance. 			fire) shall be located and easily accessible around the engine test bench.	
3	<i>Engine dismounting from test stand during firing.</i>	Engine plume may be directed towards the tank stand and/or the control room (containing the operators).	Operators (students/staff)	Potential to cause damage to test site equipment and burn to personnel. Hearing and eyesight damage is also possible.	<ul style="list-style-type: none"> All test operations shall be conducted 10m away from the engine, behind a blast-proof shield, in a well-ventilated room. Significantly reducing the risk to operators. The control system has an integrated emergency stop button, which, as indicated in the SOP, shall be pressed if such an event were to occur. The engine is safely secured to the test stand using jubilee clips and straps, preventing significant lateral movements. 	3	2	6	N
4	<i>Flashback from the engine to the feed system tanks.</i>	Could cause an internal feed system fire which may result in tank rupture and/or an uncontrollable fire.	Operators (students/staff)	Fire injury to personnel and damage to equipment. Feed line or valve failure / possible ignition / shrapnel.	<ul style="list-style-type: none"> All test operations shall be conducted 10m away from the engine, behind a blast-proof shield, in a well-ventilated room. A positive pressure difference of at least 10 Bar across the injector (i.e., between the feed system and the engine's combustion chamber) shall be maintained throughout the burn, with the injector acting as a check valve reducing the risk to operators by preventing any pressure oscillations causing reverse flow into feed lines. 	4	2	8	N

5	<i>Power cut during firing.</i>	Engine becomes uncontrollable from the remote-control unit.	Operators (student s/staff)	The engine may burn for longer than desired, increasing the risk of engine failure and overheating the surrounding test stand area.	<ul style="list-style-type: none"> All solenoid valves selected are designed to fail-shut. Thus, preventing the flow of oxidiser/fuel to the engine and stopping the combustion process. The Nitrogen purge line has normally open valves, to allow the whole system to be purged and extinguished with the high pressure nitrogen. 	2	2	4	N
6	<i>Electric shock.</i>	Electrocution of an operator from the 230 VAC power supplies.	Operators (student s/staff)	A double insulated wiring connection may become exposed and contact personnel resulting in burns and/or a cardiac arrest.	<ul style="list-style-type: none"> The control system is designed to be 12VDC (within the control room) and 24VDC (by the engine) power systems, using step-down transformers to ensure a safe operating voltage. The wiring within the control room is insulated by the control box and the box is grounded to the floor of the control room. The more exposed 230VAC cable on the tank stand is covered to reduce the risk of contact when live. 	4	1	4	N
7	<i>Gas tank's toppling.</i>	Physical impact and/or dangerously expelling combustion fluids.	Operators (student s/staff)	Nearby persons may endure a high energy impact resulting in significant physical harm if a tank connector were to break-off a tank.	<ul style="list-style-type: none"> The tanks shall be secured to their places using multiple sandbags and keeping them far from the thrust trail of the engine. The feed line will incorporate a plastic tube before the feed line goes to the injector. This plastic tube will carry the thrust deviations and protects from transference of big loads to the steel pipes and the tanks. All operators will remain at least 10m away from the engine during firing and behind a blast proof shield. Operators must wear safety boots during preparation and testing. 	3	1	3	N
8	<i>Personnel contact with hot parts post firing.</i>	Heat damage to skin	Operators (student s/staff)	Minor injury from burns	<ul style="list-style-type: none"> Warning signs and barriers to be put in place immediately pre-firing Operators only to approach engine after ambient temperature achieved – determined visually and using thermal hand sensors. Operators to use heat-resistant protective gloves when handling hardware post-burn 	3	1	3	N
9	<i>Combustion after firing terminates</i>	External heating of rocket engine chamber.	Operators (student s/staff)	Cosmetic damage to motor, burns to operators	<ul style="list-style-type: none"> Ensure equipment is clean, no loose, potentially flammable items within range of motor plume. Purge each feed line and the engine with nitrogen gas after every burn. 	2	2	4	N

	eg from fuel slivers.			inspecting after firing.	<ul style="list-style-type: none"> CO₂ and dry powder fire extinguisher(s) to be available during test fire – can be used to extinguish any post-test burning. 				
10	<i>Upstream leakage of gas: N₂O / O₂ / N₂ - during loading / ignition / hot fire / purge.</i>	High pressure gas leak: fire and / or asphyxiant.	Operators (student s/staff)	Minor injury from ejected gas Damage to instrumentation and feed system	<ul style="list-style-type: none"> Low pressure gas test of plumbing (10 Bar) – balance between pressure required for MEOP + safety factor hydraulic test, and risk from high pressure gas in event of a mechanical failure. PPE (full face masks and fire-retardant suits) to be worn during loading. All operator staff to be remote (min 10m and behind a blast proof shield) during firing. All plumbing connections double checked for leaks with soapy water. 	3	2	6	Hydraulic cold flow test of fully assembled plumbing, from tanks to injector.
11	<i>Burn through of engine chamber</i>	Burn the internal side of the casing, melt it, and deform the surface. Causes corrosion of the metal during cool down after the burn out.	Operators (student s/staff)	Cosmetic damage to motor, minor burns to operators inspecting after firing, damage to the casing making it prone to failure.	<ul style="list-style-type: none"> The chamber casing will be painted to protect from corrosion, and completely covered with a thick layer (5 mm) of cork liner to protect from the combustion of the engine. The thickness of the casing is 6 mm to protect from any burn through. Thicker metal makes it difficult for conductive heat transfer within the 6.5 seconds burn 	2	2	4	N
12	<i>Nozzle failure</i>	Nozzle breaks, the exhaust flow is deviated, due to cracked nozzle, creating unresolved loads on structure. blocks the combustion chamber outflow, makes it a high pressurized and high temperature gas cylinder, with explosive potential.	Operators (student s/staff)	Potential to cause damage to test site equipment, may damage the engine setup, may cause a big explosion.	<ul style="list-style-type: none"> The nozzle is tested through simulations for higher than worst loading. The graphite nozzle sits on nozzle casing with 2 compressive radial O-rings, creating sealed outer zone. The fitting of nozzle and nozzle casing is tolerance fit of 0.1 mm, making it difficult to break and create a space pocket in the combustion chamber. 	4	2	8	N
13	<i>Nozzle blockage and overpressure of chamber</i>	Blocks the combustion chamber, makes it a high pressurized and high temperature gas cylinder, with explosive potential.	Operators (student s/staff)	Potential to cause damage to test site equipment, may damage the engine setup, may cause a big explosion	<ul style="list-style-type: none"> If the nozzle is blocked and/or the chamber is overpressured, the rear end of the nozzle casing with 2 mm of steel layer fails and pops out the graphite nozzle. This releases the internal overpressure and saves crucial components from damaging. 	4	2	8	N
14	<i>Overpressure of</i>	High pressure of 33.5 bars, but low velocity	Operators	Potential harm to equipment, any	<ul style="list-style-type: none"> The thickness of combustion chamber is considered with a big margin to be 6 mm. 	4	1	4	N

	<i>combustion chamber</i>	causes pressure builds up, which may crack/rupture the chamber.	(student s/staff)	personnel standing close, or in unsafe manner	<ul style="list-style-type: none"> The chamber has been water pressure tested up to 50 bars as pre-requisite tests. 				
15	<i>Structural failure due to vibrations, heat and thrust loads</i>	The test stand, structure or any interface can fail due to vibrational loads, heat loads, and thrust loads	Operators (student s/staff)	Potential harm to equipment, any personnel standing close, or in unsafe manner	<ul style="list-style-type: none"> The design of components has been thoroughly tested against possible worst thrust loads, heat loads, and vibrational loads. A minimum of 1.5 factor of safety was targeted and achieved, at every component and interface. 	3	2	6	N
16	<i>Malfunctioning or failure of feed line component (valves, regulators)</i>	Valves and regulators malfunction due to unexpected pressure load, internal mechanical failure, or electrical failure	Operators (student s/staff)	The leakage of N ₂ O may concentrate the surrounding atmosphere and make it hazardous. O ₂ leak may lead to fire explosion.	<ul style="list-style-type: none"> The feed line components are checked for valid certifications before putting in all together. The valves and regulators will be tested during the cold flow test to ensure no leaks or failure occurrence. The components will be sealed with Teflon tape and copper thread locker to eliminate any sliver of opening and ensure tight connections at all the interfaces. 	4	2	8	N
17	<i>Leakage from feed line pipes</i>	Feed line pipe connections not tight enough, the pipes used are of low quality, causing cracks due to high pressured flow.	Operators (student s/staff)	The leakage of N ₂ O may concentrate the surrounding atmosphere and make it hazardous. O ₂ leak may lead to fire explosion.	<ul style="list-style-type: none"> The feed line pipes are 3/8 in steel Swagelok pressure fluid pipes. They cross the threshold limit established through calculations. Valid certifications for the pipes is checked. The feed pipes will be tested during the cold flow test to ensure no leaks or failure occurrence. The pipes will be sealed with Teflon tape and copper thread locker to eliminate any sliver of opening and ensure tight connections at all the interfaces. 	4	1	4	N
18	<i>Improper assembly, misalignment</i>	May lead to gaps in interfaces, weakening the structure, single point failures, the exhaust plume will not be in the anticipated direction	Operators (student s/staff)	Potential harm to structure, if not enclosed, the exhaust plume can pollute the surroundings	<ul style="list-style-type: none"> The assembly is checked for correct alignment using handset inclinometer at each step of the assembly and integration. The fixtures prepared aid in correctly aligning the line assembly onto the test stand for correct alignment for the plume. The setup will be tested during cold flow test to ensure proper alignment has been achieved. The structure is capable enough to take unanticipated loads with a safety factor of 1.5 	3	2	6	N
19	<i>Ignition failure or delayed ignition</i>	Uncontrolled propellant buildup or incomplete combustion. Affects the recorded engine performance. The	Operators (student s/staff)	Incomplete combustion means intermittent species (CO, NO,	<ul style="list-style-type: none"> The ignition will be tested before the actual test firing. The burning of the Nichrome wire (28 AWG) will be measured, with the required distance to keep the controls behind the blast cover. 	3	2	6	N

		required voltage for ignition is a potential danger.		NOx) existing in the exhaust which will be harmful to personnel	<ul style="list-style-type: none"> The required voltage may be potentially dangerous and will always be shielded. The data acquisition system shall have enough storage to allow for no or bad readings, which will be removed in post processing of the obtained results. This will be correlated with the firing through the camera feed. 				
20	<i>Noise, shockwave, or acoustic hazard during firing</i>	The noise and acoustic hazard are inevitable in test firing. Acoustic vibrations may shake components in surrounding, like tanks, cameras, sensor placement	Operators (students/staff)	Large noise may be harmful to human ears. May cause nearby equipment to shake due to acoustic vibrations	<ul style="list-style-type: none"> The tanks and cameras will be fixed in place of sandbags. The tower containing the electronics will be shielded by a wooden board to protect from shock waves and any kind of explosion. The operators shall always wear headphones. The sensor readings may have jitters, which can be removed in post processing of the obtained results. The test facility area will be alerted before the testing. The area will be blocked from any outsider to enter. 	2	3		N
21	<i>After-firing Exhaust</i>	The exhaust after test firing may contain unburnt combustion products (like CO, NO, NOx) which are dangerous to humans, and may react with equipment.	Operators (students/staff)	Potential to cause damage to test site equipment. Hazardous to humans and nearby personnel.	<ul style="list-style-type: none"> To clear up the surroundings from large exhaust concentration, electric fans will be used kept at sufficient distance to avoid any hazardous reaction of the unburnt particles in the exhaust. The purging through nitrogen gas will be extended to ensure safety. The setup will be placed near to the outside gate of the test house to keep the system in an open atmosphere. The area will be kept closed for a certain pre-determined time to ensure the exhaust is completely dissipated and there's no chance of harm from the exhaust to the personnel or equipment anymore. 	3	3		N

PERSONAL PROTECTIVE EQUIPMENT (PPE):											
	For every item of PPE required, specify the type and other relevant information below: <ul style="list-style-type: none"> • 1 x LABORATORY COAT (PER OPERATOR) • 1 x SAFETY GLASSES (PER OPERATOR) • 1 x SAFETY GLOVES (PER OPERATOR) • 1 x SAFETY HEADPHONES (PER OPERATOR) • 1 x SAFETY BOOTS (PER OPERATOR) 										
	Type	Other relevant information <i>e.g material, level of protection, etc.</i>									

Emergency Planning Arrangements relating to operations/event

	In event of emergency ring x 2222 or 01234 752999. For an ambulance ring 999, then direct the ambulance to the test site.
--	---

Risk Rating Matrix

RISK MATRIX					
Consequence Likelihood	Negligible (1)	Minor (2)	Medium (3)	Major (4)	Severe (5)
Almost Certain (5)	5	10	15	20	25
Likely (4)	4	8	12	16	20
Possible (3)	3	6	9	12	15
Unlikely (2)	2	4	6	8	10
Very Unlikely (1)	1	2	3	4	5

Rating	Interpretation	Authorisation
≤ 6 = Low Risk	Acceptable but ensure that controls are maintained	Line Manager or equivalent
8 -12 = Medium Risk	Adequate but look to improve if reasonably practicable	Line Manager or equivalent
15 – 25 = Unacceptable Risk	STOP activity and make immediate improvements	PVC School/Director of PSU

CONSEQUENCE (considered WITH controls in place)		
5	Severe	<ul style="list-style-type: none"> Fatality (ies) Severe or chronic illnesses or permanent life changing impact
4	Major	<ul style="list-style-type: none"> Injury such as fracture of bones, dislocation, or acute ill health e.g. occupational asthma, occupational dermatitis
3	Medium	<ul style="list-style-type: none"> An injury that requires first aid treatment and subsequent treatment by health care professional No lost time illnesses and no chronic/acute health effects
2	Minor	<ul style="list-style-type: none"> An injury that requires basic first aid treatment such as administering a plaster, individual able to continue at work e.g. minor cuts, bruising, abrasions, strains or sprains
1	Negligible	<ul style="list-style-type: none"> Superficial or no physical injury or health effects

LIKELIHOOD (considered WITH controls in place)		
5	Almost Certain	<ul style="list-style-type: none"> Will occur/greater than a likelihood of 1 in 1 (yr)
4	Likely	<ul style="list-style-type: none"> Known to occur/probably occurs most circumstances/No greater than a likelihood of 1 in every 10
3	Possible	<ul style="list-style-type: none"> Might occur /no greater than a likelihood of 1 in 1000
2	Unlikely	<ul style="list-style-type: none"> Not likely/could occur at some time/no greater than a likelihood of 1 in 10,000
1	Very Unlikely	<ul style="list-style-type: none"> May only occur in exceptional circumstances/no greater than a likelihood of 1 in 100,000

11.9.2 Test House 11 CranSEDS HRMTS Risk Review

Overview

The aspect that attracts numerous students to choose Cranfield is the robust practicality facilitated by our testing and engineering facilities. In pursuit of further progress, the CranSEDS university space association has initiated a project centred around the design of a 300 N hybrid rocket engine utilizing HDPE and N_2O . Initially introduced in 2020, the project's overarching objective is to incorporate the hybrid engine into a rocket eventually and subsequently venture into the realm of liquid engine development.

Test House 11 was chosen as the site for the engine test. This involved the installation of a custom test bench in receiving it, assembly, integration, and testing of the feed line system, controls and electronics system, and thorough safety inspections before commencing the firing sequence.

Hazards, Consequences, and Control

First of all, if personnel must be allowed to move around the test site in the presence of the installed engine, it is essential that they be properly supervised by a qualified operator. To meet this requirement, an appropriate member will be appointed as the operator to oversee the set of on-site actions. An additional member will be considered if needed. Without oversight, no work will take place.

Regarding the various risks considered related to the system, they can be found in the associated risk assessment form. This document, therefore, lists by severity and probability the various hazards that the operator and the members present on-site might encounter.

For instance, let's consider a primary risk: the possibility of engine flashback reaching the feed system tanks. This scenario, classified as moderate, has the potential to ignite a fire within the internal feed system, leading to tank rupture and/or an unmanageable blaze. Therefore, it is highly recommended to carry out all test operations at a distance of 10 meters from the engine while positioned behind a shield that is designed to withstand blasts. These operations should take place in a well-ventilated room. Furthermore, it is crucial to maintain a positive pressure difference of at least 10 bars across the injector throughout the burning process. This pressure differential acts as a safeguard by preventing any pressure fluctuations that could lead to a reverse flow into the feed lines. Finally, for added protection, extra check valves and/or flame arrestors can be installed in the feed system after the injector. Since the market-available flame arrestors are marked up to 25 bars, it was decided to employ a separate small 10-litre run tank between the main nitrous oxide tank and the combustion chamber. The run tank is filled using a dip tube and is operated by a pneumatic-controlled valve for the feed of nitrous oxide into the engine.

Conclusion

We have an exciting project ahead that will elevate our learning experience. While there are certainly risks involved, we are confident in our ability to minimize them to a satisfactory extent. The crucial element in achieving this is ensuring complete supervision at all times, and it is important to note that no tasks will be undertaken without the presence of an operator.

11.9.3 COSHHA Assessment for Nitrous Oxide

The COSHH assessment stands for the Control of Substances Hazardous to Health. A COSHH assessment concentrates on the hazards and risks of hazardous substances in your workplace.

Since the oxygen and nitrogen to be used are already available in the test facility of the university, the existing COSHH assessments for the gases are used. However, the nitrous oxide, which needs to be bought this year, requires an individual-specific COSHH assessment to be bought and used for the hybrid engine test firing. This assessment is a 2-page document attached in this section, as described hereon.



Standard COSHH Assessment

STANDARD COSHH ASSESSMENT <i>This form is only to be used after completing the COSHH flow chart in Appendix A.</i>							Ref. No:	Date:	
							HY23-03 Rev.00	05.06.2023	
TASK / PROCESS / ACTIVITY/LOCATION: <i>What will be done? Where and when will this work be carried out?</i>									
Gases will be used at various stages of firing procedure for a hybrid rocket engine firing on a horizontal test bed, during feed line fill, ignition, combustion, and purging the system.									
PERSONS EXPOSED:									
Staff	<input checked="" type="checkbox"/>	Students	<input checked="" type="checkbox"/>	Visitors	<input type="checkbox"/>	Other (specify):			
HAZARDOUS SUBSTANCES: <i>What will be used? What is the materials physical form? (e.g. powder, dust, granular, liquid, solution, gas)</i>									
Nitrous oxide – pressurized gas To be used as oxidiser in a hybrid engine with high density polyethylene as the solid fuel.									
STOCK QUANTITY: <i>What is the quantity of the stock/substance container?</i>			PROCESS QUANTITY: <i>What is the quantity used in the process?</i>			FREQUENCY:		DURATION:	
Nitrous Oxide: Type W tank (to be bought from BOC)			10% margin considered Nitrous Oxide: 1.2 litres per hot test firing			Process quantity used once per firing (4 planned hot firings in June)		Less than or up to 8 seconds	
HAZARD CLASSIFICATION:									
Physical				Health				Environment	
<input type="checkbox"/>	<input checked="" type="checkbox"/>	<input checked="" type="checkbox"/>	<input type="checkbox"/>	<input type="checkbox"/>	<input type="checkbox"/>	<input type="checkbox"/>			
ROUTES OF EXPOSURE:									
Eye Contact	<input checked="" type="checkbox"/>	Skin Contact	<input checked="" type="checkbox"/>	Inhalation	<input checked="" type="checkbox"/>	Ingestion	<input type="checkbox"/>	Injection	<input type="checkbox"/>
Specific storage requirements: Consider chemical incompatibility, segregation, etc.									
All gases stored in separate pressurized containers with following pressure ratings: - Nitrous oxide: 44.5 bars (Main engine oxidiser)									
All containers should be stored upright and kept at moderate temperatures. Containers shall be kept away from open flames or other sources of ignition. Valve operation shall avoid any abrupt closure or opening, eliminating any chance of shock propagation through the feed line. In lieu of pressure decay during combustion, the supply tank shall maintain a minimum pressure of 4 bars eliminating risk of combustion instability. Pressurized Nitrogen (already available in test facility at Cranfield University) will be used as a purge gas for the whole system.									

PERSONAL PROTECTIVE EQUIPMENT (PPE):						
For every item of PPE required, specify the type and other relevant information below:						
Type	Other relevant information (e.g material, level of protection, etc.)					
Eye protection	Eye goggles required at minimum, if possible face masks should be worn when handling highly pressurized gases.					
Clothing	Long sleeved clothing should be worn when handling pressurized gases. Shorts should not be worn.					
Are additional controls required?		No <input checked="" type="checkbox"/> Yes <input type="checkbox"/> If yes, complete RAMP (Appendix D).				
EMERGENCY PRECAUTIONS						
Eyes:	Nitrous Oxide – Remove contact lenses if any, rinse eyes with warm water for several minutes, seek medical attention.					
Inhalation:	Nitrous Oxide – Remove exposed person from contaminated area immediately, move to fresh air and seek medical attention.					
Skin:	Nitrous Oxide – Immediately submerge the affected body part in warm water, soak it in for a while and remove the exposed person from the area.					
Ingestion:	N/A					
Spill:	N/A					
Fire:	Extinguish using Water, powder, foam, CO ₂ (oxidising element, apply as required by burning material)					
Risk Rating			S⁸ 3	L⁹ 3	Total¹⁰ 9 (Moderate Risk)	
AUTHORISATION						
Assessor:	Triyan Pal Arora			Date:	05.06.2023	
Reviewer:				Date:		
Authoriser:				Date:		

8. See Appendix G for severity definitions and scoring. Severity should be based on information including the worst case illness.

9. See Appendix G for likelihood definitions and scoring. Likelihood should be based on how likely ill health is to occur. Good existing controls will reduce the likelihood.

10. The total existing risk rating is determined by Severity x Likelihood. See Appendix H.

11.10 Project Gantt Chart

The Project Gantt Chart describes the overall flow and plan of the project from the initial phase in December up till the end of the competition in July. The Gantt chart contains information for the internal and external important dates for the competition, club, team as a whole, and sub-teams, including systems, propulsion, structures, controls, and manufacturing. The Gantt has been prepared in Excel and has been compressed into a single page below for your reference.

HYDRA HRMTS 22-23 Project Schedule